Sand in Short Supply

Modelling of Bedforms, Roughness and Sediment Transport in Rivers under Supply-Limited Conditions

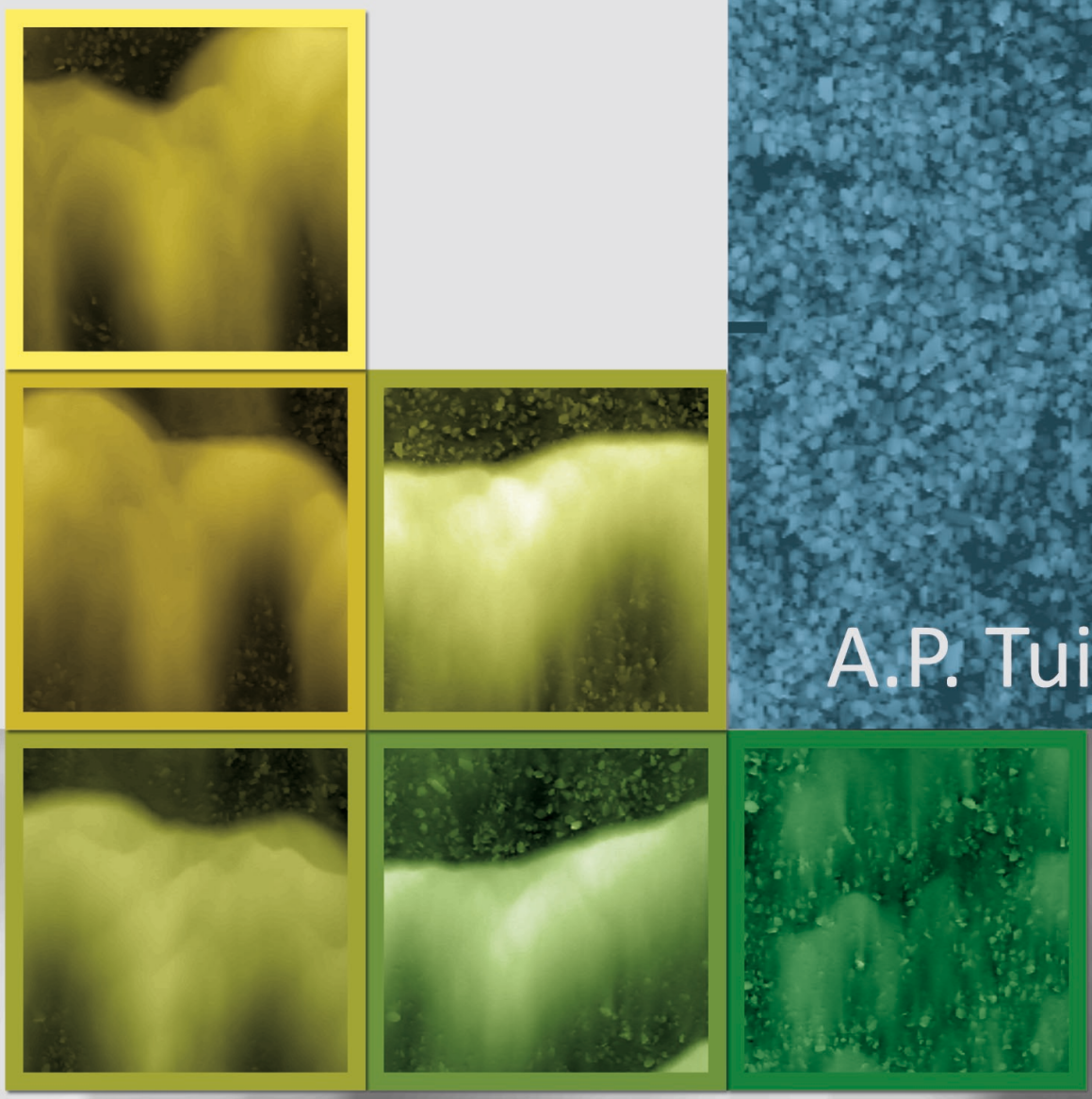

A.P. Tuijnder

SAND IN SHORT SUPPLY

MODELLING OF BEDFORMS, ROUGHNESS AND SEDIMENT TRANSPORT IN RIVERS UNDER SUPPLY-LIMITED CONDITIONS

A.P. TUIJNDER

Promotion committee

prof. dr. F. Eising	University of Twente, chairman/secretary
prof. dr. S.J.M.H. Hulscher	University of Twente, promotor
dr. ir. J.S. Ribberink	University of Twente, assistant-promotor
prof. dr.-ing. A. Dittrich	Technical University of Braunschweig
dr. ir. C.M. Dohmen-Janssen	University of Twente
prof. dr. ir. J.A.M. Kuipers	University of Twente
prof. dr. ir. L.C. Van Rijn	University of Utrecht
dr. ir. C.J. Sloff	Delft University of Technology

This research is supported by:

The Technology Foundation STW, applied science division of NWO and the technology programme of the Ministry of Economic Affairs of the Netherlands as part of the VICI project 'Rough Water' (project number TCB.6231).

The Delft Cluster program 'Natural Hazards', work package A2 River Morphology (WP CT 043211).

Deltares TO-project: "Rivierkundige onderzoeksthema's", subproject "Los zand, grind, en harde klei" No. 1200186-002.

Printed by Wöhrmann Print Service, Zutphen, the Netherlands

ISBN 978-90-9025123-3

SAND IN SHORT SUPPLY

MODELLING OF BEDFORMS, ROUGHNESS AND SEDIMENT TRANSPORT IN RIVERS UNDER SUPPLY-LIMITED CONDITIONS

PROEFSCHRIFT

ter verkrijging van
de graad van doctor aan de Universiteit Twente,
op gezag van de rector magnificus,
prof. dr. H. Brinksma,
volgens besluit van het College voor Promoties
in het openbaar te verdedigen
op donderdag 1 april 2010 om 15.00 uur

door

Adriaan Pieter Tuijnder
geboren op 29 januari 1980
te Dordrecht

This thesis is approved by:

prof. dr. S.J.M.H. Hulscher	promotor
dr. ir. J.S. Ribberink	assistant-promotor

‘Mijn waarnemingen zijn zelden waar; toch blijf ik ze nemen.’

(Simon Carmiggelt)

Voor de drie vrouwen van wie ik het meeste houd.

Preface

How I end up in the gutter

It is very unfortunate that one has to make choices in life. Already at a young age I was aware of that: I reportedly shouted in anger: 'Ik wil alles!!!' (I want everything!!!). I definitely wanted to understand both all things technical and natural. I was actually quite worried that we would run out of oxygen if we would continue chopping forests, and annoyed that LEGO would not make parts to properly build a gear box the same way as found in cars. Therefore making the choice for the right study was difficult; there are so many interesting subjects. In high school I was certain that I would do an engineering study like applied physics, mechanical or civil engineering. Because at that time I had the opinion that computational predictions and technical design are the main purposes of science and engineering. It had to be combined with something earth-science-like though, and therefore I opted for technical earth sciences at the TU-Delft. The curriculum and staff were too focused on mining and well-drilling too my taste and I found the books on geomorphology and geology that my girlfriend Ilse was reading much more compelling. Therefore I soon switched to physical geography at the Univeristy of Utrecht. No Ilse, I did not at all make that switch because I wanted to be around you all the time, that was just a fortunate side-effect. I never regretted the choice and found it a very interesting study, especially the courses on fluid mechanics, sediment transport and river and coastal morphology. Although I would have liked to learn more about mathematical modelling of morphodynamics than possible within the scope of the study. Luckily, Aart Kroon gave me all freedom to choose a graduation topic and I measured and modelled the ground water flow in beach plane 'de Horst' on the island of Texel. I started to really understand the meaning of a differential equation for the first time during the writing of my master's thesis and found it really fascinating to compare numerical computations with field measurements. After my graduation I worked at the Netherlands Environmental Assessment Agency (RIVM/MNP), where my collegues were all enthusiastic ecologists and I learned a lot about the geographical distribution of plant and birds species. But soon I realized that I would much rather do geographical research and I contacted Aart again to see whether there were any opportunities. We (well, mostly he) prepared a research proposal, but in the mean time he moved to Denmark and I got the possibility to start my PhD-research in the hydraulic roughness research project 'Rough Water' of Suzanne Hulscher.

That is what eventually got me into the gutter.

I mean into a flume of course. The flumes proved to be a very natural habitat for a geographer with a strong technical interest. It is your own private bit of nature, with you in control over the boundary conditions. What's more: you get to play with pumps, cranes, sensors and

computers. Calibrating, testing, programming, data analysis, the first glimpse of a trend in your data: can work be more versatile and interesting than this?

So how did I end up studying the effects of 'supply limitation' – a limited volume of sediment on the riverbed that can be transported – on river dunes, hydraulic roughness and sediment transport?

This focus developed during the first year or so. My daily supervisor, Jan Ribberink, gave me another research proposal for inspiration and ideas. This had a focus on suspended sediment transport modelling in large scale morphological models. In my eyes this was quite a different focus than described in Suzanne's research proposal. This confused me a bit, but at the same time it also gave me the freedom to find out what my own interests really were. A key concept in both research proposals was 'graded sediment' (a grain size mixture), and since bedforms play a key role in almost anything that happens on and in the riverbed, I was interested in the relation between bedform characteristics and sediment mixture characteristics. I found a paper by Maarten Kleinhans (Kleinhans et al., 2005), which made me realize that there was a lot to be learned about the influence of supply-limitation on bedform type. In fact I was suprised to learn that there was hardly any quantitative knowledge on the prediction of bedform dimensions under supply-limited conditions. I often asked myself: why did this subject receive so little attention? Is it because the answers are too obvious or the subject too unimportant? Gradually, by talking to other people, a.o. my user-committee, I started to realize that it would be worthwhile to study this topic. Moreover, the possibility of doing experiments at the TU-Braunschweig provided a good opportunity to study the relation between the dune characteristics and sediment supply. There I had my research topic for the years to follow.

Once the experiments, which were conducted at the TU-Braunscheig, were under way, my confidence that I would be able to finish the study started to grow. Back in Enschede, I enjoyed the data analysis and it appeared that papers are much easier to write if you have a nice set of data. The result of 4½ years of hard work are summarized in this thesis. I hope that you will enjoy reading it as much as I enjoyed writing it.

Words of thanks

I'll start with Jan: I consider myself lucky that you were my daily supervisor. Your experience, patience and precision were just what I needed. I learned a lot from you and I enjoy working with you. Suzanne: It took me a bit longer to get to know you, mainly because we did not talk as often, because I wanted to have some serious results to show to you. I discovered that your 'listening frown' doesn't mean that your annoyed at all; you're just concentrated. I really appreciated your patience and positive view on things when I was overly critical. Thanks for your confidence that I would give a useful contribution to your Rough Water project.

I also want to thank all my WEM-colleagues for the support, discussions, chats and the nice working atmosphere in general. A few people I want to mention in particular. Daniëlle, Rolien, Andries and Freek: it was really useful and nice to have regular discussions with the DRAF group when I just started. Andries, I was glad that I had a travelling companion and hotel roommate at conferences every now and then. Saskia, Jebbe, Judith and Pieter: your were just very nice fellow PhD-students it was great to share experiences with people who are doing the same thing. Blanca and Rianne, you were great roommates I couldn't hide much from you but that's okay; I really appreciated the help, support and chats. Blanca: it is great that you just tell me to take it easy when I'm stressing out. Jolanthe: it was great to have a long-time friend as a colleague with the same supervisors. They thought they had to evaluate us, but we evaluated them probably more often. I'm sure you'll manage to wrap up soon as well. Rolien: our exchange of ideas, opinions and papers was really valuable. The time spent on our common commute was time well spent. I'm glad you want to back me up during my defense as paranymph.

Matthieu: you joined me for the experiments for your masters thesis work. I found it an exciting time, but it was initially also a quite stress-full time. Stress was not what you were waiting for at that time, but you handled it well in the end and you produced a good masters thesis. I was really happy that you wanted to stay at the WEM group to do additional experiments with vertical sorting; these have proved very valuable. Thank you for your cooperation and help, and good luck with your own PhD-research. Stephan: thanks for your help with the vertical sorting experiments. I think your MSc-thesis is coming together nicely now; success finishing it.

Ich möchte mich auch ganz herzlich bei meinen Kollegen in Braunschweig bedanken. Ich fühlte mich bei euch am LWI ganz schnell zu Hause. Klaus, Bernd, Joe und Katinka: herzlichen Dank für die viele Hilfe von Euch. Thomas und Henrich: Danke für die Gemütlichkeit und schönen Ausflüge die wir gemacht haben und viel Erfolg mit euren Diss. Ich hoffe wir sehen uns nochmal. Ein herzliches Dankeschön auch an die Werkstatt für die vielen Sachen die Herr Appelthauer, Herr Neumann und Herr Lehmann gebaut haben. Allerdings hätten ohne Uwe Ecklebe die ganzen Versuche gar kein Zweck gehabt, denn ohne Ihn hätte die Messelektronik nicht funktioniert, dafür herzlichen Dank. Zum Schluss, aber nicht weniger Wichtig: Herzlichen Dank an Professor Dittrich das er mir die Möglichkeit gegeben hat solange an seinem Institut zu arbeiten. Viele Deutschland Vorurteile sind überholt, aber zwei haben sich als wahr herausgestellt: Wurst und Bier sind wirklich wichtige Sachen für Deutsche, aber zu Recht, denn ich werde mich an die vielen gemütlichen Mahlzeiten und so mancher Diskussion über einem Bier gerne erinnern.

Furthermore I would like to express my thanks to some people from other institutions. My user committee proved to be very useful. In the beginning I was a bit unsure as to what I would have to offer you. But in the end it proved to be useful for both sides. Therefore I want

to thank Hendrik Havinga, Kees Sloff, Arjan Sieben and Gert-Jan Akkerman for their input, critical questions and motivational words. The morphological simulations were carried out in cooperation with Deltares. I want to thank Willem Ottevanger, Aukje Spruyt, Bert Jagers and Kees Sloff for their help. Astrid Blom and Maarten Kleinhans: thank you for your suggestions, papers, comments and support, especially in the earliest phase when I was looking for a research topic. Aart Kroon: Thank you for your support when I wanted to start my research. I'm glad to live on the right side of IJssel now ;-)

Theo en Aja: jullie zijn echt fantastische schoonouders. Niet officieel weliswaar, maar dat is omdat we trouw belangrijker vinden dan trouwen. Aja, laat je niet in de maling door me. Je bent echt een zeldzaam lief mens. Sorry dat ik niet alles geloof wat je ergens leest of hoort, maar jij gelooft ook maar dat helft van wat ik zeg. Wat zeer verstandig is, want zeker de 50% van de dingen die ik uitkraam is onzin. Helaas kies jij altijd precies de verkeerde 50% uit om te geloven.

De laatste woorden zijn voor de mensen aan wie ik dit proefschrift opgedragen heb.

Ma, voor jou ben ik blijkbaar een open boek want je weet altijd precies welke 50% te geloven. Jammer dat jullie (Marja en jij) zo ver weg wonen en we elkaar niet zo vaak zien. Maar dat is mijn eigen schuld, moet ik maar niet in Deventer gaan wonen. Gelukkig bestaat er zoiet als de telefoon. Fijn dat je begrijpt dat ik niet altijd zin heb om in alle detail te vertellen wat ik die dag gedaan heb. Soms wil je namelijk gewoon je werk even vergeten. Bovendien doe ik meestal de hele dag saaie dingen. Ma: ik weet dat je het vaak moeilijk hebt bij mijlpalen, je had ze graag met papa gedeeld. Pas achteraf realiseer ik me wat voor verschrikkelijk sterke, goede moeder je was, en bent natuurlijk. Ik ben dan ook echt onwijs trots op je.

Kleine zusjes worden groot, kopen huizen en gaan trouwen. Toe maar. Marja, ik ben blij dat het goed me je gaat; zelfs een leuke baan komt binnenkort goed. Ik wil graag je getuige zijn op je bruiloft want Erik is een prima kerel. Maar eerst mag je mijn getuige zijn. Ik hoop dat ik het alleen af kan, maar ben blij dat je er als paranimf bij bent. Verzin maar vast een list om de aandacht af te leiden als ik onzin uitkraam.

En tot slot Ilse: bedankt, omdat je bent wie je bent en voor wat je voor me bent.

Arjan, Februari 2010

Die Welt ist so leer, wenn man nur Berge, Flüsse und Städte darin denkt, aber hie und da Iemand zu wissen, der mit uns übereinstimmt, mit dem wir auch stillschweigend fortleben, das macht uns dieses Erdenrund erst zu einem bewohnten Garten.

Johan Wolfgang von Goethe - Wilhelm Meister's Lehrjahre

Table of Contents

Summary

River dunes play an important role in many processes that take place on the riverbed. The dimensions of the dunes determine the hydraulic roughness of the river bed to a large extent. This roughness in turn, determines the flow depth and velocity for a given channel geometry and discharge. While the flow determines the sediment transport that formed the dunes in the fist place. In this way an interdependent system exists of flow characteristics, bed forms, bed roughness and sediment transport, and a change in one factor has consequences for each other factor.

In this thesis, the effect of a limited volume of mobile sediment on the river bed –a supply limitation– on this system is studied. The new insights into these effects are used to formulate new models and adapt existing model concepts to predict average dune height and length, hydraulic roughness and sediment transport rate.

The relationship between the availability of mobile sediment and dune geometry, bed roughness and sediment transport rate is studied in an extensive set of new flume experiments. In these flume experiments, 59 in total, the average layer thickness of mobile sediment is varied and the reactions of the bedforms, the roughness and sediment transport are measured.

Under supply-limited conditions, the bedform dimensions do not reach the equilibrium dimensions that are reached with an unlimited sediment supply (alluvial conditions). The limited volume of mobile sediment leads to smaller dunes and to flow exposure of the underlying immobile layer between the dunes. This causes a lower bedform roughness and, if the underlying layer is coarser, a higher grain roughness. Furthermore, the transport rate decreases compared to alluvial conditions.

The observed relationships between the dune dimensions and layer thickness collapse to one relationship for height and one for length if they are scaled with the alluvial dune height and length. This characteristic is used to formulate a function that extends the applicability of existing alluvial dune height and length predictors to the supply-limited regime.

The roughness variation due to supply limitation is partly caused by the variation in bedform dimensions and partly by the varying exposure of the usually coarser immobile sublayer. It appears that the decreasing bedform roughness with increasing supply limitation can be predicted with existing bedform roughness predictors if the predicted supply-limited bedform dimensions are used as input. The grain roughness varies with varying supply limitation because of the varying coverage and infilling of the coarser gravel layer with the finer mobile sediment that forms the bedforms. A model to predict the fractional coverage of

the immobile layer with bedforms is proposed. This model enables us to make a separation between the prediction of the grain roughness for the immobile layer and for the bedforms.

With a decreasing average layer thickness of the mobile sediment, a decreasing sand transport rate is observed for a constant flow velocity and water depth. This can be explained by I) a reducing bed shear stress due to decreasing bedform dimensions and II) a decreasing coverage of the bed with bedload sediment. A model concept for sediment transport under supply-limited conditions is presented that takes these processes into account. This transport model is shown to be able to reproduce the results from the lab experiments well.

The model concepts for bedform dimensions, roughness and sediment transport that are proposed in this study are first tested independently using the experimental data. Subsequently, the model concepts are combined into an integrated model that predicts the bedform height and length, the immobile layer exposure, the grain and bedform roughness and the sediment transport including the interactions between these parameters. This integrated model is tested by applying it to the experimental data sets. A comparison with an alluvial model shows that the new supply-limited method results in much better predictions.

Finally, the new transport model for supply-limited conditions is applied in the framework of a morphological modelling package (Delft3D). Three flume experiments with non-uniform initial conditions have been conducted to have a reference data set. In these experiments a sand wave propagated over an immobile gravel layer. The morphological development that was observed in these experiments is simulated with the morphological model. A comparison of the results of these experiments to morphological simulations using the new model concepts and existing model concepts shows that the new morphological model gives better predictions of the morphological development.

Samenvatting

Rivierduinen spelen een belangrijke rol in veel processen op de bodem van de rivier. De grootte van de duinen bepaalt grotendeels de hydraulische ruwheid van de rivierbodem. Deze ruwheid bepaalt op zijn beurt de waterstand en stroomsnelheid voor een gegeven dwarsdoorsnede, verhang en afvoer. Terwijl het sedimenttransport, dat de duinen vormde, weer door de stromingsomstandigheden wordt bepaald. Er is daardoor sprake van een systeem waarbij de stromingsomstandigheden, de bodemvormen, de ruwheid en het sedimenttransport onderling afhankelijk zijn. Een verandering in één van deze componenten beïnvloedt alle andere componenten.

In dit proefschrift wordt het effect van een beperkte beschikbaarheid van mobiel sediment (supply limitation) op dit systeem bestudeerd. De nieuwe inzichten in deze effecten worden gebruikt om nieuwe modellen voor het voorspellen van de gemiddelde duinhoogte en –lengte, de hydraulische ruwheid en het sedimenttransport te ontwikkelen en om bestaande modellen aan te passen.

De relatie tussen de beschikbaarheid van mobiel sediment en de duingeometrie, de bodemruwheid en het sedimenttransport wordt bestudeerd met de resultaten van een uitgebreide serie experimenten. In deze experimenten, 59 in totaal, wordt de laag met mobiel sediment in dikte gevarieerd waarbij de reacties van de bodemvormen, de ruwheid en het sedimenttransport wordt gemeten.

Bij een beperkte beschikbaarheid van mobiel sediment bereiken de duinen niet de afmetingen die ze bij een onbeperkte beschikbaarheid, de zogenaamde alluviale condities, bereiken. Het beperkte volume aan mobiel sediment leidt tot kleinere duinen waarbij de onderliggende vaste laag aan het oppervlak komt. Hierdoor is de door bodemvormen veroorzaakte ruwheid kleiner en, als de onderliggende laag grover is, de korrelruwheid groter. Verder neemt het sediment transport af.

De verschillende relaties tussen de duinafmetingen en de laagdikte van het mobiele sediment die voor verschillende stromingsomstandigheden zijn waargenomen, kunnen worden beschreven met één relatie wanneer de duinhoogte en lengte worden geschaald met de alluviale duinhoogte en lengte. Deze eigenschap wordt gebruikt om een functie te formuleren die de toepasbaarheid van bestaande modellen voor duinhoogte en lengte uitbreidt naar het ‘supply-limited’ regime.

De ruwheidsvariatie die wordt veroorzaakt door supply limitation wordt deels veroorzaakt door de variatie in bodemvormgrootte en deels doordat de meestal grovere onderlaag aan het

oppervlak komt. De afnemende ruwheid bij een afnemende bodemvormgrootte blijkt te kunnen worden voorspeld door bestaande modellen voor bodemvormruwheid te gebruiken met voorspelde supply-limited bodemvorm afmetingen als invoer. De korrelruwheid varieert door supply limitation doordat de bedekking en de opvulling van grovere onderlaag met het fijnere sediment dat de bodemvormen vormt varieert. Er wordt een model voorgesteld dat voorspelt wat het relatieve oppervlak van de bodem is dat met bodemvormen is bedekt. Dit stelt ons in staat om de korrelruwheid apart te voorspellen voor de grovere, niet-mobiele laag en het fijnere, mobiele sediment in de bodemvormen.

Bij een afnemende gemiddelde laagdikte van het mobiele sediment wordt een afnemend sedimenttransport geobserveerd bij gelijkblijvende stroomsnelheid en waterdiepte. Dit kan worden verklaard door I) een afnemende bodemschuifspanning door afnemende bodemvorm afmetingen en II) een afnemende bedekking van de bodem met transporteerbaar sediment. Er wordt een modelconcept voorgesteld voor sediment transport dat rekening houdt met deze processen en er wordt getoond dat dit model goed in staat is de resultaten van de stroomgootexperimenten terug te voorspellen.

De voorgestelde modelconcepten voor bodemvormafmetingen, ruwheid en transport worden in deze studie eerst onafhankelijk van elkaar getest met de experimentele data. Daarna worden ze gecombineerd tot een geïntegreerd model dat de bodemvormhoogte en -lengte, de bedekking van de vaste onderlaag, de korrel- en bodemvormruwheid en het sedimenttransport voorspelt, inclusief de onderlinge afhankelijkheden tussen deze parameters. Dit geïntegreerde model wordt getest door het toe te passen op de experimentele data. Een vergelijking met een alluviaal model toont aan het nieuwe supply-limited model veel betere voorspellingen oplevert.

Tot slot wordt het nieuwe transportmodel voor supply-limited omstandigheden toegepast binnen het raamwerk van een morfologisch modelleerpakket (Delft3D). Om vergelijkingsmateriaal te hebben zijn drie stroomgootexperimenten met niet uniforme initiële condities uitgevoerd. In deze experimenten bewoog een zandgolf zich voort over een niet mobiele grindlaag. De morfologische ontwikkeling die werd waargenomen tijdens deze experimenten wordt met het morfologische model gesimuleerd. Een vergelijking van de experimentele resultaten met de morfologische simulaties met de nieuwe modelconcepten en bestaande modelconcepten laat zien dat de nieuwe model concepten leiden tot betere voorspellingen van de morfologische ontwikkeling.

Chapter 1

Introduction

1.1 Context

People tend to live near coasts and rivers because rivers and seas provide an important means of transportation, a source of food and rivers are a major fresh water supply. The need to manage rivers -and coasts equally- is increasing because of the increasing number of people and increasing economic activity. We want to prevent flooding, as cheaply as possible, and still be able to use the river for navigation while also satisfying ecological demands. That is challenging.

River managers try to optimise the increasing demands on a river system using a number of tools: physical scale models, pilot projects, expert knowledge and numerical models for hydraulics and river bed morphology. This thesis contributes to the development of this last tool, the numerical river models for hydraulics and morphology. Due to the rapidly increasing computer capacity it is now feasible to create 2D process-based numerical models that can simulate the natural development of the river bed and the effects of interventions in the low water bed and flood planes. These morphological models have become important tools for the design of measures in rivers and channels (Having et al., 2009). However, the knowledge of the processes that are simulated is still incomplete. This leads to a reduced accuracy and increased uncertainty in the predictions. The goal of this study is to improve the understanding of some of these processes, more specifically "supply-limited sediment transport", and reduce the uncertainty by incorporating new process knowledge into models through physics based empirical model concepts. This provides river managers with a better tool to weigh different options for river management.

1.2 The role of roughness in morphological river models

In morphological models a feedback-loop is solved between the river bed morphology and the flow that causes the sediment transport and therefore changes in the bed morphology. The bed roughness plays an important role in these models at two places. Firstly, the bed roughness determines the water depth and flow velocity for a given discharge and channel morphology. Secondly, an accurate bed roughness is essential for sediment transport rate predictions. The transport rate is mainly dependent on the shear stress, which is directly related to the bed roughness.

It is still too calculation-intensive to solve energy losses from a detailed bed geometry for many kilometres, as is needed in river models. This is currently only feasible on a much smaller scale, with domains in the order of meters: the scale of experiments (e.g. Nabi, 2008;

Giri and Shimizu, 2006). Instead the bed roughness parameters relate bed characteristics to the depth-averaged flow velocity or time-averaged vertical flow profiles (Keulegan, 1938). Therefore the bed roughness prediction has an important role in morphological models.

Bed roughness prediction is traditionally separated into the prediction of roughness due to skin friction with the bed sediment and the net drag force caused by flow over bedforms (e.g. Yalin, 1964; Engelund and Hansen, 1967; Engelund, 1977). The sudden expansion behind bedforms causes a turbulent wake where energy is dissipated through internal friction. Existing (semi-) empirical models derived to predict the bed roughness therefore require the input of predicted bedform dimensions (e.g. Yalin, 1964; Engelund, 1977; Van Rijn, 1984; Van der Mark, 2009) or implicitly include the effect of bedform geometry (Engelund and Hansen, 1967). The split of bed roughness into a grain related part and a bedform related part is illustrated with a figure from Engelund and Hansen (1967) (Figure 1.1). This figure shows a gradually increasing grain shear stress (τ') with increasing velocity (V) and, especially if dunes are present, an additional form drag related shear stress (τ''). This illustrates that knowledge of the bed state and the bedform dimensions is important for roughness prediction.

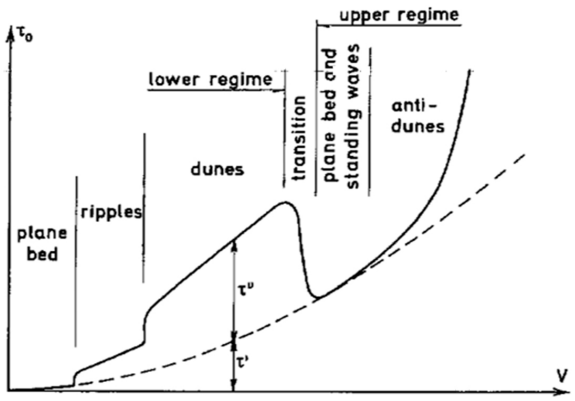

Figure 1.1: Explanatory figure from Engelund and Hansen (1967) that relates the boundary shear stress (τ_0) to the increasing flow velocity (V). The jumps in the bed shear stress are related to transitions in the bedform regime.

1.3 Bedform regimes

The type of bedform that occurs is in most studies related to a flow strength parameter and a grain size parameter (e.g. Simons and Richardson, 1966; Southard and Boguchwal, 1990; Van den Berg and Van Gelder, 1993). In the low flow regime ripples and dunes are distinguished. The low flow regime roughly occurs if the Froude number is much smaller than one (e.g. Engelund, 1982). Ripples are relatively low compared to the water depth and have a relatively large height to length ratio. Current ripples only develop if the grain size is less than 0.8 mm. Dunes on the other hand, have a relatively low height to length ratio and their dimensions are strongly related to the water depth (Van Rijn, 1984; Yalin, 1977). The dune length is several times the water depth and the dunes reach heights up to one third of the water depth. Ripples do not form and dunes are becoming washed out if the flow strength approaches the

transition towards the upper regime. In the upper flow regime, the dunes are washed out and a mobile flat bed or anti-dunes can develop. For the prediction of the dune and ripple dimensions empirical models are available as well (e.g. Gill, 1971; Fredsøe, 1982; Yalin, 1985; Van Rijn, 1984). However, these bed state predictors and bedform dimension predictors have been developed for the simplest case where the bed sediment is uniform, i.e. all grains have approximately the same dimensions, and the bedform formation is not limited by the amount of available sediment, the so-called alluvial conditions (Photo 1.1).

Photo 1.1: Dunes in an alluvial flume experiment. The flow direction was from top to bottom.

Bed state prediction for a non-uniform sediment, also known as a graded sediment, is more complex than for a uniform sediment. Whether a graded sediment exhibits more complex behaviour than a uniform sediment depends a.o. on whether the initiation of motion for the various size fractions is approximately equal. The critical shear stress for initiation of motion of each size fraction in unimodal grain size mixtures is approximately equal to that of the median grain size of the mixture (D_{50}). For bimodal sediments, the critical shear stress varies with grain size (Kleinhans and Van Rijn, 2002; Wilcock, 1993). This can, depending on the flow conditions, cause partial mobility of the bed sediment.

Different bedform types are reported due to partial mobility and grain size sorting compared to bedforms in uniform sediment. Bedform types that are typically associated with partial mobility conditions are: sand ribbons (McLelland et al., 1999; Kleinhans et al., 2002), barchanoid dunes, isolated dunes and sediment starved dunes (Kleinhans et al., 2002; Endo et al., 2005; Dreano et al., 2008; Carling et al., 2000), bedload sheets (Dietrich et al., 1989) and low-relief bedforms (Bennett and Bridge, 1995; Livesey et al., 1998).

Sand ribbons and bedload sheets are low relief bedforms. Sand ribbons are flow parallel sand ridges, where the sediment transport concentrates due to a feedback with lateral secondary currents (McLelland et al., 1999). Bedload sheets on the other hand are a grain size sorting related feature where a graded sediment moves as a very thin layer, a few grain diameters in thickness (Whiting et al., 1988). Isolated dunes, sediment starved dunes and barchanoid dunes are different types of supply-limited dunes. These bedforms are observed if the amount of transportable sediment on top of an immobile layer is limited. Isolated dunes are separated from other dunes by an area without mobile sediment. Sediment starved dunes are dunes that do not develop to the full-grown dimensions of alluvial dunes but remain smaller (Photo 1.3).

Barchanoid dunes are dunes with a specific morphology: they are flow transverse, crescent shaped dunes, with downstream pointing tips (Photo 1.2).

Photos 1.2 (l) and 1.3 (r): The left photo shows flow parallel sand ribbons in which small barchanoid bedforms have developed. This situation develops if little mobile sediment is present on the immobile bed. The right photo shows sediment-starved dunes. These dunes are supply limited rather than depth limited. Both photos come from data-set IV presented later in this thesis.

1.4 Supply limitation

The additional bed states that are possible in graded sediments can largely be attributed to the effect of supply-limitation (Dietrich et al., 1989; Kleinhans et al., 2002; Kuhnle et al., 2006; Dreano et al., 2008 and this thesis). If the coarsest part of the sediment mixture cannot be transported, a coarser immobile layer can develop through vertical sorting of grain size fractions (Blom et al., 2003; Wilcock and McArdell, 1997). This layer prevents entrainment of the underlying sediment and thus limits the availability of sediment for bedform formation to the volume present on top of the coarse layer. The availability of sediment is a primary control on the bedform development. A limited volume of bedload sediment leads either to smaller dimensions, the sediment starved bedforms (Tuijnder et al., 2009) or fewer isolated bedforms (Carling et al., 2000; Kleijwegt, 1992).

The author uses the terms isolation and sediment starvation to discern between two reactions of bedforms to a supply-limitation. For a certain sediment availability the dune height and the area where the immobile layer is exposed are related. This can be explained as follows. The sediment availability per dune is Λd; where Λ is the length between consecutive dunes and, d is the average sediment layer thickness (see Fig. 1.2). The length Λ is split into a length where the immobile layer is exposed ($p\Lambda$) and where it is covered by the dune ($(1\text{-}p)\Lambda$). The available sediment is present in the dune while no sediment is present where the immobile layer is

exposed. The weighted average of the sediment volume over the length Λ is therefore given by:

$$\Lambda d = (1-p)\Lambda^{1}/_{2}\Delta \qquad \text{(Eq. 1.1)}$$

Here it has been assumed that the dunes are triangular, with a height Δ. This means that the dune height and the exposed length between dunes are related for a certain sediment layer thickness (d = constant) through the following relation:

$$d = (1-p)^{1}/_{2}\Delta \qquad \text{(Eq. 1.2)}$$

Figure 1.2 illustrates two possible realisations of the distribution of bedforms over the immobile layer. The exposed area of the immobile layer is small if the bedforms remain small and the exposed area increases if the bedforms become larger. The increase of p as a reaction to supply-limitation is the isolation reaction of bedforms; the decrease of Δ is the sediment starvation reaction. In principle any combination of these reactions is possible. However, the bedforms that develop in supply-limited experiments are predominantly sediment starved (Kuhnle et al., 2006; Dreano et al., 2008; and this thesis). Since bedform dimension predictors for supply-limited conditions are not yet available, the relation between average layer thickness, immobile layer exposure and the dune shape and dimensions is not yet known. This relation is subject of study in this thesis.

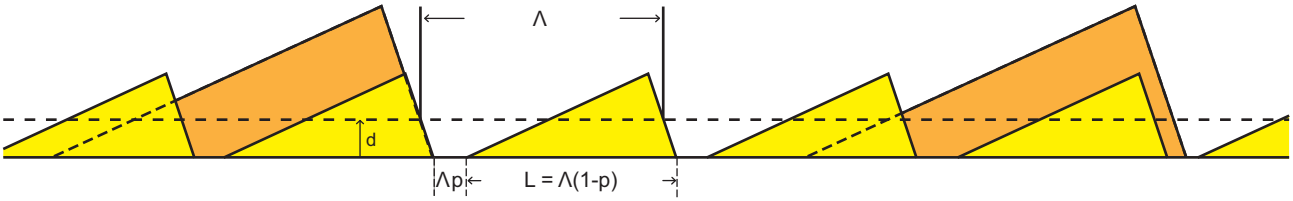

Figure 1.2: Two realisations of bedform height and space between bedforms for the same sediment availability (d). The large bedforms have bedform height Δ = 4 d and therefore p = 0.5. The small bedforms have a bedform height Δ = 2,22 d and therefore p = 0.1.

The severity of the supply limitation can be expressed using the ratio of the average layer thickness of bedload sediment (d) to the layer thickness required for alluvial conditions (d_0)(Struiksma, 1985) or the alluvial bedform height (Δ_0)(Tuijnder et al., 2009). Or it can be characterised with the ratio of the actual, supply-limited sediment transport rate (s) to the transport capacity (s_0) (Van der Zwaard, 1974 and Dietrich et al., 1989). This layer thickness ratio and transport rate ratio are related. The transport rate (s) depends on the availability of bedload sediment for transport (d). With decreasing sediment availability the transport rate also decreases. However, few model concepts are available that can describe this relation.

Model concepts for supply-limited conditions

Bed state prediction is relevant for roughness prediction since it is necessary to know what type of bedform will develop before the dimensions of the bedforms can be predicted. Some

model concepts for bed state prediction under partial transport and supply-limited conditions have been proposed (Kleinhans et al., 2002; Venditti et al., 2008). However, models for the prediction of the bedform dimensions under supply-limited conditions are required in order to predict roughness using form-drag models. Unfortunately, relatively few predictive model concepts for the supply-limited regime have been developed.

Carling (2000) published an extensive description of supply-limited dunes in the Rhine. The presence of isolated dunes on a bed composed of gravel is described. These dunes are often depth limited. A qualitative model concept is proposed to describe the dynamics of the bedform behaviour in relation to the passage of flood waves.

A study regarding ripple development under supply-limited conditions was conducted by Rauen et al. (2009). It is concluded that an empirical relaxation equation by Coleman et al. (2005), which describes development rate of ripples, can also be applied in the supply-limited regime. However, the supply-limited steady state needs to be specified and cannot be predicted.

To the best of the author's knowledge no model concepts are available for the prediction of dune dimensions under supply-limited conditions. However, a model concept for supply-limited bed roughness is available in which supply-limited bedform behaviour plays a central role. Van der Zwaard (1974) carried out a study on the relation between supply-limited transport of sand over a gravel layer and bed roughness. In flume experiments with a varying supply limitation it is shown that the bed roughness decreases with a decreasing sediment supply. It is also shown that a minimum roughness exists if the coarser immobile layer is partly covered with bedload sediment but too little sediment is present for significant bedform formation with the associated form drag generation. The coarse layer becomes more exposed if the sediment supply decreases further; this causes an increasing roughness. Van der Zwaard presents a model concept to predict this variation. Unfortunately, the observed behaviour of the supply-limited bedforms is reported scarcely. The independent parameter of choice is the ratio s/s_0, because a limited transport rate was imposed in the flume experiments. This parameter is inconvenient if one wishes to calculate the supply-limited transport rate from local conditions like sediment characteristics, transport layer thickness and hydraulical parameters.

For transport rate prediction the distinction between conditional and permanent supply limitation is relevant. A partial transport model may be applicable if the immobile layer is not very different in grain size from the bedload sediment. Since this situation can be considered a partial mobility problem, model concepts like the surface based transport model by Wilcock (2003) or Parker (1990) can be considered. However, prediction of the (surface based) grain size distribution that is input to the transport model may be problematic. Choices are required about what part of the immobile layer is part of the grain size distribution that is

relevant as input for the transport model. However, application of such concepts for an unconditional supply limitation, where the immobile layer is much coarser than the bedload sediment, is outside the validity regime of the concepts (Van der Scheer et al., 2001).

Struiksma (1999) presents an alternative approach for calculation of the supply-limited transport rate from local conditions. This concept considers the average layer thickness of the bedload sediment. It is assumed that the transport rate starts to decrease below a certain minimum average layer thickness for alluvial transport. It decreases until no mobile sediment is present and the transport rate reaches zero. Between the alluvial rate and zero an interpolation is assumed that is related to the transport layer thickness. The bed roughness is assumed to be constant and equal to the alluvial bed roughness. This method has been applied successfully for relatively short fixed layers in an otherwise alluvial environment (Struiksma, 1999).

1.5 Occurrence of supply-limited conditions

Graded sediments, more specifically sand-gravel mixtures, can be partially mobile and form a pavement that temporarily limits the sediment availability. If the shear stress increases, first a part of the immobile layer is entrained and pavement may reform at a lower level. With further increasing shear stresses, the pavement may be mobilized completely, which removes the supply limitation. This type of supply-limitation is conditional, in the sense that all present grain size fractions can become mobile and the supply limitation vanishes if the shear stress increases (e.g. Curran and Wilcock, 2005; Blom et al., 2003).

Armour layer development can cause a more permanent supply limitation. An armour layer is, depending on its development, still stable under moderate flood waves or even strong flood waves if the armour layer is fully developed (Koll and Dittrich, 2001). This means that bedload on an armour layer may remain supply-limited with increasing shear stress. Under strong floods armour layers still may break up, causing transport of all size fractions.

Obviously, supply limitation can also occur on permanently immobile layers. Due to dam building and discharge regulation, armour layers can develop that are permanently stable. Otherwise, permanent immobile layers that cause supply limitation can be formed by bedrock outcrops or can consist of clay or peat layers that are hard to erode. Supply-limited conditions develop if there is fine sediment input into such a river reach, for example from bank collapse, reservoir flushing or tributary channels.

The essential difference between the permanent and conditionally supply-limited appears with increasing shear stress. An increasing shear stress causes a decreasing supply limitation for the conditionally supply-limited conditions since a larger part or even the entire grain size distribution is mobilised. But on permanently immobile layers an increasing shear stress does not have to lead to a decreasing supply limitation. The supply-limitation becomes relatively

stronger with increasing shear stress if the bedform dimensions increase with increasing shear stress, as is generally the case in the lower flow conditions. In that case, more sediment is needed to reach alluvial dune dimensions and the relative sediment availability (d/Δ_0) decreases if the sediment volume remains constant. In nature on the other hand, a flood wave may introduce additional sediment into the system and reduce the supply limitation (Kleinhans et al., 2002).

The Netherlands are located in the Delta of three rivers, the Scheldt (de Schelde in Dutch), the Meuse (de Maas) and the Rhine (de Rijn), see Figure 1.3. Alluvial conditions can be expected to dominate in a delta area since the rivers are essentially flowing through their own deposits. This is the more general definition of an alluvial river. Nevertheless, supply limitation can be expected in different situations in the Netherlands. The upper reaches of the river Meuse (Border Meuse) have a gravel bed, with locally fine sand deposits underneath. Erosion of the gravel layer could cause transport of sand over a gravel bed. The first kilometres of the Pannerdens Canal and the River IJssel are relatively rich in gravel due to an uneven sediment distribution at the bifurcations (Frings, 2007). Development of immobile layers with supply-limited transport could be possible under low flow conditions at these locations. Bed level measurements show that the bed level amplitude at these locations is reduced (Sieben, 2008), possibly due to effects of supply-limitation.

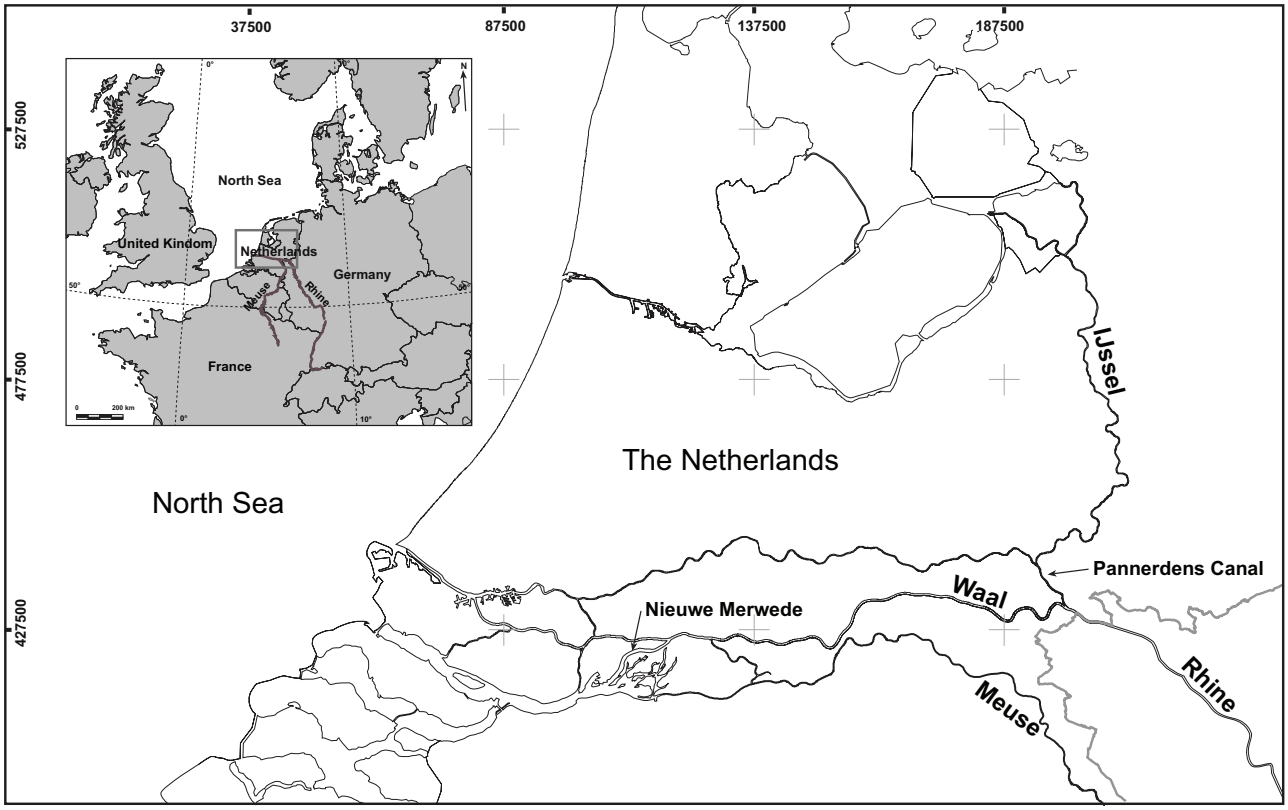

Figure 1.3, Map of the rivers in the Netherlands. The insert map shows the position of the map in North-West Europe. The grid that is shown is the Dutch RD-grid.

In the river Waal, immobile layers have been constructed to prevent the formation of deep outer bends. This causes an increased flow velocity in the inner bends and therefore a wider navigation channel (Sloff and Mosselman, 2006). The sediment transport over these immobile layers is supply-limited. The studies of Van der Zwaard (1974) into bed roughness of sediment transport over immobile layers and Struiksma (1985) into sediment transport prediction on immobile layers have been conducted in the context of the design of these measures. Finally, erosion resistant layers of peat are present in the river Nieuwe Merwede. Here supply-limited sediment transport occurs over the peat layers.

1.6 Goals, objectives and research questions

Problem formulation

To summarise the above it can be said that most empirical models for bedform dimensions, roughness and sediment transport rate predictions are not valid in the supply-limited regime. Few model concepts explicitly take the supply limitation into account. Yet supply limitation has a large impact on processes and ignoring it generally leads to overprediction of bedform dimensions, roughness and sediment transport. This makes morphological modelling of rivers where supply-limited conditions occur uncertain.

Focus of the present research

In this thesis, the focus is on the lower-flow regime as it occurs in the lower to middle reaches of many rivers among which the Dutch rivers. Sand constitutes a large part of the bed sediment in the lower reaches of most rivers, due to longitudinal sorting (Paola et al., 1992; Frings, 2007). This combination of lower regime conditions and sand is favourable for dune formation under alluvial conditions. Because dunes can generate considerable form-drag, the influence of supply limitation on bedform dimensions in the dune regime will be studied.

Sand-gravel mixtures have been studied because these are most relevant for the conditions in the lower to middle reaches of rivers. The results are applicable to permanent as well as conditionally supply-limited cases where a sand-gravel mixture forms a pavement with transport of the finest fractions on top. Furthermore, the study focuses on supply-limited bedload transport in conditions where supply-limited bedforms migrate over an immobile layer such as pavements and armour layers.

The study is not focussed on the more upstream river reaches, especially in mountainous areas, where the river bed generally becomes much coarser and where at the same time the bed slopes usually are higher. Grain size ratios of 100-1000 between the transported and immobile sediment are typical in those environments and the transport through the void space of the immobile layer and suspended transport over it become important processes (Grams, 2006). This regime is excluded from the present study.

1.7 Research objectives and questions

The main research objective is to increase the present understanding of morphological processes of river beds in supply-limited conditions. The limited bedform development due to supply limitation is important for the bed roughness and shear stress prediction and therefore for the transport rate prediction and the morphological development. Therefore research questions have been formulated for these subjects:

Prediction of dimensions of supply-limited dunes:

I. What is the influence of the volume of bedload sediment as present on top of an immobile layer on the bedform characteristics in general, and particularly on the average bedform dimensions?

II. How can the bedform dimensions be predicted under supply-limited conditions?

Roughness prediction:

III. What is the effect of variation in supply-limitation on the bedform roughness and the grain roughness?

IV. In what way can the roughness prediction for supply-limited conditions be improved?

Transport rate and morphological development:

V. How can the sediment transport be calculated in supply-limited situations from the local flow and sediment conditions on top of an immobile layer?

VI. How can morphological simulations be improved in case of supply-limited sediment transport?

1.8 Research strategy and thesis outline

The basis for the answers to the research questions and the development of the model concepts in this thesis lies in several different series of flume experiments that have been carried out to study varying degrees of supply limitation under different boundary conditions. The setup and conditions of the experimental sets are described in Chapter 2. The results of the experiments are discussed in the subsequent chapters, where they are also used for model development and model testing.

In Chapter 3 the experimental data is analysed to find a relation between the bedform characteristics and the degree of supply limitation. The relation between the bedform length and height and the average sand layer thickness on top of the immobile layer is explored in detail. Subsequently, a model concept is presented that extends the validity of alluvial dune height and length predictors into the supply-limited regime.

In Chapter 4, first the roughness variation as observed in the experiments is presented and related to the supply-limitation. Subsequently, a model for bed roughness under supply-limited conditions is formulated. The bedform dimension model that was presented in Chapter 3 is combined with a bedform roughness predictor to predict the variation in bedform roughness with supply-limitation. The coverage of the immobile gravel layer with mobile sand plays an important role in determining the grain roughness. Therefore, a model to predict the fractional coverage of the immobile layer is introduced. Furthermore, a grain roughness model is formulated. The combined bedform roughness and grain roughness models are tested using the experimental data. Finally, an integrated bed roughness model, that uses the previously introduced sub-models for bedform dimensions, immobile layer coverage and bed roughness is presented and is also tested using the experimental data.

In Chapter 5 the experimental results regarding the sediment transport rate are presented and the relation between the transport rate and the supply-limitation is explored. Next, it is shown that the decreasing sediment transport rate with decreasing sediment supply can be explained by the effect of reducing shear stress and reducing coverage of the bed with bedload sediment. A model concept is presented that takes the sediment availability into account to calculate the supply-limited sediment transport. This model uses the sub-models for bedform dimensions, immobile layer coverage and bed roughness from Chapters 3 and 4. This model is first tested using the data from equilibrium experiments. Subsequently, the model is tested in the context of a morphological model. A set of new morphological (non-equilibrium) experiments with supply-limited transport of sand over a gravel layer is presented and the observed morphological development is compared to the simulated morphological development using the new model concepts for supply-limited transport, bed roughness and bedform dimensions.

Chapter 6 is the closing chapter; here the overall results are discussed and conclusions and recommendations for further research are summarised.

Chapter 2

Experiments with Supply-Limited Conditions

The setup, procedures and programme of the experimental work are described in this chapter. Furthermore some basic average results for the experiments are presented. Interpretation of the results is done in the following chapters. All experiments have been conducted in the hydraulics laboratory of the Leichtweiss Institute (LWI) of the Technical University of Braunschweig in Germany. The experiments of Data Set I (DS-I), DS-II and DS-IV have been conducted by the author. The experiments of DS-III and IV have been conducted by Matthieu Spekkers, who also assisted with the experiments of DS-I.

2.1 Data set I: Fixed layer experiments small flume

The experiments of DS-I have been conducted as a pre-study for the experiments of DS-II. The goal of these experiments was to study the effects of increasing sand availability on top of a gravel layer on the transport rate, the bedform dimensions and the bed roughness. To study this, a gravel layer was installed in a flume and the amount of sand on top of the gravel layer was increased stepwise between experiments. The experiments have been conducted in a small flume with simple equipment since these experiments are a pre-study.

Setup

The dimensions of the flume that was used are 7 m x 0.3 m. The gravel layer was installed with a slope because we wanted to realize an equilibrium flow and the flume was not tiltable. The sand was distributed evenly over the length of the flume before an experiment. During a run, the sediment was recirculated by hand. At the downstream end of the flume a sand trap was present (See photo 2.1), which was emptied regularly using a siphon. The sand discharge was determined by weighing the water sediment mixture and determining its volume and the time between measurements. The sand was fed back to the upstream end of the flume gradually by hand. The water discharge was measured using an inductive flow measurement device. The water level varied between experiments due to the different roughness that developed since uniform flow was maintained.

During the experiments the water levels along the flume were measured using a 'Wasser Harfe'. This setup consists of static pressure measurement tubes, distributed along the flume, which are connected to glass cylinders in which the water level is measured using a point gauge. The small holes in the measurement tubes react slowly to the water level variations; this makes an accurate observation of the average water level possible.

The bed level was measured with a laser distance meter that was mounted on a measurement carriage. Unfortunately, the bed level meter could not be used submerged during the experiment. Therefore the bed level was measured after carefully draining the flume.

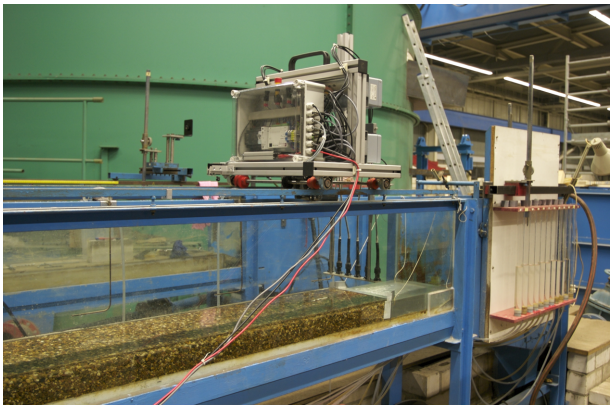

Photo 2.1: Downstream section of the small flume. On top of the flume the measurement carriage for the bed level profiles is visible. On the right hand side the glass tubes for the water level measurements can be seen. The gray box in the flume is the sand trap.

Experimental programme

Between the experiments only the sand layer thickness was varied. The average layer thickness of the sand was increased from 0.6 cm to 2.7 cm in 6 steps. The layer thickness was determined by taking an average value of the difference of the laser bed level scans of the gravel layer before the experiments and after an experiment. The layer thickness is reported in Table 2.1 for each experiment.

The discharge and the sediments characteristics were the same for all experiments of DS-I. The discharge (Q) was 20 l/s, which resulted in a flow velocity (u) of approximately 0.52 m/s. The gravel used for DS-I was a bit coarser than the gravel used in the other data sets. The gravel between the 11.2 and 16 mm sieves has been used so the average grain size was approximately 13.6 mm. The sand that was used is a well-sorted quartz sand with D_{50} = 0.8 mm and is the same sand as used in the other data sets. A grain size distribution is shown in section 2.2.

Procedure

Before an experiment the sand layer was distributed evenly over the length of the flume. The flume was slowly filled with water to a level higher than used in the experiment. Next, the required discharge was established and the downstream weir was gradually lowered to reduce the water level to approximately the required water level. The time registration of the sediment transport recirculation was started as soon as the sediment transport started. After a few minutes (±5 min) the water levels were measured. The water level data were entered into a laptop to calculate the slope and display the water level, bed level and water depth profiles. If required, the weir was adjusted to create a uniform flow. This was repeated regularly. The sand trap was emptied using a siphon and the time of emptying was registered. The emptying interval depended on the transport rate; it was usually emptied between two bedforms entering the trap. This procedure was continued for a couple of hours (2-3 h). The

bedform dimensions reached their maximum within approximately 15 minutes. Therefore, this was sufficient to get a good measurement of the bedform dimensions, the roughness and the transport rate. The laser bed level meter was used to make bed level profiles. Two profiles were made, one approximately in the middle of the experiment and one at the end. The flume was slowly drained in order to make a laser scan for the bed level measurements. After the first bed level profile the flume was slowly filled again and the experimental procedure was resumed. Finally, the bed level surface was scanned with a laser sensor to capture the 3D bedform morphology after each experiment.

Results

Table 2.1 shows the average values of the key experimental parameters over the equilibrium period. Between the experiments the average sand layer thickness on top of the gravel layer (d) was increased gradually. The value of d reported here is the averaged difference between the measured gravel layer level and the bed level after the experiment. The water depth (h) increased slightly, going from a supply-limited to an alluvial situation, due to an increase in form drag.

Exp Nr	d [m]	Q [m^3/s]	h [m]	I_e [m]	τ_b [m]	Δ [m]	Λ [m]	s [g/s]
1	0.006	0.020	0.12	0.0019	1.64	0.011	0.42	4.7
2	0.010	0.020	0.12	0.0021	1.81	0.019	0.54	7.1
3	0.013	0.020	0.13	0.0022	2.06	0.021	0.54	6.1
4	0.015	0.020	0.13	0.0022	2.21	0.025	0.63	6.1
5	0.018	0.020	0.13	0.0018	1.71	0.026	0.62	6.2
6	0.022	0.020	0.13	0.0023	2.37	0.029	0.66	6.3
7	0.027	0.020	0.13	0.0024	2.42	0.032	1.08	7.4

Table 2.1: Conditions and average results of DS-I. The sediment discharge (s) is the sediment transport rate for the entire flume width.

The total boundary shear stress has been calculated from the slope of the energy level (I_e), subsequently the bed shear stress (τ_b) has been calculated using the method of Vanoni and Brooks (1957) as explained in Appendix I. For this flume the sidewalls are not assumed to be hydraulically smooth because of the rough seams between the glass windows and the presence of the thin water level tubes in the flow. Instead is has been assumed that the glass wall with the tubes can be assigned an equivalent roughness height $k_{s,w}$. A special set of experiments with an immobile gravel bed and a water depth variation between 5 and 20 cm has been conducted to estimate the wall roughness. The procedure to estimate the $k_{s,w}$ value is described in Spekkers (2007). The wall roughness correction procedure is also explained in Appendix I.

The bedform height (Δ) and length (Λ) have been determined using the procedure described in Van der Mark and Blom (2007). This method is explained in Appendix II. The bed level profiles with the bedforms recognized using this procedure have been checked by hand. Sometimes gravel particles are recognized as dunes, if the dunes are small and a gravel layer

is present. Furthermore, small bumps near the average bed level were sometimes recognized as dunes, this was corrected by hand for this data set, whereas for the other experiments the filter window was adapted (See Appendix II).

2.2 Data set II: Fixed layer experiments large flume

Just like the pre-study experiments of DS-I, the goal of these experiments is to study the effects of increasing sand availability on top of a gravel layer on the transport rate of the sand, the bedform dimensions and the bed roughness. However, a much larger and automated experimental setup was used to carry out the experiments. The main idea behind the experiments is the same: a gravel layer is installed in the flume and the volume of sand that is transported on top is increased stepwise.

Experimental Setup

The experiments were conducted in a sediment recirculation flume (See Figure 2.1). This flume had a width of 2 m and an approximate length of 30 m. The width was reduced to 1 m for the experiments. A constant head tank above the flume supplied the flume with water. The discharge in the supply pipe was measured with an IDM, an Inductive Discharge Measurement device. The accuracy of this device is approximately 1% of the measured discharge according to its specifications. A test of the IDM with a V-shaped weir gave approximately the same result. At the end of the flume a funnel caught the sediment discharge. The sediment was pumped back to the upstream end with a small water discharge (±20 l/s) using a recirculation pump. In the return pipe another IDM measured the discharge.

In the sediment return pipe a turbidity sensor was present as well. Near the downstream weir a second turbidity sensor measured the background turbidity of the water. The difference between the two sensors gave the turbidity caused by the sand in the return pipe. A calibration curve was made to calculate the sediment concentration from this turbidity difference. The sediment transport was calculated by multiplying the concentration and the discharge.

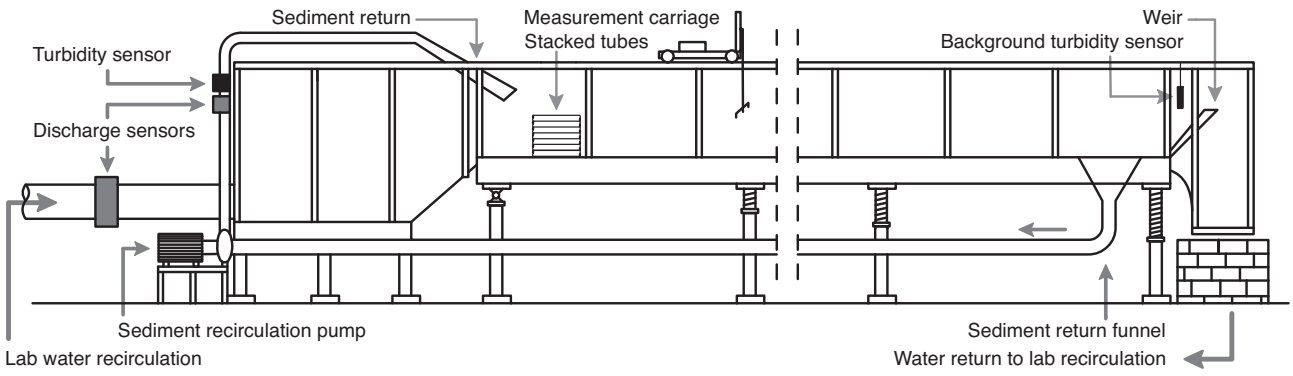

Figure 2.1: Side view of the used flume setup. The supply of water came from a constant-head tank ca 5 m above the level of the flume. The flume is supported by jacks that allow the flume to be tilted to realize an equilibrium flow.

At the upstream end of the flume a sediment feeder distributed the sediment water mixture over the width of the flume. Directly downstream, the water flowed through stacked tubes (see Photo 2.3) that break down large-scale turbulence from the water inflow and the sediment return.

Over a length of 17.45 m the bed and water level were measured continuously using echo sensors that were mounted on a measurement carriage. The measurements were taken from x = 6.3 to x = 23.75, where x = 0 is located at the upstream end of the flume, at the location of the pivoting point. The carriage measured the bed level at three parallel transects; at y = 0.165, 0.500 and 0.835 m, where y = 0 is the left sidewall when looking downstream. The flume bottom is z = 0. The water level was measured approximately in the centre of the flow. The accuracy of the bed level measurements was tested by repeatedly measuring a fixed profile. The vertical standard deviation was less than 1 mm, while the horizontal standard deviation was approximately 3 mm. In the horizontal direction the accuracy was limited by the area of the measurement surface of the echo sounders. The radius of the measurement surface was a few centimetres. Therefore, the ultrasound measurements are suitable for measuring the large-scale features of the dunes, but the grain scale cannot be resolved. The accuracy of the sensor for the water level is comparable to the bed level sensors. The measurement carriage pulled itself along a toothed belt with a stepping motor. The speed of the carriage was constant. A sensor on the carriage measured the presence of markers at precisely known locations along the flume. The position of the carriage was interpolated between these markers. This positional accuracy that was achieved this way is in the order of a 1-2 mm. It took about three minutes to measure a bed and water level profile.

The signals from all sensors were sampled by an A/D converter at 100 Hz. A PC stored the average over 1 s for the turbidity sensors and the IDMs. All data from the bed and water level sensors were stored. Every 3 minutes the latest data were processed in order to monitor the development in the flume. The flume slope and downstream weir were manually adjusted to create uniform flow. Once equilibrium conditions were established the setup could continue measuring automatically without further adjustments. This way long uninterrupted measurements were possible.

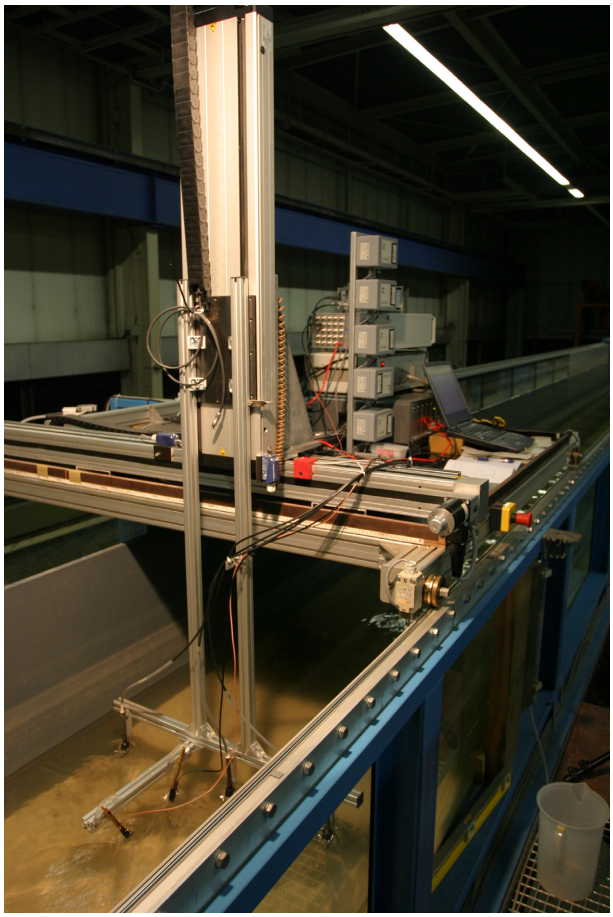

Photo 2.3 (above): Stacked tubes to reduce large scale turbulence from the water inlet tank and sediment recirculation.

Photo 2.2 (left): The measurement carriage for the large flume

The measurement carriage was also equipped with the laser distance sensor. This sensor has a much smaller measurement surface, 3 x 0.2 mm and was used to make 3D bed surface scans. A control program for the carriage positioned the laser to take measurements of an area of 5 m x 0.8 m in the measurements section. This procedure is very time consuming: depending on the bedform height a measurement took approximately 7 or 14 hours. Therefore these measurements were only taken after each experiment of Series 1 (see below).

Experimental programme

The experimental programme consisted of 5 series of experiments. Within each series the sand layer thickness was varied. Between the series the hydraulic conditions were varied; see Table 2.2. Series 1 was the central series, with a water depth of 0.20 m and flow velocity of 0.52 m/s. In the other series either the water depth or the flow velocity was varied. Series 4 should have been executed with a flow velocity of 0.67 m/s. But it appeared that the maximum shear stress on the immobile layer increased with increasing dune height. The immobile layer started to become mobile and therefore the experiments were continued with a lower flow velocity. Because of time constraints this series was not continued until alluvial conditions were reached.

Apart from these series a few alluvial experiments were conducted before the supply-limited experiments were started. These were done to test the setup and gain some experience. These experiments were conducted with a water depth of 0.25 m and are reported in Table 2.4 as

Series 6. The experimental data from these tests have been used to do calibrations of alluvial models for sediment transport and dune height in the following chapters.

For all experiments in DS-II the same sediments have been used. The grain size distributions are shown in Figure 2.2. The sand fraction consists of quartz; the grains are well rounded and have a high sphericity. The density is 2650 kg/m^3. The gravel is sub-rounded to rounded with a variable sphericity. The gravel has a mixed mineral composition which has not been determined in detail. The density is probably below 2650 kg/m^3.

Series	h [m]	u [m/s]
1	0.20	0.52
2	0.30	0.52
3	0.15	0.52
4	0.20	0.58-0.67
5	0.20	0.46

Table 2.2: Hydraulic conditions for the series of DS-II.

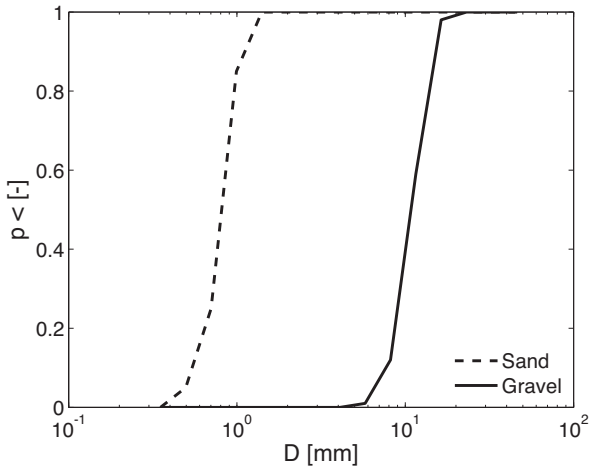

Figure 2.2 (left): Grain size distributions of the used sediments. p is the fraction of the distribution that is smaller than D.

	D_{10}	D_{50}	D_{90}	σ_g
Sand	0.6	0.8	1.2	1.3
Gravel	7.8	10.9	15.4	1.3

Table 2.3: Characteristics of the used grain size distributions. The columns D_{10}, D_{50} and D_{90} indicate the grain size (mm) where respectively 10, 50 and 90% of the sediment is finer. The column σ_g shows the geometric standard deviation, the definition of σ_g is given in Appendix 3.

Procedure

A gravel layer of constant thickness (± 4 cm) was installed before the experiments and stayed in place during all experiments. The sand was distributed evenly over the gravel layer along the length of the flume. The flume slope was set to a bed slope that was close to the bed slope required for equilibrium flow. The downstream weir was set to a higher setting than required for equilibrium flow. The flume was slowly filled from both the downstream side and upstream side. The experiment was started once the flume was filled. The required discharge was set and the recirculation pumped was started. Next, the weir was lowered and the measurement program was started. From that moment, every three minutes a water level profile and bed level profile were available to estimate whether adjustments to the weir level and bed slope were necessary to establish equilibrium flow. Usually equilibrium flow was established after a few corrections of the slope and weir. The development of the process was

checked regularly until it was clear that a steady state had been measured for a while. At the end of the experiment, the discharge was stopped and the flume was drained slowly in order not to disturb the bedforms. Finally, the program for the bed surface scan with the laser was started.

Results

The results of these experiments, in terms of averages of the parameters over the equilibrium period, are reported in Table 2.4. The total shear stress has been calculated from the gradient of the energy level over the measurement section (I_e). The bed shear stress (τ_b) has been calculated with the wall roughness correction method proposed by Vanoni and Brooks (1957). Once the bed shear stress has been calculated, the bed roughness height ($k_{s,b}$) can also be calculated from the Chézy equation and the White-Colebrook equation. These procedures for wall roughness and bed roughness calculation are explained in Appendix I. The dune dimensions have again been determined using the bedform tool by Van der Mark and Blom (2007) as explained in Appendix III. The alluvial bedform dimensions (Δ_0 and Λ_0) are the asymptotic values to which the dune dimensions develop with increasing sand layer thickness (d) under alluvial conditions as described in Chapter 3. The sand layer thickness that is reported here is the average difference between the immobile layer level and the bed level after the experiment as measured with the ultra sound sensors. The sediment transport (s) has been calculated from the turbidity and discharge measurements. The dune celerity (c) is reported since it provides a validation opportunity for the sediment transport. The dune celerity has been determined by visually estimating the average dune migration speed in dune migration graphs. The procedure is explained in Section 5.2. The last two columns report the estimated coverage of the immobile layer with dunes. The column $p_{z<ztil}$ reports the fraction of the bed level measured below the level of the top of the immobile layer (z_{til}) using the ultra sound sensors. The top of the gravel layer is assumed to be at a level $z_{til} = z_{cl} + \frac{1}{2}D_{cl}$, where z_{cl} is the average level of the gravel layer and D_{cl} is the gravel layer grain size. The column p_{cl} reports the fraction of the bed where the gravel layer is exposed. This was visually estimated using the bed surface scans of Series 1.

Exp Nr	d [m]	Q [m^3/s]	h [m]	I_e [-]	τ_b [N/m^2]	$k_{s,b}$ [m]	Δ [m]	Λ [m]	Δ_0 [m]	Λ_0 [m]	s [g/s]	c [m/h]	$p_{z<ztil}$ [m]	p_{cl} [-]
1-1	0.000	0.074	0.20	0.0007	1.25	0.007	0.000	0.00	0.080	1.41	0.0	0.0	0.92	1.00
1-2	0.003	0.105	0.20	0.0008	1.33	0.008	0.006	0.26	0.080	1.41	4.3	2.5	0.77	0.50
1-3	0.003	0.104	0.20	0.0008	1.38	0.008	0.006	0.29	0.080	1.41	3.8	2.5	0.71	0.50
1-4	0.011	0.104	0.20	0.0008	1.35	0.008	0.024	0.64	0.080	1.41	11.6	2.3	0.28	0.33
1-5	0.012	0.106	0.20	0.0008	1.41	0.008	0.023	0.65	0.080	1.41	7.9	2.3	0.27	0.33
1-6	0.020	0.105	0.20	0.0012	2.06	0.011	0.040	0.84	0.080	1.41	15.0	2.3	0.21	0.20
1-7	0.041	0.104	0.20	0.0016	2.87	0.013	0.057	1.13	0.080	1.41	21.2	1.9	0.06	0.10
1-8	0.068	0.104	0.20	0.0018	3.37	0.014	0.076	1.34	0.080	1.41	26.6	1.9	0.02	0.00
1-9	0.097	0.104	0.20	0.0019	3.32	0.015	0.077	1.46	0.080	1.41	25.5	1.9	0.00	0.00
1-10 (a)	0.161	0.105	0.20	0.0022	3.97	0.016	0.077	1.44	0.080	1.41	31.8	1.9	0	0.00
2-1	0.000	0.151	0.30	0.0008	2.17	0.007	0.000	0.00	0.091	1.49	0.0	0.0	0.96	
2-2	0.003	0.156	0.30	0.0006	1.36	0.006	0.007	0.34	0.091	1.49	3.9	2.5	0.78	
2-3	0.011	0.157	0.30	0.0004	0.90	0.004	0.024	0.74	0.091	1.49	6.0	1.3	0.31	
2-4	0.019	0.156	0.30	0.0007	1.66	0.007	0.042	0.90	0.091	1.49	9.9	1.2	0.27	
2-5	0.039	0.153	0.30	0.0008	2.06	0.007	0.065	1.23	0.091	1.49	13.6	0.9	0.12	
2-6	0.067	0.157	0.29	0.0012	3.18	0.010	0.080	1.33	0.091	1.49	20.1	1.4	0.03	
2-7	0.095	0.157	0.30	0.0009	2.24	0.008	0.086	1.64	0.091	1.49	16.5	1.0	0.01	
3-1	0.004	0.079	0.15	0.0013	1.74	0.012	0.008	0.34	0.067	1.31	4.6	5.0	0.58	
3-2	0.011	0.079	0.15	0.0012	1.56	0.012	0.022	0.64	0.067	1.31	10.8	3.0	0.24	
3-3	0.021	0.077	0.15	0.0014	1.94	0.013	0.035	0.84	0.067	1.31	15.1	2.0	0.14	
3-4	0.037	0.078	0.16	0.0014	1.95	0.013	0.048	1.06	0.067	1.31	18.1	2.0	0.04	
3-5	0.067	0.079	0.15	0.0020	2.88	0.017	0.059	1.26	0.067	1.31	15.2	2.0	0.01	
3-6 (a)	0.160	0.080	0.15	0.0026	3.70	0.019	0.068	1.37	0.067	1.31	32.1	2.7	0	
4-1	0.004	0.135	0.20	0.0012	2.07	0.011	0.007	0.29	0.081	1.06	17.9	9.0	0.65	
4-2	0.012	0.135	0.20	0.0017	3.01	0.014	0.028	0.69	0.081	1.06	35.0	8.0	0.31	
4-3	0.021	0.116	0.20	0.0016	2.82	0.013	0.042	0.86	0.081	1.06	26.2	3.5	0.21	
4-4	0.039	0.116	0.20	0.0021	3.91	0.015	0.059	1.03	0.081	1.06	38.2	3.5	0.08	
5-1	0.003	0.093	0.20	0.0006	1.05	0.006	0.007	0.34	0.069	1.32	2.1	1.1	0.69	
5-2	0.004	0.093	0.20	0.0007	1.12	0.007	0.006	0.32	0.069	1.32	1.5	1.0	0.62	
5-3	0.009	0.092	0.20	0.0006	0.92	0.006	0.016	0.76	0.069	1.32	3.2	1.0	0.24	
5-4	0.019	0.093	0.20	0.0006	1.05	0.006	0.033	0.95	0.069	1.32	6.0	0.9	0.15	
5-5	0.038	0.093	0.20	0.0008	1.43	0.008	0.052	1.20	0.069	1.32	10.0	0.8	0.06	
5-6	0.065	0.093	0.20	0.0012	2.24	0.011	0.067	1.37	0.069	1.32	11.1	0.7	0.01	
5-7 (a)	0.160	0.094	0.20	0.0015	2.84	0.013	0.070	1.39	0.069	1.32	14.5	1.0	0	
6-1 (a)	0.160	0.130	0.25	0.0017	3.87	0.012	0.083	1.47			25.2	1.6	0	
6-2 (a)	0.157	0.135	0.25	0.0020	4.71	0.013	0.084	1.46				1.9	0	
6-3 (a)	0.160	0.150	0.26	0.0022	5.21	0.014	0.095	1.49			45.2	2.5	0	

Table 2.4: Conditions and average results for the experiments of DS-II. The sediment discharge (s) is the sediment transport rate for the entire flume width (1 m). The (a) in the first column signifies an alluvial experiment.

2.3 Data set III: Vertical sorting experiment small flume

The vertical sorting experiments have one important difference with the previously described experiments: the experiments have been conducted with a mixture of sand and gravel in the flume, instead of preinstalled layers of sand and gravel. The conditions were such that gravel in large concentrations was immobile, but in low concentrations some gravel was mobile because the sand matrix was mobile. Some gravel was initially mobile, until a coarser gravel layer had formed due to vertical sorting. The goal of these experiments is to study the vertical sorting that develops if this mixture is transported. More specifically, these experiments have been conducted to provide insight in the relation between the initial gravel content of the mixture and the thickness and concentration of the gravel layer and the average sand layer thickness on top of the immobile gravel layer.

The study of the vertical sorting falls outside the scope of this thesis. These results will be published elsewhere. However, an immobile layer had developed in the final supply-limited equilibrium conditions, with –depending on the initial gravel content– a sand layer of limited thickness on top. The data collected in these final situations are used to validate the model concepts for bedform dimensions prediction and bed roughness prediction in Chapter 4 of this thesis.

Setup

These experiments are a pre-study to the experiments of DS-IV and were conducted in a small non-tiltable flume like the experiments of DS-I. The flume is similar to the flume used for DS-I but it is 1 m shorter (0.3 x 6 m) and it is equipped with a sediment recirculation system. This made long flume runs possible, which was required to reach an equilibrium sorting profile. The discharge through the return pipe was 4.7 l/s, which was measured using an IDM. The main water discharge came from a constant head tank several meters higher. This discharge was determined by measuring the water level in the stilling tank with a sharp crested rectangular weir. The discharge was calculated from the water level difference between the water in the tank and the crest of the weir with a weir formula. The discharge was regulated with a valve until the total discharge, including the sediment recirculation, was 29 l/s.

The bed and water level were measured with the same sensors as were used for DS-II. These sensors were mounted on the measurement carriage that was also used for DS-I. However, the controlling electronics did not allow a full automation of the measurements. Therefore the carriage was started regularly by hand.

Procedure

Before an experiment, the sand and gravel were thoroughly mixed and installed in the flume with a slope of 0.001. See Figure 2.3 and Table 2.5 for information on the used grain size distributions. Sediment storages in the sediment recirculation were filled with some sand to prevent erosion or sedimentation just after the start of the experiment. To start an

experiment, the flume was slowly filled with water. Subsequently, the discharge was set to 29 l/s, the recirculation was started and the weir was lowered to give a quasi-equilibrium flow. The water level was observed with the measurement carriage every 5 – 15 minutes. These observations were used to keep the water level slope at 0.001 and the depth 0.18 m. Stationary conditions developed quickly in the experiment without gravel. This experiment lasted for approximately 7 hours. Stationary conditions developed much more slowly in the other experiments with gravel because the vertical sorting had to develop. First, observations were taken for 5-7 hours in the experiments with gravel. Then, the experiments were left to run unattended for approximately 15 hours. Finally, observations of the final equilibrium were taken for a few more hours. The bed was photographed and the vertical sorting was measured after the experiments. Furthermore, the vertical sorting was measured by excavating the bed in layers of 10 – 15 mm at six places along the flume and by taking wax cores at three locations.

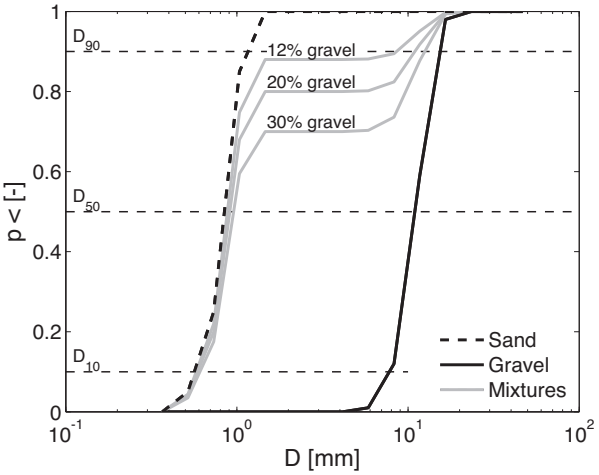

Figure 2.3: The sand and gravel have been mixed to 3 new grain size distributions with 12, 20 and 30% gravel.

	% Gravel	D_{10}	D_{50}	D_{90}	σ_g
Sand	0	0.6	0.8	1.2	1.3
Gravel	100	7.8	10.9	15.4	1.3
Mixtures	12	0.6	0.9	8.5	2.4
	20	0.6	0.9	11	2.9
	30	0.6	1.0	12	3.4

Table 2.5: Characteristics of the used grain size distributions.

Results

The averages of the key parameters of these experiments are reported in Table 2.6. The bed shear stress and bedform dimensions were calculated the same way as for DS-I.

The sand layer thickness (d) was not an imposed variable in these experiments. The varying gravel concentration led to differences in the average transport layer thickness that developed. In the previously described experiments, this layer thickness could be determined by subtracting the average level of the gravel layer from the average bed level. This time, the gravel layer level could not be measured before the experiments. Instead, the level of the immobile layer had to be determined from the bed level profiles of each experiment. The gravel layer level was determined by finding the lowest bed level that was observed in the bed level profiles of each experiment. This only works if the bed level measurements are done often enough to capture the occurrence of the deepest troughs everywhere. This has been

tested after the experiments by stopping the sediment feed and eroding the bed until the sediment transport stopped. It appeared that the gravel layer level did not decrease. This confirmed the validity of the immobile layer level estimations from the deepest dune troughs. Only in the upstream part of the flume, near the sediment feed, the gravel layer level decreased further. This was outside the observation area.

Exp Nr	% Gravel	Q [m³/s]	h [m]	I_e [-]	τ_b [N/m²]	d [m]	Δ [m]	Λ [m]
1	30	0.029	0.18	0.0014	1.51	0.006	0.012	0.30
2	20	0.029	0.18	0.0016	2.06	0.013	0.025	0.71
3	12	0.029	0.18	0.0018	2.84	0.017	0.030	0.72
4	0	0.029	0.19	0.0018	2.27	0.021	0.037	0.87

Table 2.6: Conditions and average results for the experiments of DS-III.

2.4 Data set IV: Vertical sorting experiment large flume

After the pre-study experiments of DS-III, the same type of experiment has been repeated in the large flume for DS-IV. The large flume has some advantages over the small flume that improve the quality of the observations. Equilibrium flow can be realized more accurately due to the greater length and the tilting mechanism. Moreover, the greater length allows more bedforms to be present in the observation area. Finally, the measurement carriage is fully automated and can therefore make measurements continuously.

The experimental setup is the same as that setup described for DS-II. Only a gravel sieve has been added in the recirculation funnel as shown in Photo 2.4. This sieve caught the small gravel discharge that existed until the immobile layer had formed.

Photo 2.4: Gravel sieve in the sediment recirculation funnel.

	% Gravel	D_{10}	D_{50}	D_{90}	σ_g
Sand	0	0.6	0.8	1.2	1.3
Gravel	100	7.8	10.9	15.4	1.3
Mixtures	5	0.6	0.9	1.3	1.9
	10	0.6	0.9	4.1	2.3
	15	0.6	0.9	9.7	2.6
	20	0.6	0.9	10.9	2.9

Table 2.7: Characteristic grain sizes (mm) and the geometric standard deviation of the used grain size distributions.

ExpNr	% gravel	u [m/s]	h [m]
1	5	0.52	0.2
2	10	0.52	0.2
3	15	0.52	0.2
4	15	0.52	0.3
5	15	0.60	0.2
6	20	0.52	0.2

Table 2.8: Boundary conditions for experiments of DS-IV.

Programme

The measurements programme, see Table 2.8, has been designed to complement the experiments of DS-II. The water depth and flow velocity in the experiments correspond with those of DS-II. Therefore, no alluvial experiment is included in the programme. The initial grain size distribution of the experiments is shown in Figure 2.4 and the grain size characteristics are tabulated in Table 2.7. The sand and gravel that are used to create the sediment mixtures are the same as used in the other experiments. In Experiment 4 and 5 the gravel content is not varied, instead the water depth and flow velocity are varied.

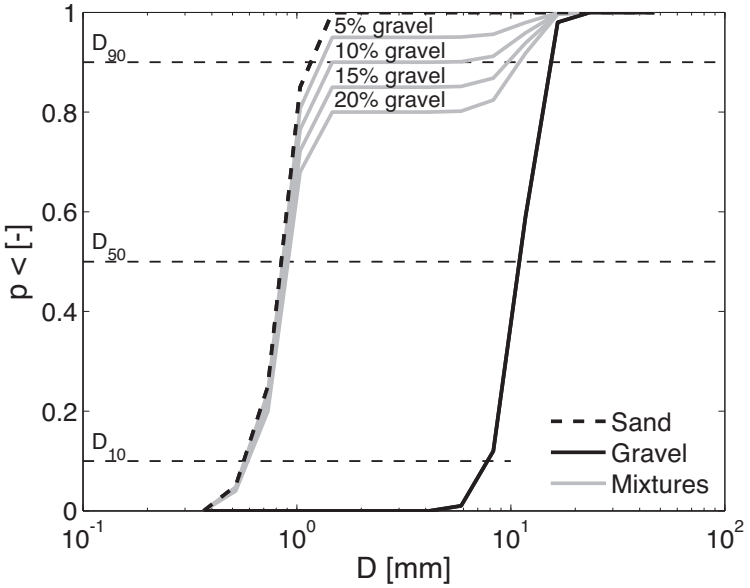

Figure 2.4: The sand and gravel have been mixed to 4 new grain size distributions.

Procedure

Before an experiment, the sand and gravel were thoroughly mixed and installed in the flume. The sediment layer was installed with a constant layer thickness. The procedure during the experiment was the same as described for DS-II and aimed to realize and maintain an equilibrium flow during the experiments. After each experiment the bed was photographed and the vertical sorting was measured. To measure the vertical sorting, the level of the top of

each gravel particle within a 0.15 x 0.15 m sampling area, was measured to a level of 8 – 10 below the average bed level. Vertical sand and gravel concentration profiles have been calculated from this data. For all experiments, 7 bed level samples were taken every 2 m along the *x*-axis in the centre of the flume (at y = 0.5 m). For Exp. 1 and 2 additional samples were taken near the sidewall, with the sampling centre 0.16 m from the sidewall. This allows the study of lateral variation in sorting. The study of these vertical sorting profiles falls outside the scope of this thesis. These results will be published elsewhere.

Results

The averages over the equilibrium periods of the experiments are reported in Table 2.9. Whether equilibrium conditions were reached was mainly judged from a graph that shows the deepest trough that has occurred at each location. This depth gradually increases until the gravel has formed an immobile layer. This gravel burial occurs fast in the beginning. The burial rate decreases and after 24 hours hardly any change was observed anymore. Therefore, equilibrium observations were taken from 24 hours to the end of the experiments after 48 hours, or in one case 31 hours. The bedform dimensions and the shear stress have been determined the same way as for DS-II. The average transport layer thickness has been determined the same way as for DS-III.

Exp Nr	t [h]	% Gravel	Q [m^3/s]	h [m]	I_e [-]	τ_b [N/m^2]	d [m]	Δ [m]	Λ [m]
1	48	5	0.104	0.20	0.0015	2.81	0.070	0.062	1.06
2	48	10	0.104	0.20	0.0013	2.31	0.046	0.052	0.98
3	48	15	0.104	0.20	0.0011	1.93	0.034	0.046	0.83
4	48	15	0.156	0.30	0.0006	1.50	0.026	0.044	0.91
5	48	15	0.120	0.20	0.0017	2.98	0.031	0.048	0.86
6	31	20	0.104	0.20	0.0009	1.54	0.016	0.031	0.76

Table 2.9: Conditions and average results for the experiments of DS-IV.

2.5 Data set V: Experiments smooth immobile layer

The goal of the experiments of DS-V was to test whether the roughness of the immobile layer plays an important role in determining the type of supply-limited bedform that develops. In order to test this, these experiments were conducted with a smooth immobile layer instead of a gravel layer. The experiments of DS-V are the same in setup as the experiments of DS-II. The immobile layer is the bottom of the flume; this consists of smooth painted steel and some smooth PVC sheets.

The conditions in the experiments correspond with those of Series 5 of DS-II. Therefore the alluvial dune dimensions of these conditions are known. The experimental procedure and methods to derive the bedform dimensions and bed shear stress are the same as described for DS-II.

Exp Nr	d [m]	Q [m^3/s]	h [m]	I_e [-]	τ_b [N/m^2]	Δ [m]	Λ [m]
1	0.010	0.094	0.20	0.0003	0.52	0.022	1.00
2	0.020	0.094	0.20	0.0005	0.87	0.034	0.92
3	0.040	0.094	0.21	0.0013	2.42	0.056	1.01

Table 2.10: Conditions and average results for the experiments of DS-IV.

Photo 2.5: Bedforms formed on a smooth immobile layer.

Chapter 3

An Experimental Study into the Geometry of Supply-Limited Dunes*

Abstract

The relationship between dune geometry and the volume of mobile sediment was studied in flume experiments. In these flume experiments, the volume of mobile sediment on top of an immobile coarse sediment layer was increased stepwise and the bedform characteristics were observed. A strong relationship was found between the volume that is mobile – and therefore available for bedform formation – and the dune dimensions and regularity. If the sediment supply is limited, dunes are smaller and more regular. Series of experiments with a decreasing supply limitation were conducted for different flow velocities and water depths. The relationship between the dune dimensions and the available volume is different for each series. The observed relationships between dune dimensions and layer thickness collapse to one relationship for height and one for length if scaling parameters are introduced. Current models for bedform dimensions under alluvial conditions can be extended to partial transport conditions using this relationship.

3.1 Introduction

Bedforms on river beds are important for water level predictions, which are essential to prevent floods and keep rivers navigable. The bedforms - especially dunes - are a primary source of roughness and therefore a major factor in determining water levels (Simons and Richardson, 1966). The hydraulic roughness induced by dunes depends on their dimensions. Therefore, models to predict dune dimensions from flow and sediment characteristics have been formulated (e.g. Gill, 1971; Fredsøe, 1982; Van Rijn, 1984; Zhang, 1999).

These models are based on full mobility conditions, under which the sediment transport is not supply-limited. In the case of a supply limitation, the sediment delivery from upstream is smaller than the local transport capacity while local entrainment of more sediment is prevented by a layer of immobile sediment. This causes a limitation in the volume of mobile sediment from which bedforms can be formed. The unerodable layer may have formed naturally, as can happen when the bed shear stress can transport only a part of the bed sediment (partial transport). Or the unerodable layer may be man-made, as an erosion prevention measure. In sand-gravel mixtures, partial transport conditions are common and

* This chapter has been published as: Tuijnder, A. P., Ribberink, J. S., and Hulscher, S. J. M. H. (2009). An experimental study into the geometry of supply-limited dunes. *Sedimentology*, *56*(6), 1713-1727.

supply-limited bedforms have been observed (e.g. McCulloch and Janda, 1964; Whiting et al., 1988; Chiew, 1991; Bennett and Bridge, 1995; McLelland et al., 1999; Carling et al., 2000; Kleinhans et al., 2002; Blom et al., 2003; Kuhnle et al., 2006; Tuijnder et al., 2007; Dreano et al., 2008). Generally, the supply-limited bedforms that were observed have a lower relief than the bedforms observed in sandy beds, which have alluvial conditions. This has implications for the bedform-induced roughness: with reducing bedform dimensions, the bed roughness decreases (Van der Zwaard, 1974; Tuijnder et al., 2007).

To improve the prediction of roughness in morphological models, we would like to be able to predict the bedform dimensions under supply-limited conditions. Therefore, we conducted flume experiments to study the dependency of the dune dimensions on the supply limitation. The setup of these experiments is explained in Section 3.2. In these experiments, we wanted to study the relation between the sediment availability and the characteristics - especially the average length and height - of the bedforms that developed. The results of these experiments are presented in Section 3.3. In Section 3.4, we propose scaling parameters to describe the observed variation in bedform dimensions with the varying supply limitation. Finally, in Sections 3.5 and 3.6, the results are compared with previous observations of bedforms under supply-limited conditions and our conclusions from this study are presented.

3.2 Experimental setup

The dependency of a dune's geometry on the supply limitation was studied in experiments in a sediment-recirculating flume (Fig. 3.1). The flume had a width of 1 m and a length of 30 m; the effective length for measurements of dune morphology was approximately 17 m. The slope of the flow could be varied, so it was possible to realize a uniform flow at the desired discharge and water depth.

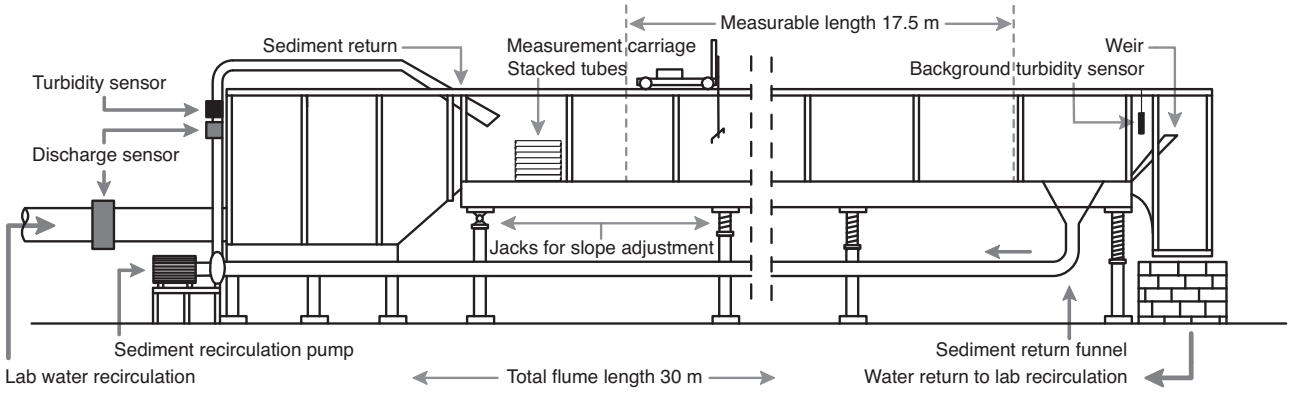

Figure 3.1: Side view of the used flume setup. The supply of water came from a constant-head tank approximately 5m above the level of the flume. The flume is supported by jacks that allow the flume to be tilted to realize an equilibrium flow.

A gravel layer was installed in the flume prior to the experiments. The gravel layer consisted of almost uniform gravel with 86% of the weight between 8 and 16 mm (Table 3.1). The grain size of the gravel layer had been chosen such that it remained stable under the shear stresses

observed in the experiments. The sediment that was transported over the coarse layer consisted of uniform quartz sand with a D_{50} of 0.8 mm (Fig. 3.2).

Sand layer						
D min	0	0.35	0.50	0.71	1.00	>1.4
D max	< 0.35	0.50	0.71	1.00	1.4	∞
Frac [-]	0.00	0.05	0.20	0.60	0.15	0.00
Gravel layer						
D min	0	4.0	5.0	8.0	11.2	>16
D max	< 4.0	5.0	8.0	11.2	16	∞
Frac [-]	0.001	0.01	0.11	0.47	0.39	0.02

Table 3.1: Result of sieve analysis of the used sediments. D min and D max are the minimum and maximum of the grain size classes in mm. The sand has a uniform distribution with a D_{50} of 0.8 mm. The table shows that the bulk of the sediment used for the gravel layer is between 8 and 16 mm.

Series	*h* [m]	*u* [m/s]
1	0.20	0.52
2	0.30	0.52
3	0.15	0.52
4	0.20	0.58-0.67
5	0.20	0.46

Table 3.2: Hydraulic conditions imposed in the different experimental series.

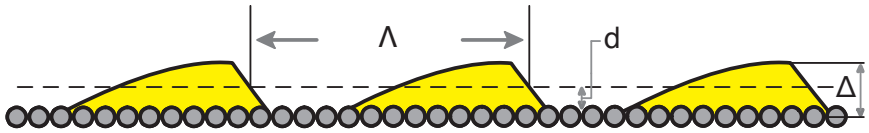

Figure 3.2: Schematic illustration of the experimental conditions. Bedforms formed from mobile sand migrate over an immobile gravel layer. The dashed line indicates the average sand layer thickness d. The length between consecutive crossings of the lee side of the dune with the average height is the bedform length Λ. The height difference between the crest and the downstream trough is the bedform height, Δ.

The experiments formed five series, each with a constant water depth and flow velocity (Table 3.2). During each experiment the volume of sand remained constant because the sediment was recirculated. The sediment discharged at the downstream end of the flume was fed back to the upstream end of the flume. For each series, the volume of sand on the coarse layer increased with each experiment, thereby decreasing the supply limitation. The volume of sand - including pores - on the coarse layer is expressed per square meter as the average layer thickness *d* (Table 3.3). It was determined by subtracting the measured level of the coarse layer from the measured level of the sand bed and averaging over the flume length and the equilibrium period.

The objective of the individual experiments was to take measurements of the bed morphology for that combination of layer thickness and flow conditions. It took some time before the conditions in the flume reached equilibrium after the start of an experiment. The bedform dimensions, sediment transport and bed roughness developed toward the equilibrium conditions. The slope of the bed and the level of the downstream weir were regularly adjusted to maintain uniform flow conditions at the desired water level during this adaptation period. The experiment was continued without further adjustment once the conditions were varying around a mean, and thus were in equilibrium. Under supply-limited conditions, less variation

in the conditions was observed over time than was the case under alluvial conditions. Therefore the experiments were continued for a few hours after an equilibrium had been reached under supply-limited conditions, while the observations were continued for up to two days under alluvial conditions (Table 3.3). The measurements from the equilibrium periods were used for the analysis of the bedform characteristics.

ExpNr Ser-Exp	t [day]	d [m]	Q [l/s]	h [m]	I_e [‰]	τ_b [N/m²]	C_b [m½/s]	Δ [m]	σ_Δ [m]	Λ [m]	σ_Λ [m]
1-1	0.00	0.000	74.3	0.20	-0.7	1.25	32.9	0	0	0	0
1-2	1.00	0.003	103.9	0.20	-0.8	1.33	44.7	0.005	0.003	0.23	0.14
1-3	0.14	0.003	104.8	0.20	-0.8	1.38	44.0	0.006	0.002	0.21	0.13
1-4	0.18	0.011	104.2	0.20	-0.8	1.48	42.4	0.023	0.005	0.63	0.11
1-5	0.05	0.012	106.0	0.20	-0.9	1.51	42.7	0.023	0.005	0.64	0.12
1-6	0.32	0.020	104.5	0.20	-1.3	2.20	35.1	0.039	0.010	0.82	0.20
1-7	0.71	0.041	104.3	0.20	-1.6	2.90	30.4	0.055	0.017	1.06	0.36
1-8	0.73	0.070	104.3	0.20	-1.9	3.51	28.0	0.068	0.024	1.19	0.48
1-9	0.68	0.097	104.4	0.20	-1.9	3.35	29.0	0.072	0.027	1.31	0.63
1-10	0.89	0.161	105.3	0.20	-2.4	4.27	25.8	0.072	0.029	1.28	0.69
2-1	0.00	0.000	150.6	0.30	-0.8	2.17	33.5	0	0	0	0
2-2	0.26	0.003	156.3	0.30	-0.6	1.36	44.5	0.006	0.003	0.25	0.17
2-3	0.24	0.011	156.8	0.30	-0.5	1.18	48.2	0.024	0.006	0.73	0.16
2-4	0.33	0.019	155.6	0.30	-0.8	1.93	37.0	0.041	0.008	0.89	0.17
2-5	0.36	0.039	152.6	0.30	-0.9	2.18	34.3	0.064	0.015	1.21	0.26
2-6	0.59	0.067	157.1	0.29	-1.2	3.00	30.7	0.078	0.024	1.27	0.43
2-7	0.95	0.095	157.2	0.30	-1.0	2.47	33.2	0.082	0.028	1.51	0.61
3-1	0.14	0.004	78.7	0.15	-1.3	1.74	39.7	0.007	0.004	0.25	0.14
3-2	0.47	0.011	79.0	0.15	-1.2	1.63	41.0	0.021	0.006	0.62	0.16
3-3	0.12	0.021	76.8	0.15	-1.5	2.02	36.0	0.034	0.009	0.81	0.22
3-4	0.95	0.037	77.8	0.16	-1.5	2.12	34.2	0.046	0.015	0.98	0.38
3-5	0.30	0.067	78.5	0.15	-2.0	2.80	30.5	0.056	0.019	1.12	0.52
3-6	0.86	0.160	80.2	0.15	-2.8	3.94	26.2	0.062	0.026	1.20	0.63
4-1	0.11	0.003	134.7	0.20	-1.2	2.07	46.4	0.006	0.003	0.22	0.13
4-2	0.12	0.012	135.1	0.20	-1.8	3.12	37.8	0.028	0.008	0.68	0.19
4-3	0.17	0.021	116.0	0.20	-1.6	2.94	33.6	0.041	0.011	0.84	0.25
4-4	0.91	0.039	116.3	0.20	-2.2	4.07	28.5	0.058	0.016	0.99	0.29
5-1	0.05	0.003	93.2	0.20	-0.6	1.05	45.4	0.005	0.002	0.24	0.18
5-2	0.10	0.004	93.1	0.20	-0.7	1.13	43.5	0.006	0.003	0.26	0.19
5-3	0.24	0.009	91.5	0.20	-0.7	1.12	42.7	0.016	0.005	0.75	0.17
5-4	0.50	0.019	92.9	0.20	-0.7	1.23	41.9	0.033	0.008	0.94	0.21
5-5	0.39	0.038	92.5	0.20	-0.9	1.51	37.5	0.051	0.015	1.15	0.33
5-6	0.92	0.065	93.0	0.20	-1.2	2.09	31.8	0.064	0.021	1.27	0.52
5-7	0.81	0.159	93.7	0.20	-1.5	2.74	27.4	0.065	0.023	1.25	0.46
5-8	1.47	0.160	93.7	0.20	-1.7	3.13	26.8	0.066	0.025	1.27	0.57
5-9	0.65	0.159	93.7	0.20	-1.5	2.68	27.9	0.061	0.022	1.15	0.42

Table 3.3: Overview of the key variables in the experiments: d is the average layer thickness of transport layer, Q is the water discharge, h is water depth, I_e is energy slope, τ_b is the bed shear stress, C_b is Chézy parameter related to the bed, Δ is the mean bedform height and σ_g the standard deviation of Δ, Λ is the bedform length, and σ_Λ is the standard deviation of Λ.

Measurements were made using an automated carriage that measured the bed and water level during the experiments over a length of 17.5 m with ultrasound sensors. The water level was measured approximately in the centre of the flow. The bed level was measured at three parallel transects; at y = 0.165, 0.500 and 0.835 m, where y = 0 is the left sidewall when looking downstream. The accuracy of the bed level measurements was tested by repeatedly measuring a fixed profile. The vertical standard deviation is less than 1 mm, while the

horizontal standard deviation is approximately 3 mm. In the horizontal direction the accuracy is limited by the area of the measurement surface. The radius of the measurement surface was a few centimetres. So the ultrasound measurements are suitable for measuring the large-scale features of the dunes, but the grain scale cannot be resolved. The accuracy of the sensor for the water level is comparable to that of the bed level sensors. The carriage measured the bed and water level continuously. It took about 3 minutes to take a measurements profile in one direction after which the carriage immediately started measuring in the opposite direction.

After the experiments of Series 1, a detailed scan of the bed morphology was made using a laser distance measurement instrument. This sensor has a measurement area of 0.2 x 4 mm and can therefore be used to make bed level measurements with a higher spatial resolution. In the scans made with this instrument, the bed level was measured every 1 mm in the x-direction, along the flume, and every 4 mm in the lateral y-direction. The standard deviation in the y and the z-direction, normal to the flume bottom, of these measurements is <1 mm. The positioning of the sensor in x-direction is slightly less accurate with a standard deviation of <2 mm.

The discharge from the large water recirculation system and the smaller sediment recirculation system was measured using inductive measurement devices. The accuracy of these instruments is approximately 1% according to their specifications. From these measurements, the average flow velocity was calculated by dividing the total discharge by the water depth and flume width. Subsequently the total shear stress was calculated from the gradient in the energy level, assuming equilibrium flow. The total shear stress was divided in a wall and bed-related part using the method of Vanoni and Brooks (1957). The bed shear stress (τ_b) is reported in Table 3.3.

3.3 Experimental results

Bed level observations

Between the experiments, the layer thickness was increased and therefore the bedform characteristics changed. We would first like to illustrate this with pictures from the 3D laser surface scans and examples of bed level profiles from Series 1. Figure 3.3 shows a height map of a section of 5 m from the laser surface scans. The patterns are clearly visible in this figure, but the height is not. Therefore, Fig. 3.4 shows the longitudinal bed level profiles of the centre bed level sensor. A histogram of the observed bed level elevations is shown next to the profiles in Fig. 3.4. This shows how often a certain level was observed. The profiles are just examples since a new profile was made every 3 minutes. The distribution shows the observed levels in all profiles over the equilibrium period.

In Fig. 3.3 Exp. 1-1, a scan of the gravel layer is shown. There was no sediment movement that could form bedforms since the gravel was immobile. In Exp. 1-3, a layer sand of 1 cm in depth

had been distributed over the coarse layer. A part of this sand disappeared from the active layer because it fell into the coarse layer. Another part of the sand lied at the surface but between the gravel particles. This part could not contribute to an increase in average bed level, because the relatively large measurement area of the echo sensor could not detect it. Therefore a few millimetre of sand (± 2-5 mm) is not included in the thickness of the sand layer *d*, as reported in Table 3.3. The morphological pattern that emerged in the sand layer during the experiment is visible in Fig. 3.3 Exp. 1-3. Two flow parallel stripes formed where the sand transport concentrated. Ripple-like bedforms are present in the stripes. No profiles are shown for this experiment in Fig. 3.4 because the relief is very low; the sandy bedforms formed between the gravel particles. In Exp. 1-4 and 1-5, which had the same flow conditions, the sand layer thickness has been increased again with 1 cm. The effective layer thickness is now 12 mm. In these experiments, straight-crested dunes appeared with a very regular topography. When we continued adding more sand, the bedforms grew bigger and became more irregular. This is illustrated in Fig. 3.3 and Fig. 3.4 by the disappearance of the straight crests, the appearance of the overlapping of dunes and the development of secondary bedforms on top of the larger dunes. With a further increasing sand layer thickness, the influence of the coarse layer vanished.

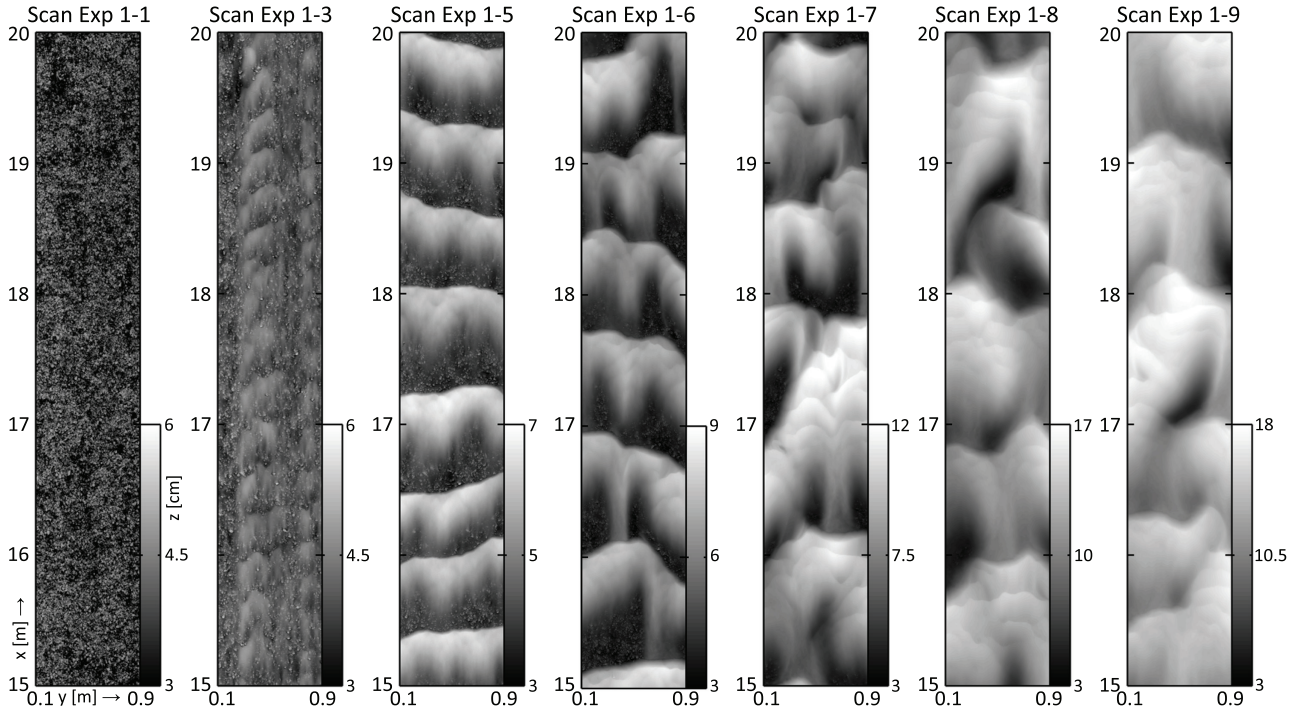

Figure 3.3: Laser surface scans from the situation after the experiments of Series 1. The color indicates the height. The mean bed level is gray. The flume sidewalls are located at 0 and 1 meter, so 10 cm is missing on both sides. Flow is from bottom to top

In Fig. 3.4 Exp. 1-4 and 1-6, the coarse layer is exposed between almost every dune. Therefore, all sand in the flume is part of a dune. No sand layer remains immobile while dunes are migrating over it, apart from the small amount of sand trapped in the pockets of the gravel layer. In Exp. 1-7, it can be seen that the troughs of the dunes are often not on the coarse layer.

A lag-deposit of sand is present under the dunes. Some troughs are deeper and reach the coarse layer. So the sediment in the lag-deposit is regularly entrained in the transport process. In Exp. 1-8 this lag-deposit has developed further. No troughs any longer reach the coarse layer in the profile shown here. In the histogram, it can be seen that the coarse layer still is exposed sometimes though; the histogram shows a peak at the level of the coarse layer. In Exp. 1-9, the lag deposit has developed further and the troughs reach the coarse layer for only < 1% of the dunes. Therefore, the influence of the supply limitation disappears in Exp. 1-9 and the dune dimensions are not significantly different from the dune dimensions of the alluvial reference experiment for Series 1, Exp. 1-10.

So, for a small sediment supply no lag deposits are observed. At some point, dunes start to coalesce and a lag-deposit starts to develop. This lag-deposit grows with the increasing sediment supply until the troughs no longer reach the coarse layer. At that point the dunes are no longer supply-limited.

In the other series (Series 2 to 5), the same experiments were performed at water depths and flow velocities different from those in Series 1. In these series similar trends were observed as will be shown in the following sections where the relation of the bedform dimensions with thickness of the sand layer is explored.

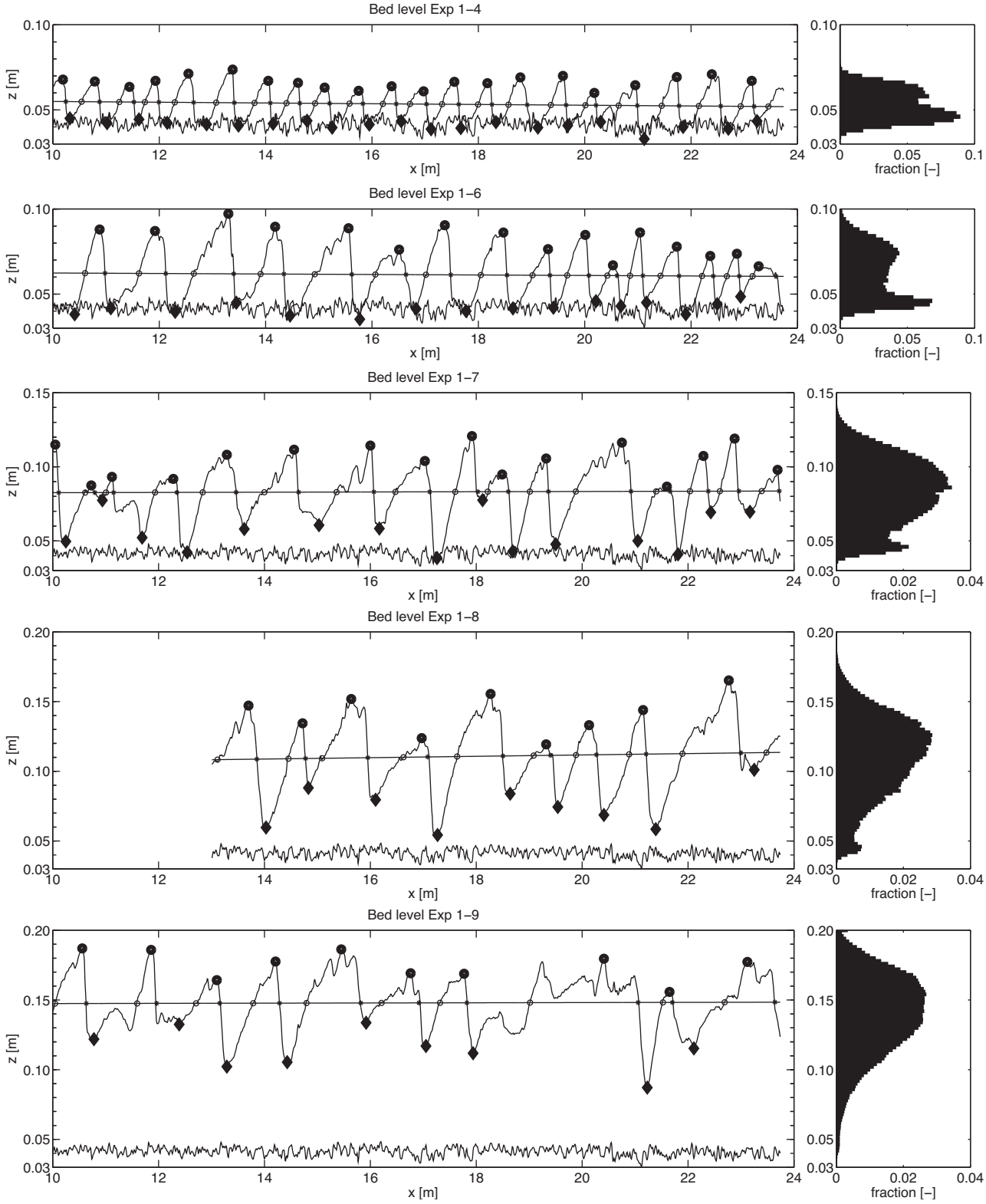

Figure 3.4: Bed level profiles from the centre bed level sensor. The irregular line at the bottom of each figure is a scan of the gravel layer. The straight line through the dunes is a linear fit line, the zero-level for the zero-crossing bedform-recognition routine. The circles and stars on the line show the zero-crossings, the diamonds and the circles mark the location of the crests and troughs as located by the zero-crossing routine. The rotated histograms at the right of the profiles show the distributions of the observed bed levels.

Method of determining the bedform dimensions

Bedform dimensions were determined from the measured bed level profiles using a 'zero-crossing' method (Van der Mark et al., 2008). In this method, the crossings of the bed level with a fitted linear trend line are recognized (Fig. 3.2). Between an up and a down crossing a crest is selected at the maximum, and between a down and an up crossing, a trough is selected at the minimum. The bedform length (Λ) is defined as the distance between successive down crossings. The bedform height (Δ) is defined as the height difference between a crest and the trough on the downstream side.

Using this method, secondary bedforms - smaller bedforms migrating on top of other bedforms - are sometimes recognized. In other studies such secondary bedforms were often removed because the researchers were only interested in dune dimensions and bedforms smaller than a certain size were not considered to be dunes (e.g. Allen, 1984; Bakker, 1982; Leclair, 2002). In this study, no minimum length or height for a dune has been defined because the bedforms vary in size due to the supply limitation. The bedforms, which we consider to be supply-limited dunes in one case, have the same dimensions as the secondary bedforms in another experiment. Therefore, a different threshold would have to be used for every experiment, making the analysis subjective. The total distribution of observed dune dimensions is analyzed here. The effect of not removing secondary bedforms is that the reported dimensions will be somewhat smaller. This effect is small because the secondary bedforms form on the crests of dunes, usually above the mean level of the bed that is used for bedform detection.

Variation in average dune dimensions with supply limitation

The bedform dimensions were determined for all profiles within the equilibrium period (25-700 profiles) of each experiment using the method explained above. The average and the standard deviation of the height and length are shown in Fig. 3.5 and 3.6. It can be seen that the average dune dimensions increase with an increasing (sand) layer thickness for all series of experiments. In Fig. 3.5A and 3.6A, the flow velocity is equal for all series (u = 0.52 m/s) and the water depth varies between the series. It can be seen that, for increasing water depths, the dunes grow to larger dimensions under alluvial conditions. The differences in average dune dimensions between the series decreases with a decreasing sediment availability.

Figures 3.5B and 3.6B show the increase in dune height and length with an increase in d for series with a constant water depth; now the flow velocity was varied between these series. The bedforms grow towards larger dimensions for series 1 (u = 0.52 m/s) than for series 5 (u = 0.46 m/s). Series 4 seems to grow towards an alluvial height that is equal to Series 1; unfortunately we lack observations for a layer thickness larger than 4 cm.

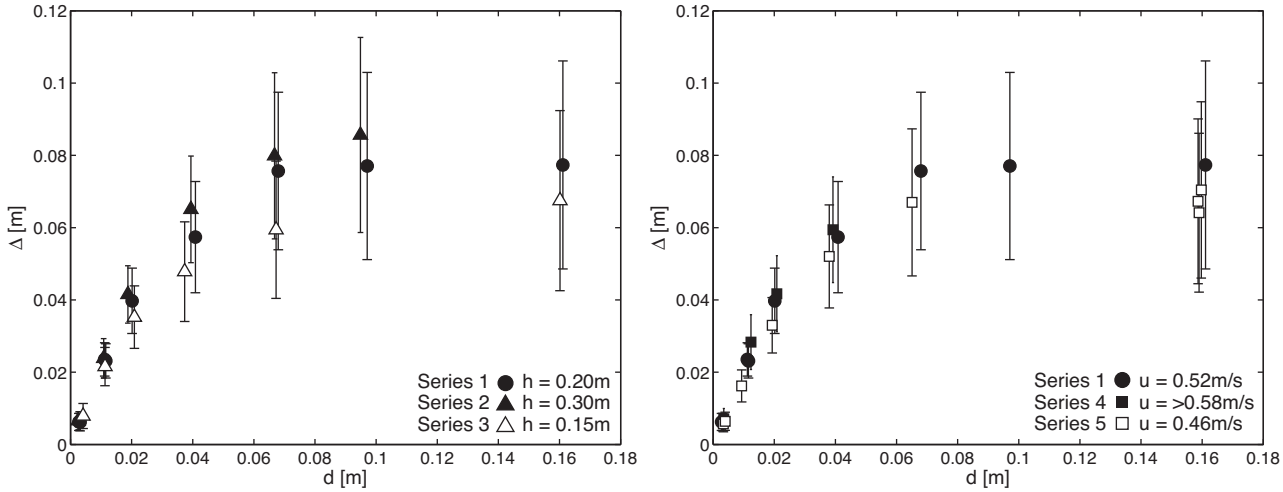

Figure 3.5a (left) and 3.5b (right): The average dune height versus the average layer thickness. The bars indicate the standard deviation of the observations.

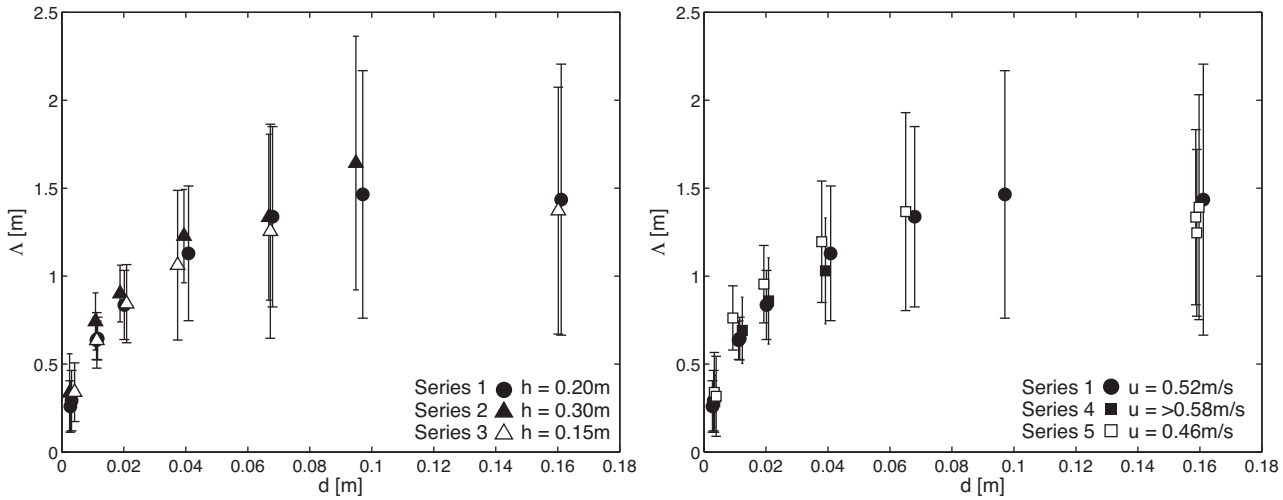

Figure 3.6a (left) and 3.6b (right): The average dune length versus the average layer thickness. The bars indicate the standard deviation of the observations.

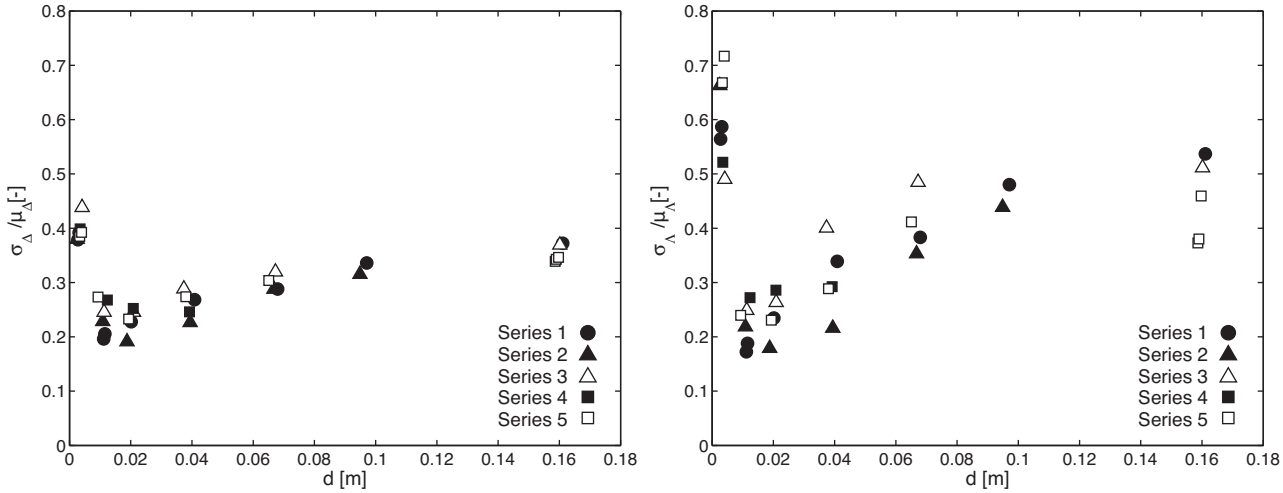

Figure 3.7a (left) and 3.7b (right): The relative standard deviation of the height (a) and length (b) versus the average layer thickness.

The bars in Fig. 3.5 show the range of 1 standard deviation in bedform height. The standard deviation (σ) increases with d. The relative standard deviation, the standard deviation divided by the average (μ), also increases with increasing sediment supply (Fig. 3.7). This shows that the supply-limited dunes are more regular than the alluvial dunes. The increase in relative standard deviation for $d \rightarrow 0$ is caused by coarse grains that are recognized as bedforms. These points can be ignored.

The dune height divided by the length, namely the dune steepness, is shown in Fig. 3.8. The steepness increases quickly with increasing sediment availability. The alluvial steepness was reached at a layer thickness of approximately 5 cm, whereas the length and the height of the dunes was still increasing, as can be seen in Fig. 3.5 and 3.6. This suggests that the dune steepness is constant in the slightly supply-limited regime. The height approaches zero for a strong supply limitation, while the length does not. See the surface scan of experiment 1-3 in Fig. 3.3: the wavelength is still clearly recognizable while the height of the bedforms is so small that the coarse layer is just covered at the crests of the dunes.

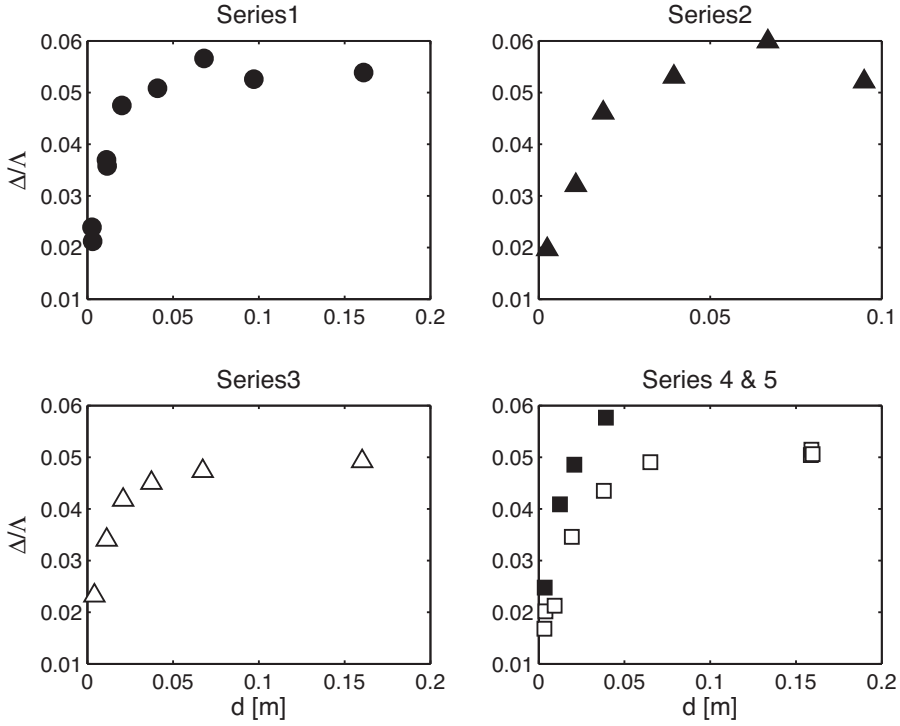

Figure 3.8: The bedform steepness, Δ/Λ, for the different series. The symbols are the same as in Figure 3.7.

The spectral development from supply-limited to alluvial conditions

A spectrum of the bed-level profiles can tell us whether dominant wavelengths are present or whether the bed consists of many different wavelengths. It has been shown that longitudinal wave number spectra show a -3 slope over a certain range for fully developed sand wave fields (Hino, 1968; Nordin and Algert, 1966; Nikora et al., 1997). This means that in a sand wave field all wavelengths are present between a certain minimum and maximum wavelength, these wavelengths are controlled by the bed shear stress and the sediment characteristics. This range of wavelengths is called the scaling region (Nikora et al., 1997).

With a further increasing sediment availability the peak in the spectrum shifts towards lower frequencies and the total variance (the area under the spectrum) increases. Gradually, the spectrum right of the peak starts to approach the -3 slope. This indicates an increasing spectral energy for wavelengths smaller than the peak wavelength. This can be attributed to the increasing presence of small bedforms superimposed on the larger ones. When the alluvial situation is approached (see Exp. 2-6 and 2-7), the well-defined peak disappears and the energy in the spectrum spreads over a wide range of frequencies. This agrees with the increasing standard deviation of bedforms lengths and heights shown in Figs 3.5 and 3.6. With an increase in the sediment availability, not only does the bedform dimensions increase, but also the bedforms become more irregular.

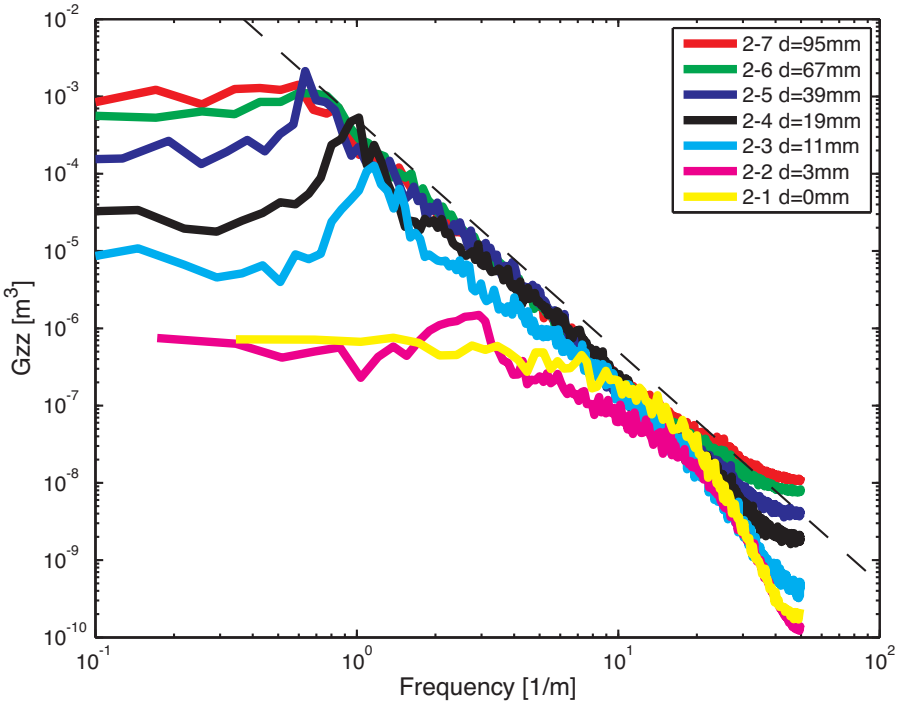

Figure 3.9: The spectra for the experiments of Series 2.

Comparison of the results from the spectral and zero crossing method

Both zero-crossing analysis and spectral analysis provide different information on the bedform characteristics. An extensive treatment of the relation between dune dimensions from a zero-crossing method and the statistical properties of bed level profiles is given in Nordin (1971).

The peak wavelength - as can be observed in the spectra - provides an alternative means to characterize the bedform length. In Fig. 3.10, the peak wavelength, Λ-peak, is compared to the mean wavelength from the zero-crossing method. The results from both methods are very similar up to a Λ-mean of about 1.2 m. Figure 3.10 shows that the observations follow the Λ-mean = Λ-peak relation, with a small systematic difference between the two methods. Up to the wavelength of ± 1.2 m the dunes are regular and their spectra are peaked. From this point on the spectra are no longer peaked, instead they tend to show an approximately equal spectral energy for all longer wavelengths. See the horizontal lines for Exp. 2-6 and 2-7 in Fig. 3.9 for wave lengths >1.4 m. Under these alluvial conditions, wavelengths longer than Λ-mean sometimes have a slightly larger spectral energy which causes a difference between the Λ-mean and Λ-peak. These peaks do not represent actual dune wavelengths, since the amplitude is very small compared to the wavelength. It suggests the presence of larger bed features (Nikora et al., 1997). It has been suggested that the characteristic wavelength in this case is the wavelength of the end of the scaling region.

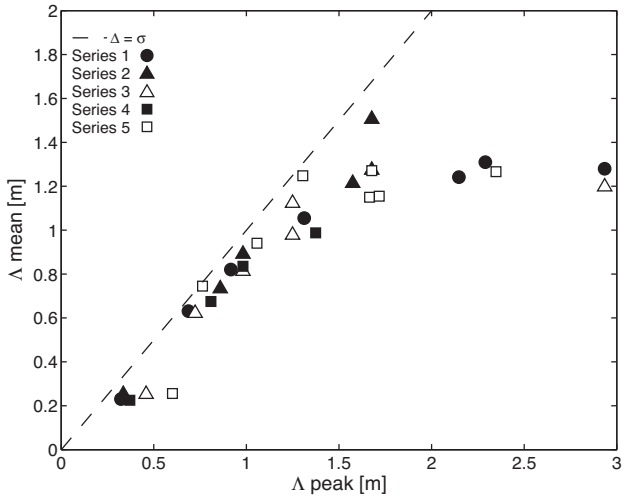

Figure 3.10: The mean bedform length versus the peak wave length from the spectra.

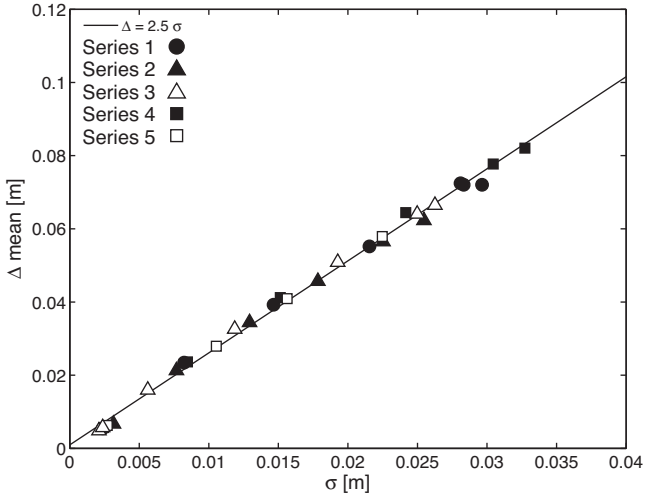

Figure 3.11: Mean bedform height versus the standard deviation from the bed level.

Unlike the bedform length, the bedform height cannot be directly read from the spectrum. However, the area under the spectrum - the total variance of the bed - is related to the bedform height. It has been shown that Δ/2 is distributed according to a Rayleigh distribution (Cartwright and Longuet-Higgins, 1956 in Nordin, 1971) if the bed elevations have a Gaussian distribution with standard deviation σ. This can be expressed as:

$$p(\Delta/2) = \frac{\Delta}{\sigma} e^{-\left(\frac{\Delta}{2\sqrt{\sigma}}\right)^2} \qquad \text{(Eq. 3.1)}$$

The bedform dimensions from the zero-crossing method reported here are averages. The mean bedform height ($\mu\Delta$) can then be calculated as follows (Bendat and Piersol, 2000):

$$\mu_\Delta = 2\sigma\sqrt{\pi/2} \approx 2.5\sigma \qquad \text{(Eq. 3.2)}$$

The mean bedform height is therefore approximately 2.5 times the standard deviation of the bed level. Figure 3.11 shows the bedform height from the zero crossing method against the standard deviation, the square root of the variance. The data points lie on a straight line with a steepness of 2.5. This agrees with the result of Cartwright and Longuet-Higgins (1956), even though the bed level distribution is not Gaussian in all experiments due to the presence of the coarse layer, see Fig. 3.4.

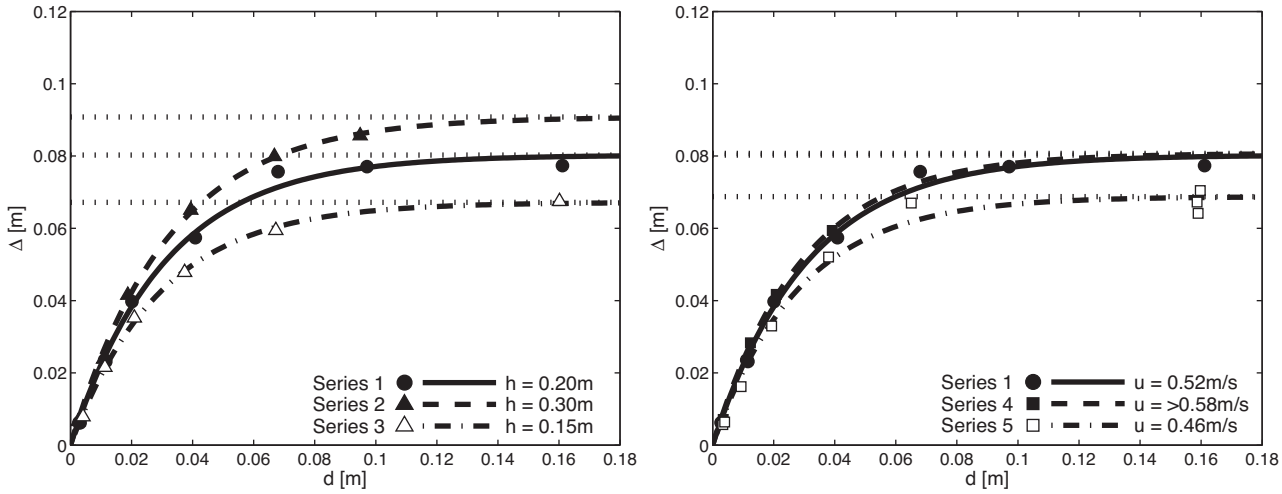

Figure 3.12a (left) and 3.12b (right): Dune height observations with fitted trend lines. The equation behind the trend line is eq. 4.3. The fits have been used to determine the asymptotic values of the dune height, which are considered to be the alluvial dune height (Δ_0).

3.4 Empirical relation between dune dimensions and supply limitation

A relation between the dune height and the sand layer thickness may be useful when predicting the bed roughness and sediment transport for supply-limited situations. Therefore we used the experimental data to derive an empirical model.

Figure 12 shows that the steepness of the fitted functions decreases with a decreasing distance to the asymptotic value, the alluvial dune height (Δ_0):

$$\frac{d\Delta}{d(d)} \sim -(\Delta - \Delta_0) \qquad \text{(Eq. 3.3)}$$

L is introduced as a characteristic length parameter to fit the model:

$$L\frac{d\Delta}{d(d)} = \Delta_0 - \Delta \qquad \text{(Eq. 3.4)}$$

Integration of this equation gives:

$$\frac{\Delta}{\Delta_0} = 1 - \exp\left(-\frac{d}{L} + C\right) \qquad \text{(Eq. 3.5)}$$

The integration constant, C, is zero because Δ = 0 for d = 0. If *L* is a constant, Eq. 3.5 suggests that there should be one relation between the relative dune height (Δ/Δ_0) and the layer thickness (*d*). Figure 3.13 shows the relative dune height against the layer thickness. It indeed shows that the measured dune heights collapse to one line when the dune height is divided by the alluvial dune height Δ_0. The dune length also shows this collapse when divided by the dune length under alluvial conditions but the scatter is larger. Unfortunately, the absolute value of *d* cannot be considered a good model parameter. If applied to a situation where the water depth and dune size are much smaller or larger, then the absolute *d* from these experiments will have no predictive power. It can be assumed that the parameter *L* is related to Δ_0, but the variation in Δ_0 in our experiments is too small to demonstrate the relation. Another set of experimental data of Dreano et al. (2008) is used for this purpose. This data has also been plotted in Fig. 3.13 and is visible to the left of our data.

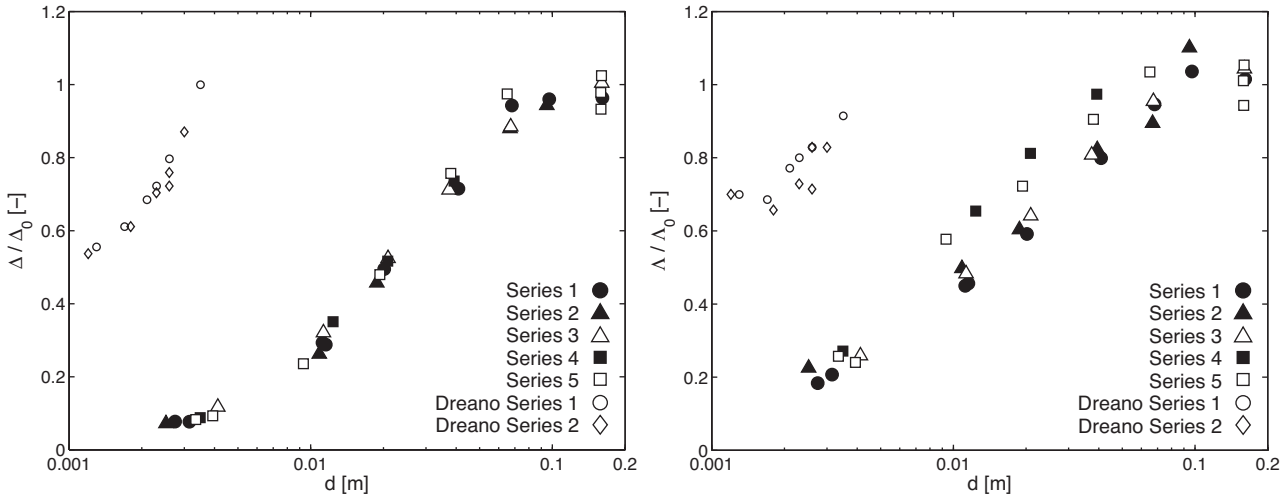

Figure 3.13a (left) and 3.13b (right): Relative dune height (Δ/Δ_0) and relative dune length (Λ/Λ_0) versus the layer thickness, on a logarithmic axis.

Several key characteristics of the experiments by Dreano et al. (2008) are mentioned here. Their experiments are comparable to the experiments presented here because the supply limitation was also systematically varied while measuring the bedform characteristics. However, the scale of their experiments is much smaller. Therefore they can provide additional information. The water depth, in a closed duct flume, was 3.5 cm compared to 20 - 30 cm in our experiments. In the experiments, glass beads - 0.1 mm in diameter with a density of 2.5 g/cm^3 - were fed into a flume and transported over a surface with glass beads glued to

it. Two series of experiments were carried out: one with 0.1 mm glass beads glued to the bed, the other with 0.25 mm. The flow discharge was constant for all experiments.

In these experiments the dune height also showed an increase with an increasing active layer thickness and increasing sediment transport rate. However, the data do not show constant alluvial dune dimensions for large *d*, which may be an indication that alluvial conditions were not yet reached in the experiments. Since the alluvial dune dimensions were unknown the alluvial value has been estimated based on the observed dune heights and the water depth in the experiments (Δ_0 = 0.6 cm Λ_0 = 7 cm).

Figure 3.14 shows the result of using the relative layer thickness (d/Δ_0) on the *x*-axis. Our experiments are still on one line, but now the data of Dreano (2008) also concentrate around the same line. This shows that the relative dune height has the same relation with the relative layer thickness for different conditions. In other words: the relative layer thickness determines to which value the relative dune height can develop.

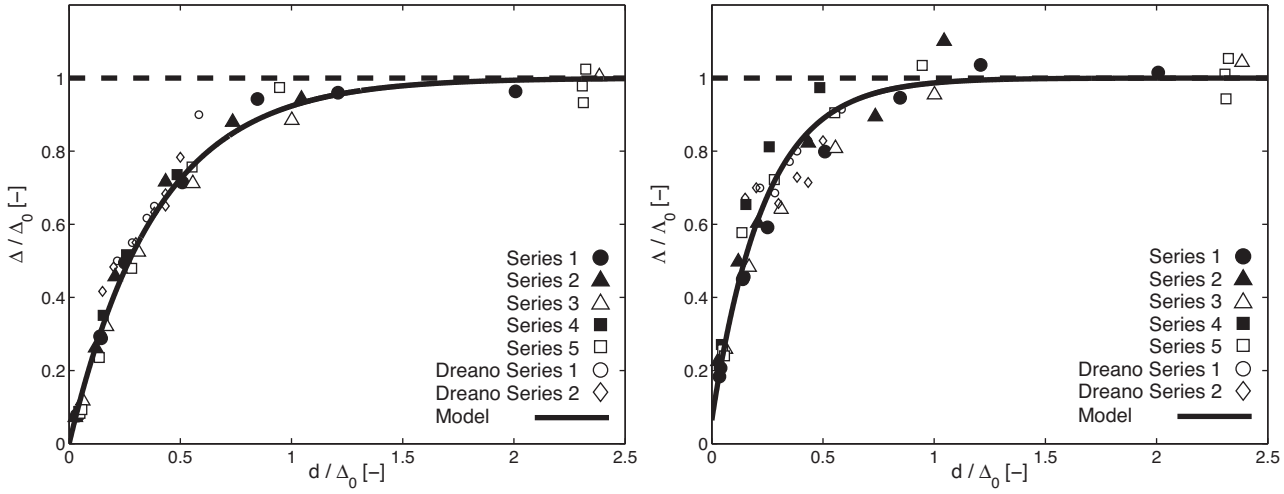

Figure 3.14a (left) and 3.14b (right): Relative dune height (a) and dune length (b) versus the relative layer thickness. The dashed line indicates the asymptotic value of the model, a relative dune height and length of 1.

This result is very insensitive to the estimated value of the alluvial dune dimension in the experiments of Dreano et al (2008). The lower limit for the alluvial dune height is the measured maximum dune height. The maximum value for the alluvial dune dimensions is approximately one-third of the water depth in the experiments. The results of Dreano et al. (2008) plot on the curve for all values between the minimum and maximum. The points only move along the curve. The assumed value for the alluvial dune height in Fig. 3.14 is 0.60 cm, which is just a little larger than the maximum observed dune height of approximately 0.52 cm.

The collapse of the data points to one relation between the relative dune height or length and the relative layer thickness gives us the opportunity to make a model for the dune dimensions under supply limitation. We propose the following equations:

If a linear relation between L and Δ_0 is assumed ($L = \alpha\Delta_0$), equation 3.5 can be expressed as:

$$\frac{\Delta}{\Delta_0} = 1 - \exp\left(\frac{-d}{\alpha_h \Delta_0}\right) \qquad \text{(Eq. 3.6)}$$

This relation has one parameter to fit, α_h, which determines the rate of adaptation to the alluvial dune height. The relation for the dune length (Eq. 3.7) is derived analogue to equation 3.6. Only the boundary condition $\Lambda = 0$ for $d = 0$ is not imposed. Because a wave length can remain while $d \rightarrow 0$ as was observed in Exp. 1-3 (Fig. 3.3) where the bedforms formed mainly between the gravel particles. Therefore the equation has an additional parameter β, which is used to fit the model to a finite bedform length for $d \rightarrow 0$.

$$\frac{\Lambda}{\Lambda_0} = 1 - \beta \exp\left(\frac{-d}{\alpha_l \Delta_0}\right) \qquad \text{(Eq. 3.7)}$$

The models were fitted to the data of our experiments using nonlinear least squares fitting. The results are $\alpha_h = 0.39$, $\alpha_l = 0.24$ and $\beta = 0.96$. These results are shown in Fig. 3.14 as the solid line through the observations.

3.5 Discussion

The main goal of this study was to investigate how the dune characteristics, most importantly the average length and height, react to a supply limitation. It was observed that the average dune height and length decrease with decreasing average layer thickness. This trend is found in other flume data and some field data as well (Kleinhans et al., 2002). The experiments of Kuhnle et al. (2006) are particularly interesting because conditions in these experiments were comparable but the cause of the supply limitation was different. A bed of a well-mixed bimodal sediment, which was a little finer than in our experiment, was subjected to increasing shear stresses. The sediment mixture was only partially mobile, creating a supply limitation under the lower flow conditions. The thickness of the transport increased and the supply limitation decreased with increasing shear stress. First, under the lowest shear stress, flow parallel strips were observed. Flow transverse bedforms with increasing bedform dimensions were observed when the shear stress increased. This was caused by an increasing sediment availability, analogous to our experiments.

A different reaction of dune characteristics to a supply limitation was found in the Rhine in Germany. Carling et al. (2000) describe the occurrence of sand dunes on top of a stable gravel lag. The available volume of sand is not enough to cover the entire bed, therefore the reach is supply limited. The dunes react to the supply limitation by forming isolated dunes rather than sediment starved dunes (nomenclature following Dalrymple and Rhodes (1995) and Carling et al. (2000)). Isolated dunes are dunes that have a varying spacing between dunes where the underlying stable base is exposed. They can develop until they are depth limited, just as

alluvial dunes. The supply limitation manifests itself in the larger space between dunes. Sediment starved dunes on the contrary, develop a smaller height and length due to the limited sediment availability. In our observations the dunes react to supply limitation by changing the length and height, thus forming sediment starved dunes as surmised by Dalrymple and Rhodes (1995). A possible cause for the difference with Carling et al. (2000) is the fact that our experiments were conducted under equilibrium conditions, while in the field the bedforms are subjected to repeated flood waves. Carling et al. (2000) provide a conceptual model for the influence of stage history on the behaviour of dunes that describes how the bed morphology is continuously adapting to the present conditions. These non-stationary effects were not studied in our experiments and therefore the model should be considered a model for equilibrium conditions.

Range of validity

In our experiments the water depth and the flow velocity were varied to incorporate their influence on the bedform dimensions in the model. The data from our experiments show that the relation between relative bedform dimensions and the relative layer thickness is independent of water depth and flow velocity. The range of water depths in our experiments was 15 to 30 cm. These water depths are far enough apart to clearly see their influence on the alluvial dune dimensions. The range in velocity was 0.46 - 0.67 m/s but the high velocity series is unfortunately not complete. The influence of the velocity was visible, but limited in range.

Scaling parameters are often valid beyond the range of observations that were used to discover them. Therefore, the dependency of the relative dune dimensions on the relative layer thickness may extend well beyond the range of parameters observed here, but this requires validation with other data sets. The fact that the data of Dreano et al. (2008) plot on the same line gives some validation for smaller dimensions, but validation is still required for larger dimensions; especially because the application of the relation will typically be on larger scale problems.

Bedform dimensions are also dependent on the grain size of the transported sediment, as shown by the dependency of most alluvial dune dimension models. However, the grain size has not been varied in our experiment. The experiments by Dreano et al. (2008) were conducted using much finer sediment than we used. The fact that the same trend was found in these experiments, suggests that the relation may be grain size independent as well.

Finally it is still unknown whether the geometry of the supply-limited bedforms is dependent on the grain diameter of the immobile gravel layer.

Application of the model

We would like to be able to predict the bed roughness in morphological and hydraulic river models based on knowledge of the characteristics of the river bed. Currently the roughness parameters are often used to calibrate the model. By accounting for more processes in the river models we hope to take a further step towards an accurately predicted roughness parameter. For roughness predictions under alluvial conditions, we could base our roughness prediction on the present models for bedform dimensions. The model presented in this paper can extend these models to incorporate partial transport conditions. Provided that the volume of available sediment for bedform formation per square meter is a predictable parameter.

3.6 Conclusions

We draw the following key conclusions from the experiments and the data analyses.

The supply limitation clearly limits the dimensions to which dunes develop. The equilibrium bedform dimensions increase with an increasing supply of sediment, which was characterized by the active layer thickness.

The irregularity of the dunes increases with increasing supply; or stated the other way around: the presence of the unerodable layer suppresses the development wavelengths other than the dominant wavelength. This is visible in the wave number spectra. Compared to the alluvial condition wavelengths both larger and smaller than the peak wavelength are missing in a supply-limited dune field.

The relative layer thickness determines the maximum relative dune height that can develop. This relation is independent of both water depth and flow velocity. Therefore, these parameters can be used to formulate a model that extends the use and usefulness of existing models for dune dimensions in the alluvial regime to the supply-limited regime.

Acknowledgments

This research project, which is part of the VICI project ROUGH WATER (project number TCB.6231), is supported by the Technology Foundation STW, applied science division of the Netherlands Organization for Scientific Research (NWO) and the technology program of the Ministry of Economic Affairs. The laboratory experiments are funded by the Delft Cluster program 'Natural Hazards', work package A2 River Morphology (WP CT 043211).

Furthermore the authors would like to thank A. Dittrich and the rest of the staff of the Leichtweiss-Institute for Hydraulic Engineering at the Technical University Braunschweig in Germany for their cooperation in the experiments. The help of master's student M. Spekkers with the flume experiments was also greatly appreciated.

Chapter 4

Riverbed Roughness Prediction under Supply-Limited Conditions*

Abstract

Under supply-limited conditions an immobile layer is present in the river bed that limits the volume of sediment available for sediment transport and bedform formation. Because of the volume limitation the bedforms are generally smaller than under alluvial conditions and the (usually coarser) immobile layer is exposed between the bedforms. These conditions have been studied in several new series of flume experiments.

It was observed that the roughness generated by dunes decreases with an increasing supply limitation. In Tuijnder et al. (2009) the relation between the supply limitation and the bedform dimensions was studied and a model to predict the dune height and length under supply-limited conditions was proposed. In this study we validate this model with new flume-experiments and we propose a new method to predict the bedform related roughness under supply-limited conditions.

Apart from the bedform roughness also the grain roughness needs to be predicted in order to predict the total bed roughness. The grain roughness varies with varying supply limitation because of the varying coverage of the gravel layer with the bedload sediment that forms the bedforms. A new model to predict the fractional coverage of the immobile layer with bedforms is proposed. This model enables us to make a separation between the prediction of the grain roughness for the immobile layer and for the bedforms.

In this study the proposed model concepts for roughness prediction are first tested independently using the experimental data. Subsequently, the model concepts are combined into an integrated roughness prediction model that predicts the bedform height and length, the immobile layer exposure, the grain roughness and the bedform roughness including the interactions between these parameters. This integrated model is tested by applying it to the experimental data sets. A comparison with an alluvial roughness model shows that the new supply-limited method results in much better roughness predictions under supply-limited conditions.

* This chapter has been submitted for publication.

4.1 Introduction

Hydraulic and morphological models are used to predict the natural development of a river or the effects of engineering measures. They can help river managers with the optimization of safety, navigability and the many other functions a river has. Accurate roughness estimations are important in hydraulic and morphological models. In hydraulic models the water levels are calculated in relation to the discharge. The bed geometry and the bed roughness determine this relation. In morphological models the bed roughness additionally plays a role in the calculation of the bed shear stress and therefore the sediment transport rates and morphological development.

The presence of bedforms on the riverbed is often a major source of roughness. Therefore, many bed roughness prediction models explicitly or implicitly include the effect of bedform dimensions (e.g. Yalin, 1964; Engelund, 1966; White et al., 1980; Van Rijn, 1984). However, these semi-empirical models are generally based on conditions with unlimited sediment availability, the so-called alluvial conditions. These models do not take a supply-limitation into account and are, therefore, unreliable in these conditions.

Photo 4.1: This photo shows a flume experiment with a supply-limited condition. The immobile gravel layer shows in the dune troughs. The limited sand presence causes reduced bedform dimensions, a decreased bed roughness and sediment transport rate.

Supply-limited conditions exist if an erosion resistant layer exists near the surface of the river bed (see Photo 4.1) and less sediment is supplied from upstream than could have been transported if all of the bed would have consisted of the bedload sediment. The amount of bedload sediment on top of the erosion resistant layer determines the actual transport capacity: the lower the sediment volume, the lower the actual transport capacity. Therefore, an equilibrium develops between the upstream supply and the volume of bedload sediment. The volume of bedload sediment decreases due to erosion, or increases due to sedimentation, until the actual transport capacity matches the upstream supply.

The volume of bedload sediment, or expressed as an average volume per square meter as average layer thickness, exerts a strong influence on the development of bedforms. Kleinhans et al. (2002) gathered flume and field data from supply-limited conditions and used it to study the bedform types and characteristics in relation to supply limitation. They relate the bedform type to the composition of the transported sediment, rather than the bed sediment composition, and to the transport layer thickness. It is described how dunes diminish and form other bedforms types, like flow parallel ribbons and barchanoid dunes, with decreasing sediment availability. A decrease in dune dimensions, or an absence of dunes, due to supply-limitation is relevant for roughness prediction. However, very few model concepts are available that predict the bed roughness and bedform dimensions under supply-limited conditions. A model for supply-limited bed roughness has been formulated by Van der Zwaard (1974). This model requires knowledge of the upstream sediment supply and is therefore difficult to apply in a predictive way. A study into ripple development under supply-limited conditions was recently carried out by Rauen et al. (2009). They conclude that an empirical relaxation equation by Coleman et al. (2005), which describes development rate of ripples, can also be applied in the supply-limited regime. However, the supply-limited steady state dimensions need to be specified and cannot be predicted.

The authors have conducted a set of flume experiments to study the relation between supply-limitation and dune characteristics because of the importance of dune dimensions in roughness prediction and the limited quantitative understanding of this relation. The results of these experiments have been used to develop a bedform dimension reduction (BDR-) function that describes the decrease in dune dimensions due to supply limitation (Tuijnder et al., 2009). These experiments also provide data on bed roughness. These data reflect the decrease in form drag with decreasing bedform dimensions. However, the increasing exposure of the usually coarser immobile layer can cause an increase in grain friction if the supply-limitation is strong.

In this study we improve the roughness prediction under supply-limited conditions by taking into account the reduction in bedform dimensions and the varying immobile layer coverage. This requires sub-models for the prediction of supply-limited bedform dimensions and exposure of the immobile layer. The data needed to develop and test these sub-models and the roughness predictions come from the experiments mentioned before. Several additional data sets with flume experiments under supply-limited conditions are only used to test the models. The experimental data for the model development and testing are described in Section 4.2.

In Section 4.3, we use this data to test the BDR-function as a predictive tool in combination with an alluvial bedform dimensions model (Van Rijn, 1984). Furthermore, a new model concept to predict the exposure of the immobile layer is proposed in this section. The results of these sub-models are used as input to a new model for supply-limited roughness. This

roughness model is an adaptation of the roughness model as proposed by Engelund (1966). These sub-models, for bedform dimensions, immobile layer exposure and roughness, are individually tested against measurements.

In Section 4.4 the model concepts are combined into a new method for roughness prediction in supply-limited and alluvial conditions based on basic input, i.e. the discharge, bed slope and the sediment characteristics. The roughness prediction is based on predicted bedform dimensions and immobile layer exposure. The results of the integrated roughness model are tested again using the measured roughness. Finally the results are discussed in Section 4.5 and the conclusions are summarized in Section 4.6.

4.2 Experimental data

The experimental data used in this study come from an extensive set of flume experiments in which the sediment transport, bedform formation, vertical sorting of sediment and roughness generation were studied. In this study the results of the experiments are used to test methods for the prediction of bedform dimensions, coarse layer exposure and bed roughness. The results of the experiments for the observed bedform dimensions and bed roughness are reported here.

The experiments have been conducted with two uniform grain size distributions, one in the sand and one in the gravel grain size range (Fig. 4.1). The flow conditions in the experiments were in the lower flow regime where dune development is expected for the sand (see e.g. Southard and Boguchwal, 1990; Van den Berg and Van Gelder, 1993), provided that enough mobile sand is present. The critical shear stress for initiation of motion for the gravel was not exceeded in the experiments. However, if these size fractions are mixed a bimodal mixture results. In this mixture, the critical shear stress of the fractions strongly depends on the concentration of the size fraction. The gravel may become mobile if its concentration is low (Curran and Wilcock, 2005). The experimental data in this study come from equilibrium situations where the gravel formed an immobile layer below the migrating bedforms. This caused a limitation of the volume of sand available for sediment transport on top of the immobile layer.

Calibration data – Data set II

The goal of the experiments in Data set II (DS-II) was to find relations between the supply limitation and the bedform dimensions and roughness. For this reason experiments were conducted with varying amounts of sand transporting over an immobile gravel layer. The gravel layer was installed before the experiments and stayed in place during all experiments. The sand was distributed evenly over the gravel layer along the length of the flume. Five series of experiments were conducted in which the layer thickness of the sand (d) was increased between experiments. In this way the supply limitation was reduced. Per series the water depth (h) and discharge (Q) were constant. During the experiments the flume slope was adjusted to maintain uniform equilibrium flow. The experiments were conducted in a sediment-recirculating flume at the Leichtweiss Institute of the Technical University Braunschweig in Germany. This flume has a width of 2 m and an approximate length of 30 m. The width was reduced to 1 m for the experiments. Over a length of 17.5 m the bed and water level was measured using echo sensors that were mounted on a measurement carriage. The total boundary shear stress was calculated from the gradient of the energy level over the measurement section. The bed shear stress (τ_b) was calculated with the wall roughness correction method proposed by Vanoni and Brooks (1957). The results of these experiments, in terms of average bed shear stress and average dune height (Δ) and length (Λ) are tabulated in Table 4.1.

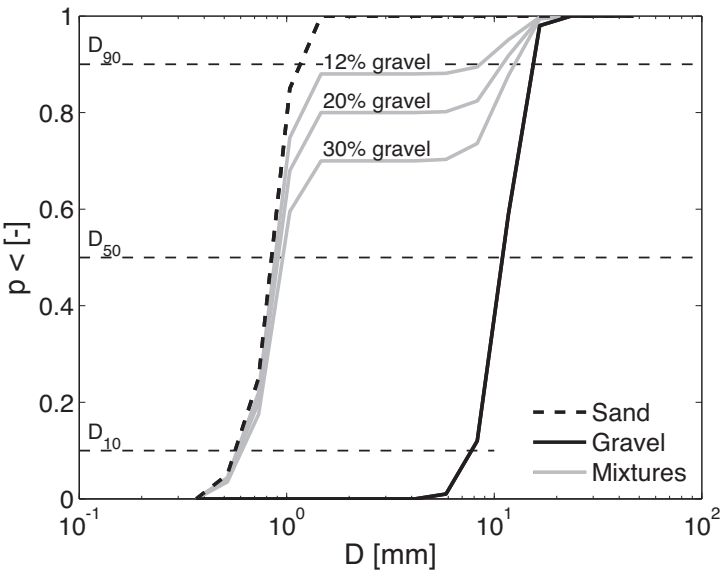

Figure 4.1: Grain size distribution of the sediment used in the experiments. The sand layer was installed on top of the gravel layer in DS-I and II. In DS-III and IV a homogeneous mixture of sand and gravel was installed in the flume. The grain size distributions of the mixtures used in DS-III are shown. The mixtures of DS-IV are similar only the sand-gravel ratio differs.

Data Set	Exp Nr	d [m]	Q [m³/s]	h [m]	I_e [-]	τ_b [N/m²]	Δ [m]	Λ [m]	Δ_0 [m]	P_{cl} [-]
II	1-1	0.000	0.074	0.20	0.0007	1.25	0.000	0.00	0.080	1.00
II	1-2	0.003	0.105	0.20	0.0008	1.33	0.006	0.26	0.080	0.50
II	1-3	0.003	0.104	0.20	0.0008	1.38	0.006	0.29	0.080	0.50
II	1-4	0.011	0.104	0.20	0.0008	1.35	0.024	0.64	0.080	0.33
II	1-5	0.012	0.106	0.20	0.0008	1.41	0.023	0.65	0.080	0.33
II	1-6	0.020	0.105	0.20	0.0012	2.06	0.040	0.84	0.080	0.20
II	1-7	0.041	0.104	0.20	0.0016	2.87	0.057	1.13	0.080	0.10
II	1-8	0.068	0.104	0.20	0.0018	3.37	0.076	1.34	0.080	0.00
II	1-9	0.097	0.104	0.20	0.0019	3.32	0.077	1.46	0.080	0.00
II (a)	1-10	0.161	0.105	0.20	0.0022	3.97	0.077	1.44	0.080	0.00
II	2-1	0.000	0.151	0.30	0.0008	2.17	0.000	0.00	0.091	
II	2-2	0.003	0.156	0.30	0.0006	1.36	0.007	0.34	0.091	
II	2-3	0.011	0.157	0.30	0.0004	0.90	0.024	0.74	0.091	
II	2-4	0.019	0.156	0.30	0.0007	1.66	0.042	0.90	0.091	
II	2-5	0.039	0.153	0.30	0.0008	2.06	0.065	1.23	0.091	
II	2-6	0.067	0.157	0.29	0.0012	3.18	0.080	1.33	0.091	
II	2-7	0.095	0.157	0.30	0.0009	2.24	0.086	1.64	0.091	
II	3-1	0.004	0.079	0.15	0.0013	1.74	0.008	0.34	0.067	
II	3-2	0.011	0.079	0.15	0.0012	1.56	0.022	0.64	0.067	
II	3-3	0.021	0.077	0.15	0.0014	1.94	0.035	0.84	0.067	
II	3-4	0.037	0.078	0.16	0.0014	1.95	0.048	1.06	0.067	
II	3-5	0.067	0.079	0.15	0.0020	2.88	0.059	1.26	0.067	
II (a)	3-6	0.160	0.080	0.15	0.0026	3.70	0.068	1.37	0.067	
II	4-1	0.004	0.135	0.20	0.0012	2.07	0.007	0.29	0.081	
II	4-2	0.012	0.135	0.20	0.0017	3.01	0.028	0.69	0.081	
II	4-3	0.021	0.116	0.20	0.0016	2.82	0.042	0.86	0.081	
II	4-4	0.039	0.116	0.20	0.0021	3.91	0.059	1.03	0.081	
II	5-1	0.003	0.093	0.20	0.0006	1.05	0.007	0.34	0.069	
II	5-2	0.004	0.093	0.20	0.0007	1.12	0.006	0.32	0.069	
II	5-3	0.009	0.092	0.20	0.0006	0.92	0.016	0.76	0.069	
II	5-4	0.019	0.093	0.20	0.0006	1.05	0.033	0.95	0.069	
II	5-5	0.038	0.093	0.20	0.0008	1.43	0.052	1.20	0.069	
II	5-6	0.065	0.093	0.20	0.0012	2.24	0.067	1.37	0.069	
II	5-7	0.159	0.094	0.20	0.0014	2.71	0.067	1.34	0.069	
II	5-8	0.159	0.094	0.20	0.0017	3.05	0.064	1.25	0.069	
II (a)	5-9	0.160	0.094	0.20	0.0015	2.84	0.070	1.39	0.069	
a	6-1	0.160	0.130	0.25	0.0017	3.87	0.083	1.47	0.083	
a	6-2	0.157	0.135	0.25	0.0020	4.71	0.084	1.46	0.084	
a	6-3	0.160	0.150	0.26	0.0022	5.21	0.095	1.49	0.095	

Table 4.1: Overview of the key variables in the experiments that form the data set that has been used for calibration and development of models for bedform dimensions and roughness prediction. The alluvial experiments are indicated with a letter 'a' in the 'Data set' column. Δ_0 is the alluvial dune dimension for the same flow velocity and water depth under alluvial conditions. p_{cl} is the relative bed area of exposed coarse immobile layer. The other symbols are defined in the text.

Validation data – Data sets I, III, IV and V

The experiments of DS-I have been conducted as a pre-study for the experiments of DS-II. The experiments in DS-I are similar in setup to the experiments in DS-II. Also in these experiments sand is transported over a pre-installed gravel layer. Between the experiments the sand layer thickness was increased. These experiments have been conducted in a smaller flume (7 m x 0.3 m) without a tilting mechanism. The bed slope was pre-installed and uniform flow had to be maintained by adjusting the downstream weir. This causes the water depth to vary slightly depending on the bed roughness that develops. The gravel layer used in DS-I was a bit coarser

than in the other experiments. The gravel between the 11.2 and 16 mm sieves has been used so the average grain size was approximately 13.6 mm.

The experiments of data set III and IV are different in their setup. In these experiment the degree of supply limitation was not determined a priori, but resulted from vertical sorting. Varying ratios of sand and gravel (see Table 4.2) were thoroughly mixed before the experiment. Vertical sorting of sand and gravel during the runs led to the development of an immobile layer that limited the further entrainment of sand from below the layer. It was observed that the immobile layer developed with less sand being transported on top of it with an increasing gravel concentration. The data used in this study is from the equilibrium situation after the development of an immobile layer. The experiments of DS-III were a pre-study to the experiments of DS-IV. For DS-III the smaller flume that was also used for DS-I has been used, while the experiments of DS-IV were conducted in the large flume.

The experiments of DS-V have been conducted with a smooth immobile layer instead of a gravel layer. This immobile layer was the flume bottom that is made of painted steel and locally of PVC sheets. Apart from that, the experimental procedure was equal to that of DS-II.

Data Set	Exp Nr	d [m]	Q [m^3/s]	h [m]	I_e [-]	τ_b [N/m^2]	Δ [m]	Λ [m]	Δ_0 [m]	Gravel [%]
I	7-1	0.006	0.020	0.12	0.0019	1.64	0.011	0.42	0.032	
I	7-2	0.010	0.020	0.12	0.0021	1.81	0.019	0.54	0.032	
I	7-3	0.013	0.020	0.13	0.0022	2.06	0.021	0.54	0.032	
I	7-4	0.015	0.020	0.13	0.0022	2.21	0.025	0.63	0.032	
I	7-5	0.018	0.020	0.13	0.0018	1.71	0.026	0.62	0.032	
I	7-6	0.022	0.020	0.13	0.0023	2.37	0.029	0.66	0.032	
I (a)	7-7	0.027	0.020	0.13	0.0024	2.42	0.032	1.08	0.032	
III	8-1	0.006	0.029	0.18	0.0014	1.51	0.012	0.30	0.039	30
III	8-2	0.013	0.029	0.18	0.0016	2.06	0.025	0.71	0.039	20
III	8-3	0.017	0.029	0.18	0.0018	2.84	0.030	0.72	0.039	12
III (a)	8-4	0.021	0.029	0.19	0.0018	2.27	0.037	0.87	0.039	0
IV	9-1	0.070	0.104	0.20	0.0015	2.81	0.062	1.06	0.080	5
IV	9-2	0.046	0.104	0.20	0.0013	2.31	0.052	0.98	0.080	10
IV	9-3	0.034	0.104	0.20	0.0011	1.93	0.046	0.83	0.080	15
IV	9-4	0.026	0.156	0.30	0.0006	1.50	0.044	0.91	0.091	15
IV	9-5	0.031	0.120	0.20	0.0017	2.98	0.048	0.86	0.080	15
IV	9-6	0.016	0.104	0.20	0.0009	1.54	0.031	0.76	0.080	20
V	10-1	0.010	0.094	0.20	0.0003	0.52	0.022	1.00	0.069	
V	10-2	0.020	0.094	0.20	0.0005	0.87	0.034	0.92	0.069	
V	10-3	0.040	0.094	0.21	0.0013	2.42	0.056	1.01	0.069	

Table 4.2: Overview of the key variables that form the data set that has been used for verification of model concepts. The column '% Gravel' indicates the percentage of gravel in the initially fully-mixed sediment mixture.

Data use

The experimental data used in this study is divided into two data sets: the calibration data set and the validation data set. The calibration data, data set II, has been used in Tuijnder et al. (2009) to develop a method to predict bedform dimensions under supply-limited conditions. This model has an important role in the roughness prediction method that is proposed below.

Therefore this data set is not an independent test for any prediction based on this supply-limited bedform dimensions model. The amount of calibration of sub-models in this study is very limited and has been done using data set II in order to reserve the other data sets for independent testing of the model concepts. Data sets I, III, IV and V are the validation data set.

Observed roughness variation

The supply limitation can be characterized using the ratio d/Δ_0. This is the ratio of the average layer thickness of the bedload sediment on top of the coarse layer (d) to the alluvial dune height (Δ_0). The parameter Δ_0 is defined as the dune height that occurs under alluvial conditions (without supply limitation) under the same flow velocity and water depth. The values of Δ_0 that have been used are reported in Table 4.1 and 4.2. The alluvial dune dimensions for DS-II are the asymptotic dune heights that are observed with increasing sediment layer thickness (Tuijnder et al., 2009). For DS-I the results from experiment 7-7 have been used as the alluvial dune height. The alluvial dune height for DS-III has been determined in a separate alluvial experiment with the same water depth and flow velocity. The experiments of DS-IV and V have been conducted under boundary conditions equal to one of the series of DS-II. Therefore the alluvial dune dimensions from the alluvial experiments of DS-II have also been used for DS-VI and DS-V.

The bed roughness varies with varying supply limitation (d/Δ_0). This is shown in Figure 4.2. The roughness is expressed as a friction coefficient that is defined as:

$$\tau_b = c_{f,b}\rho u^2 \qquad \text{(Eq. 4.1)}$$

In this function τ_b is the bed shear stress, $c_{f,b}$ is the bed friction factor, u is the cross-section averaged flow velocity and ρ the fluid density.

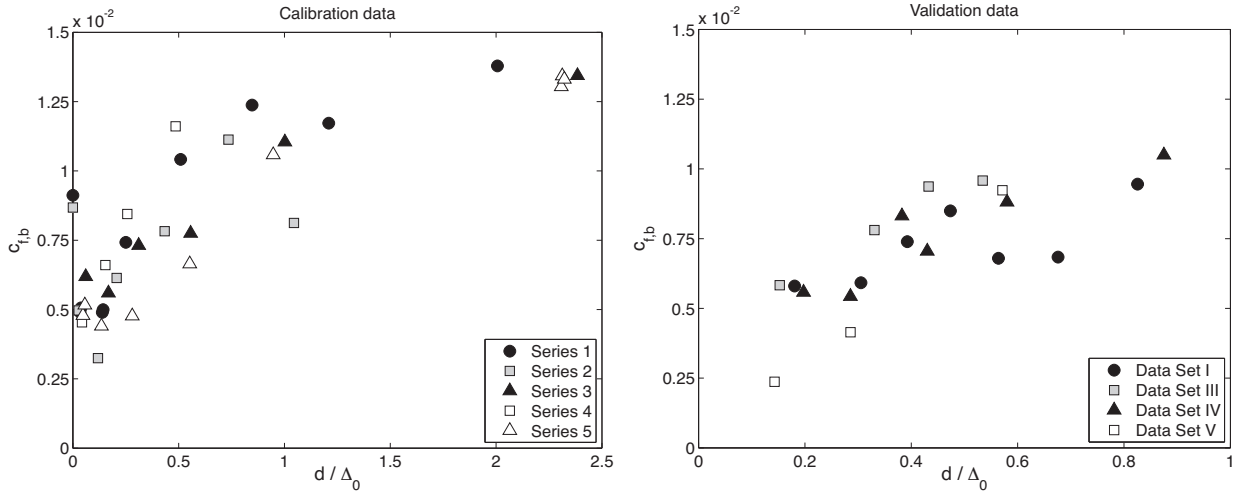

Figure 4.2: The variation in bed roughness with supply limitation (d/Δ_0).

In the left panel in Figure 4.2, first two experiments can be seen on the vertical axis; these were conducted without sand on top of the gravel layer. Therefore, all roughness can be

attributed to grain friction caused by the gravel layer. The roughness drops with increasing sediment availability ($0<d/\Delta_0<0.25$). The limited amount of sand fills in the gaps between the gravel particles and smoothes the bed in this regime. Too little sand is present for the development of dunes. An example of such a bed is given in Figure 4.3A. The roughness increases again with further increasing sediment availability ($0.25<d/\Delta_0<1$). This is caused by the increase of bedform dimensions with increasing sediment availability. An example of a bed configuration from this regime is shown in Figure 4.3B. With further increasing sediment availability ($d/\Delta_0>1$), the bed gradually becomes alluvial (Fig. 4.3C) and the roughness reaches its maximum. The roughness data from the validation data sets (Fig. 4.2 right panel) also show an increasing trend.

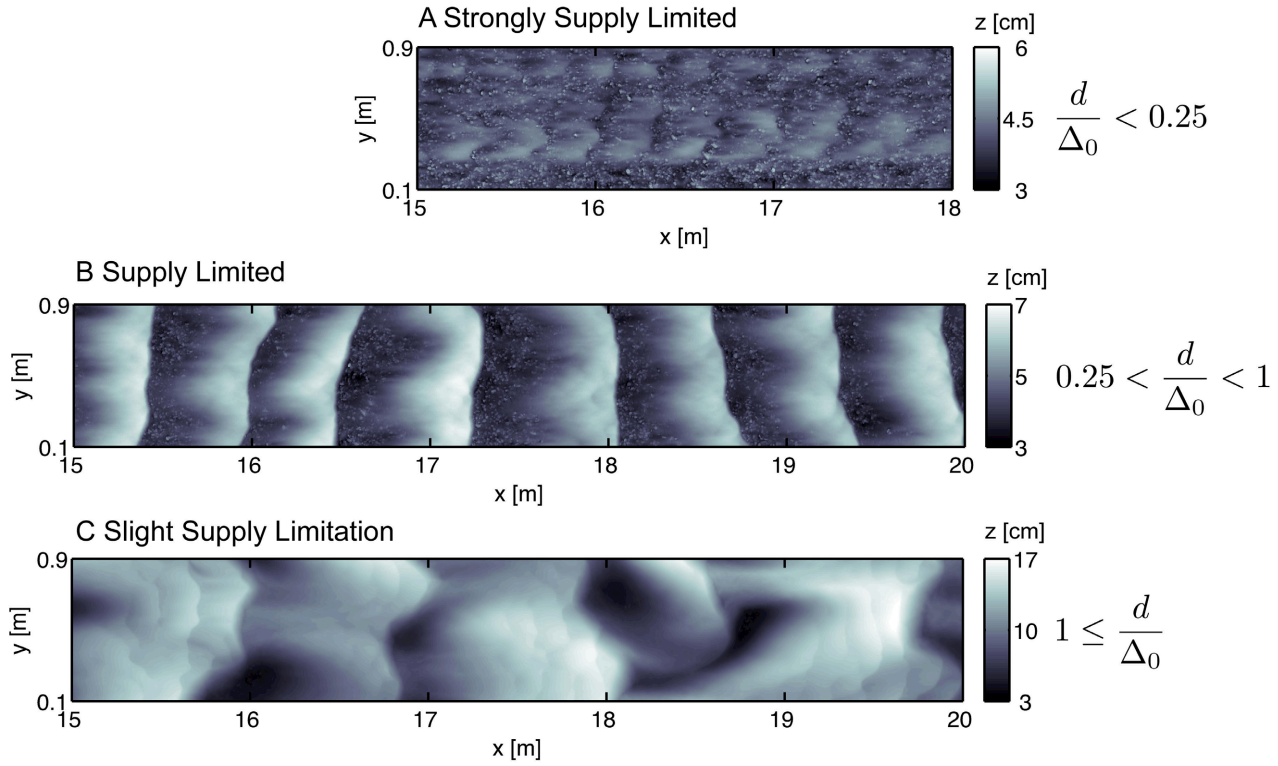

Figure 4.3: High-resolution height measurements of the bed after Exp. 1-3 (A), 1-5 (B) and 1-8 (C). Exp. 1-8 is almost alluvial ($d\approx\Delta_0$). The bedform dimensions are only slightly reduced compared to alluvial bedforms.

The decrease in dune dimensions with limited sediment supply, which causes the decreasing roughness, is shown in Figure 4.4. This Figure shows the variation in relative bedform dimensions (Δ/Δ_0) with varying supply limitation. A clear decline in bedform height with decreasing sediment availability can be seen. We consider the system to be supply limited if $d/\Delta_0 < 1$. This value is somewhat arbitrary because of the asymptotic nature of the approach of bedform dimensions towards the alluvial dimensions. However, the bedform dimension reach more than 92% of the alluvial bedform height (Tuijnder et al., 2009) and the bedform height decreases rapidly below $d/\Delta_0 = 1$. While above $d/\Delta_0 = 1$ the bedform dimensions grow gradually towards the alluvial dimensions.

Another source of roughness variation with varying supply limitation is the variation in coverage of the immobile layer. Increasing exposure of the immobile layer increases the grain shear stress if this immobile layer is coarser than the bedload sediment. If, on the contrary, the immobile layer is smoother than the bedload sediment, the grain shear stress decreases with increasing immobile layer exposure. The decrease in immobile layer exposure, with increasing *d*, is illustrated qualitatively in Figure 4.3 and quantitatively in Figure 4.7 in Section 4.3.

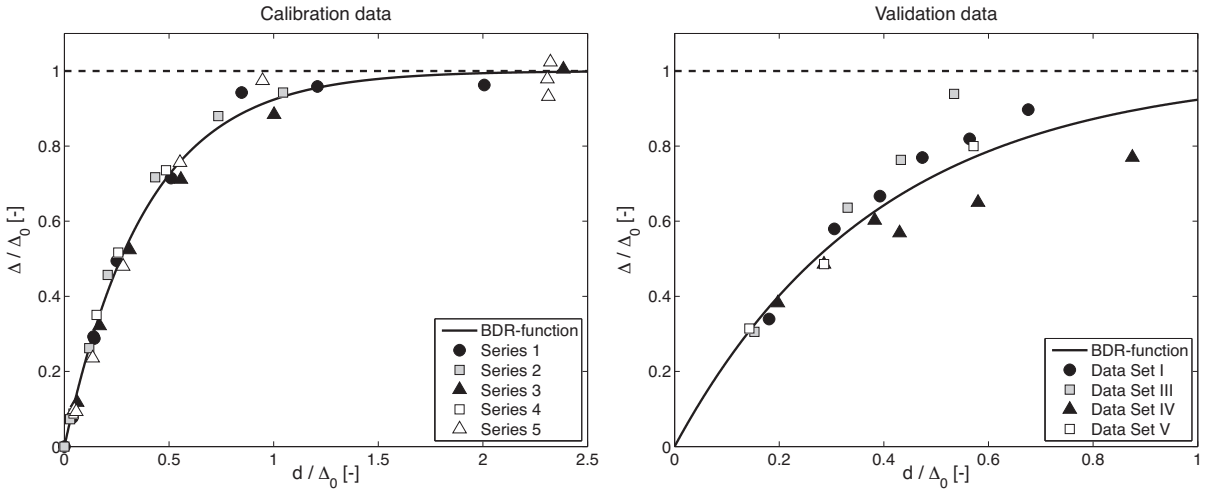

Figure 4.4: Relative dune height plotted against a measure of supply limitation (d/Δ_0). The calibration data (left Figure) is DS-II. The BDR-function is introduced in Section 4.3.

4.3 Roughness model for supply-limited conditions

In the previous section it was shown that the variations in dune dimensions and exposure of the (coarse) immobile layer cause roughness variations. For the prediction of these roughness variations we want to be able to predict the supply-limited dune dimensions and the immobile layer exposure. First methods to predict these variables are presented and tested using experimental data. Subsequently, a method to use this information for better bed roughness prediction is presented. The bed roughness predictor of Engelund (1966) is adapted for supply-limited conditions and is tested using the experimental data.

Bedform dimension prediction

The bedform dimensions, including supply-limited bedform dimensions, can be predicted if an alluvial bedform dimension prediction model is combined with the bedform dimensions reduction (BDR-) model of Tuijnder et al. (2009). This BDR-function reads as:

$$\frac{\Delta}{\Delta_0} = 1 - \exp\left(\frac{-d}{\alpha_h \Delta_0}\right) \qquad \text{(Eq. 4.2)}$$

$$\frac{\Lambda}{\Lambda_0} = 1 - \beta \exp\left(\frac{-d}{\alpha_l \Delta_0}\right) \qquad \text{(Eq. 4.3)}$$

The values of α determine the rate of increase in bedform dimensions with decreasing supply limitation (increasing d/Δ_0). The α_h = 0.39, α_l = 0.24 and β = 0.96, have been determined with the data from DS-II, the calibration data set. Figure 4.4 shows a comparison of the BDR-function with the measured data; the left panel shows a comparison with DS-II and the left panel with DS-I, III, IV and V. The application of the BDR-function to DS-II is not a test of the model since the function has been derived from DS-II. However, the application of the model to the validation data set is an independent test of this model. On average the agreement of the model with the measurements is good.

The bedform height and length predictors of Van Rijn (1984) have been selected to predict the alluvial bedform dimensions. The model reads as:

$$\frac{\Delta_0}{h} = 0.11 \left(\frac{D_{50}}{h}\right)^{0.3} \left(1 - e^{-0.5T}\right)(25 - T) \qquad \text{(Eq. 4.4)}$$

$$\Lambda_0 = 7.3h \qquad \text{(Eq. 4.5)}$$

In this function T is the bed shear stress parameter that is defined as:

$$T = \frac{\theta' - \theta_{cr}}{\theta_{cr}} \qquad \text{(Eq. 4.6)}$$

θ_{cr} is the critical shields parameter for initiation of motion. For θ_{cr} the fit of the shields curve (Shields, 1936) by Brownlie (1981) and modified by Parker has been used. This formula reads as:

$$\theta_{cr} = 1/2 \left(0.22 Re_p^{-0.6} + 0.06 * 10^{-7.7 Re_p^{-0.6}} \right) \quad \text{(Eq. 4.7)}$$

Where Re_p is the particle Reynolds number and is defined as:

$$Re_p = \frac{\sqrt{RgD_{50}} D_{50}}{\nu} \quad \text{(Eq. 4.8)}$$

The parameter R is the relative density of the sediment: $R=\rho_s/\rho_w$. The kinematic viscosity (ν) is approximately 10^{-6} at 20˚C. θ' is the grain related shields parameter calculated using:

$$\theta' = \frac{\tau'}{(\rho_s - \rho) g D_{50}} \quad \text{(Eq. 4.9)}$$

$$\tau' = c_{f,90} \rho u^2 \quad \text{(Eq. 4.10)}$$

$$c_{f,90} = g \left(18 \log \frac{12 R_b}{3 * D_{90}} \right)^{-2} \quad \text{(Eq. 4.11)}$$

This model predicts the bedform dimensions under alluvial conditions, denoted by the subscript 0.

The model for the alluvial dune dimensions has been calibrated using the alluvial experiments (indicated with an 'a' in Table 4.1) from the calibration data set. The average ratio of $\Delta_{meas}/\Delta_{pred}$ is 1.29, therefore the results of the Van Rijn dune height predictor are multiplied with this factor. The average ratio of $\Lambda_{meas}/\Lambda_{pred}$ is 0.89, also this ratio is used as a correction factor.

Figure 4.5 shows a comparison of the measured bedform dimensions with predictions using Van Rijn's model for alluvial conditions as well as this model combined with the BDR-function. The gray points are predicted using Van Rijn's model, the black points are predicted using the combined model. It can be seen that the alluvial model overpredicts the bedform dimensions under supply-limited conditions. The combined model predicts the bedform heights accurately. The scatter is a bit larger for the bedform length predictions but on average the prediction is accurate and the overprediction of the alluvial model disappears. The model results for the validation data set also show a good agreement with the measured data, although the scatter is a bit larger.

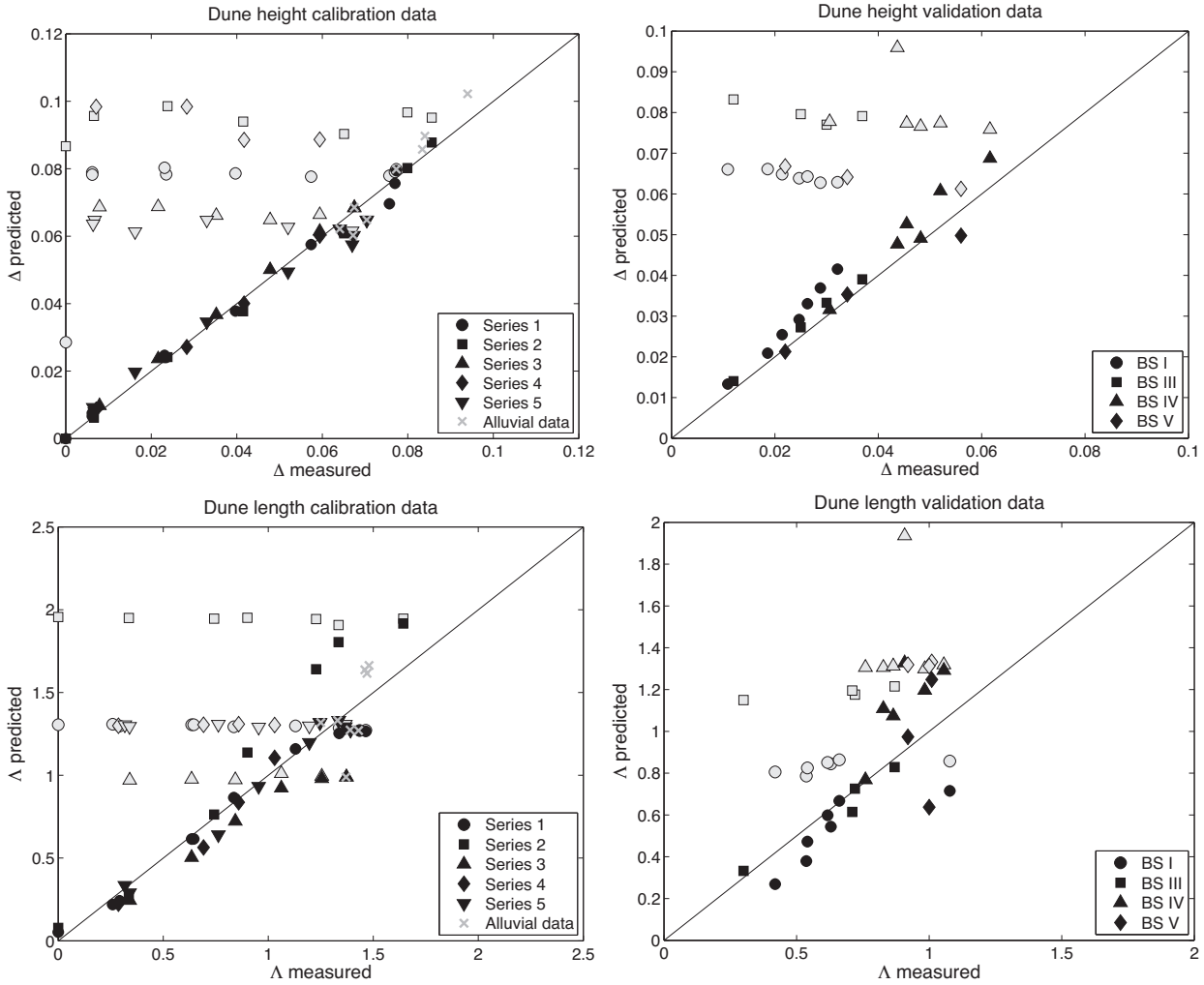

Figure 4.5: Test of the bedform dimensions prediction model. The symbols indicate the series; the gray symbols are the predictions using the Van Rijn (1984) model, the black symbols are the bedform dimensions predictions using the Van Rijn model in combination with the BDR-function.

Immobile layer coverage model

In order to predict the coverage of the coarse layer by the bedforms the vertical distribution of bed levels of a dune field around the mean bed level is considered. Although the bed level distribution of a single dune is not Gaussian because of the usually convex shape of dunes, the vertical bed level distribution of an alluvial bed with ripples and/or dunes usually can be approximated by a Gaussian distribution (Nordin, 1971). The bed level distribution tends to be slightly skewed towards the higher bed levels due to the development of deep troughs (Ribberink, 1987). Here, for simplicity, the bed level distribution of a dune field without immobile layer is considered to be Gaussian. An example of an observed bed level distribution of a practically alluvial situation is given in Figure 4.6 Exp 1-9, together with its Gaussian approximation.

Figure 4.6 shows the observed bed level distributions from DS-II Series 1. The upper panel shows the observed distribution (black line) and the lower panel shows the cumulative distribution. The top of the immobile layer (z_{til}) is assumed to be $½D_{cl}$ above the average

immobile layer level (z_{cl}): $z_{til} = z_{cl} + \frac{1}{2}D_{cl}$, where D_{cl} is the average grain size of the immobile layer. In Fig. 4.6 z_{cl} is put to zero and z_{til} is indicated with a dashed line. Most of the observed distributions show two maxima. The upper maximum is at the level where most bedform crests are present. The exposed immobile layer causes the lower maximum. In Exp 1-3 the upper maximum is missing because no dunes developed. In Exp 1-9 the immobile layer was almost completely covered with sand and the immobile layer was not observed anymore.

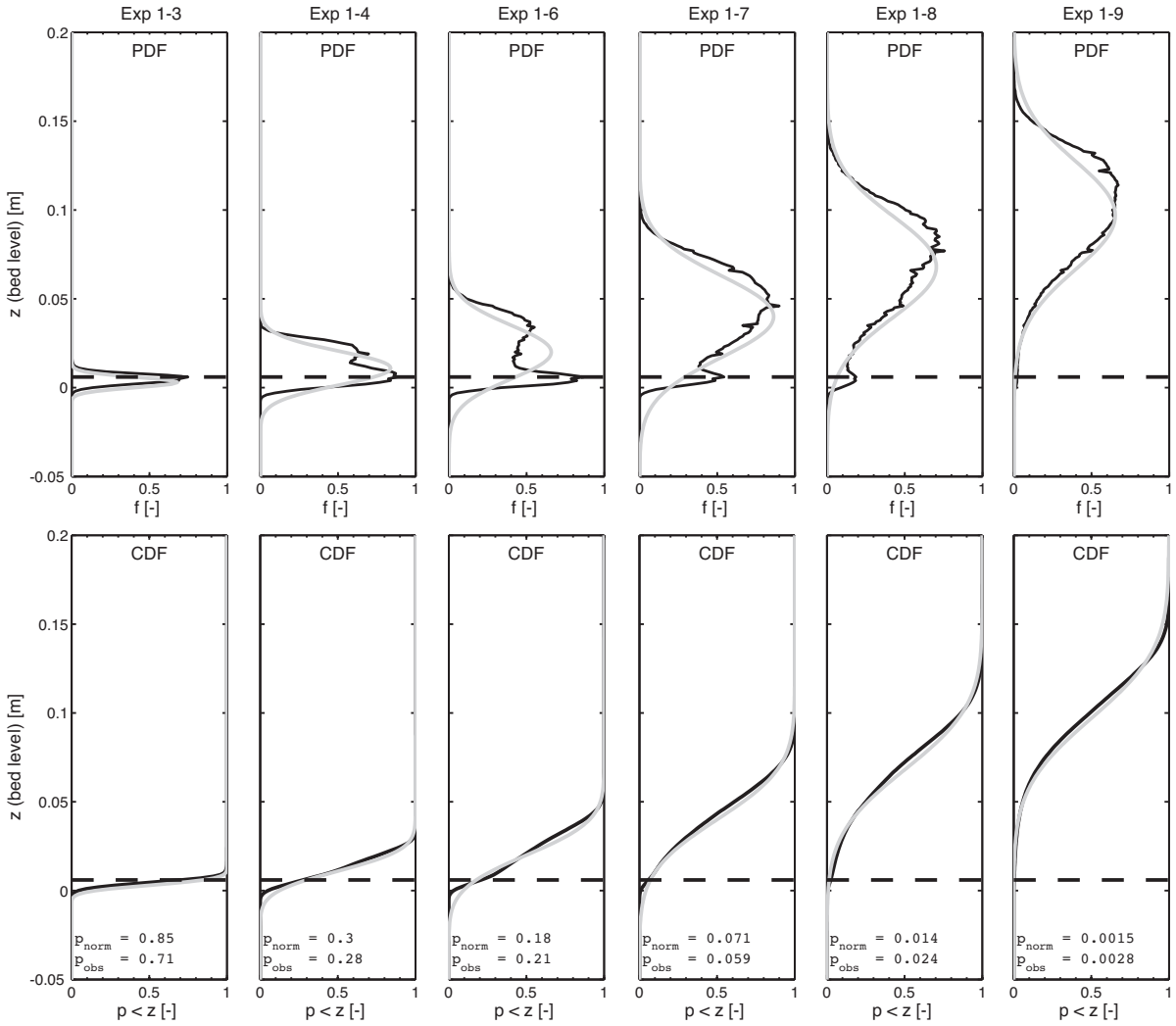

Figure 4.6: The bed level distribution is shown in the upper panels. In black the observed distribution is shown. The grey line shows the approximation of this distribution. The lower panels show a cumulative bed level distribution. This is used to estimate the how much of the coarse layer is exposed.

The trough of a dune on an immobile layer cannot develop completely because of the exposed immobile layer between the dunes. It can be hypothesised that the area where the immobile layer is exposed between two dunes is the same as the area that would otherwise develop under the level of the top of the immobile layer. This hypothesis is tested by comparing the fraction of the PDF that was observed below z_{til} (= CDF at z_{til}) to the visually estimated relative exposed area of the immobile layer as reported in Table 4.1. The bottom panel of Figure 4.6 shows the cumulative empirical distribution. The value of this distribution at the level $z = z_{til}$ should approximately agree with the exposed area estimated visually from photos of the

experiments. These values are compared in Figure 4.7. The visually estimated values are indicated with a gray square and the fraction measured below z_{til} with a black diamond. It can be seen that the exposed area decreases with increasing average layer thickness and that there is a good agreement between the two values. This confirms that the assumed value of $½D_{cl}$ is suitable for estimating the coarse layer exposure.

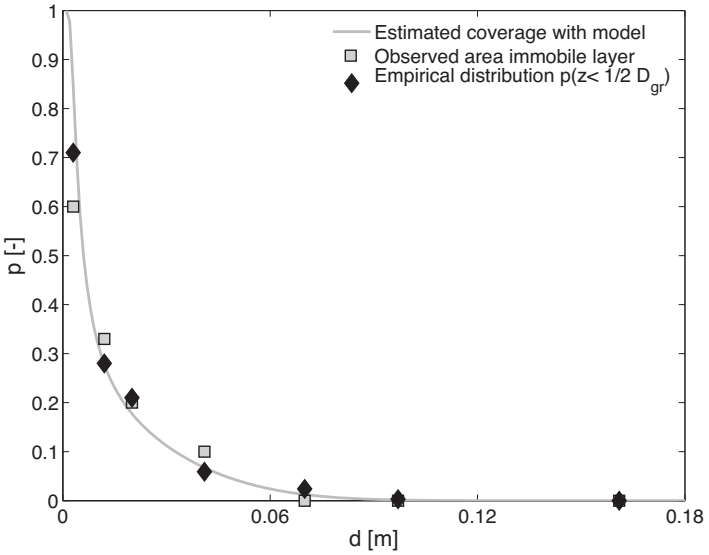

Figure 4.7: Comparison of the observed immobile layer fraction with the fraction of the bed level distribution below z = z_{til} and the modelled bed coverage.

However, the vertical bed level distribution of the supply-limited dunes needs to be known in advance in order to be able to make predictions of the immobile layer exposure. Unfortunately this distribution is unknown and therefore the Gaussian bed level distribution that develops under alluvial conditions is used as an approximation. In principle, the Gaussian distribution predicts the presence of bed levels in the troughs of the dunes below the immobile layer, which do not develop in reality. This is schematically illustrated in Figure 4.8. Therefore it is tested whether the fraction of the Gaussian distribution that is predicted under the top of the immobile layer agrees with the fraction of the bed where in the actual situation the immobile layer is exposed. The parameters of Gaussian distribution, the mean (μ) and standard deviation (σ), are estimated as follows.

The bedforms develop in the sand layer, with average layer thickness d, on top of the coarse layer, which has an average level of 0 m. Therefore the mean of the bed level distribution is at $z = d$. In Tuijnder et al. (2009) it was shown that the dune heights are related to the standard deviation of the Gaussian bed level distribution also under supply-limited conditions. In Nordin (1971) it has been shown that Δ/2 is distributed according to a Rayleigh distribution if the bed elevations have a Gaussian distribution with standard deviation σ. This can be expressed as:

$$f_{\Delta}\left(\frac{\Delta}{2}\right) = \frac{\Delta}{\sigma} e^{-\left(\frac{\Delta}{2\sqrt{\sigma}}\right)^2} \qquad \text{(Eq. 4.12)}$$

The mean of the dune heights (μ_Δ) is therefore related to the standard deviation (σ) according to (Bendat and Piersol, 2000):

$$\mu_\Delta = 2\sigma\sqrt{\frac{\pi}{2}} \approx 2.5\sigma \qquad \text{(Eq. 4.13)}$$

We use this relation to estimate the standard deviation using the predicted bedform height. The equation that describes the Gaussian (or normal) distribution reads as:

$$f_g(z) = \frac{1}{\sigma\sqrt{2\pi}} e^{-\frac{(z-\mu)^2}{2\sigma^2}} \qquad \text{(Eq. 4.14)}$$

This function is shown in Figure 4.6 in the upper panels with a gray line. This shows that this distribution indeed predicts bed level below the immobile layer. The cumulative distribution has to be evaluated at level z_{til} if we want to test whether the Gaussian distribution can be used to predict the fraction of the bed where in the immobile layer is exposed. The value of the cumulative Gaussian distribution at a level $z = z_{til}$ is calculated as:

$$p = \frac{1}{\sigma\sqrt{2\pi}} \int_{-\infty}^{z_{til}} e^{-\frac{(z-\mu)^2}{2\sigma^2}} dz \qquad \text{(Eq. 4.15)}$$

Using the definition of the error function, the proposed method for exposure estimation can be written as:

$$p = 1/2(1 - \mathrm{erf}(-t)) \qquad \text{(Eq. 4.16)}$$

with:

$$t = \frac{z_{til} - \mu}{\sigma\sqrt{2}} \qquad \text{(Eq. 4.17)}$$

$$\mu = d \qquad \text{(Eq. 4.18)}$$

$$\sigma = \frac{\Delta}{2.5} \qquad \text{(Eq. 4.19)}$$

$$z_{til} = z_{cl} + 1/2 D_{cl} \qquad \text{(Eq. 4.20)}$$

The lower panels of Figure 4.6 show the cumulative Gaussian distribution in gray. This figure shows that at the level of the top of the coarse layer the Gaussian distribution has approximately the same value as the observed bed level distribution with immobile layer.

The results of this model are shown in Figure 4.7 with the gray line. The model indeed agrees with both the visually estimated immobile layer exposure and also with the fraction of the empirical distribution below the top of the coarse layer. Therefore we conclude that this

model concept can give a good estimation of the immobile layer exposure between supply-limited dunes.

The dune length Λ is defined as the length between two consecutive crossings of the average bed level. The length of a dune from lee-toe to stoss-toe can be calculated if p is known with the following relation (see also Figure 4.8):

$$L = \Lambda(1 - p) \qquad \text{(Eq. 4.21)}$$

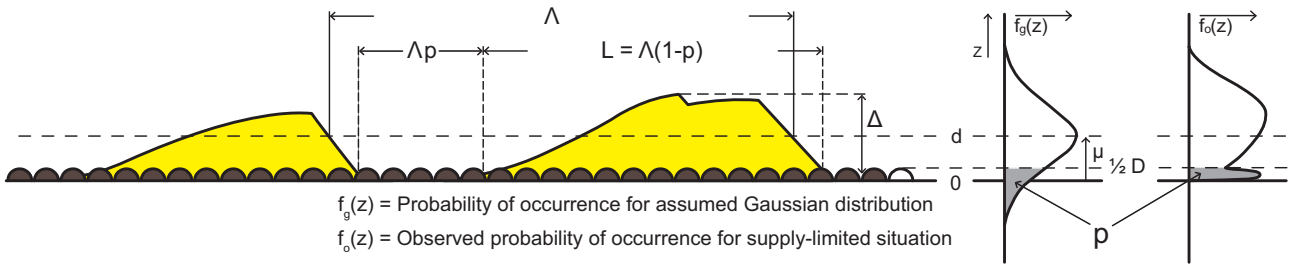

Figure 4.8: Schematic illustration of dunes on an immobile layer with the definitions of some of the important variables.

Roughness prediction

Recently Van der Mark (2009) studied the prediction of form drag caused by bedforms. In this study it was concluded that the form drag predictors by Yalin (1964) and Engelund (1966) are a good choice to predict roughness for alluvial flume data. These models have simple expressions and the more complex methods presented in Van der Mark (2009) do not perform better. However, it is also concluded that the models of Engelund and Yalin may be expected to overpredict for field conditions. For field conditions the application of the semi-analytical model presented in Van der Mark (2009) is recommended. The simpler model of Engelund is used for roughness prediction since we are dealing with flume data with a mobile bed. This model has been adapted to improve the prediction of roughness under supply-limited conditions by taking the variable coarse layer coverage and variable bedform dimensions into account. First, the alluvial model is described below and subsequently the adaptations for SL-conditions are introduced.

Engelund as well as Yalin assume that the bed shear stresses caused by grain friction and expansion losses can be added:

$$\tau_b = \tau_b' + \tau_b'' \qquad \text{(Eq. 4.22)}$$

Yalin and Engelund used different roughness parameters to express their models. For convenience only one friction factor definition is used here. The friction factor is defined in the following relation:

$$\tau_b = c_{f,b}\rho u^2 \qquad \text{(Eq. 4.23)}$$

In this equation u is the cross-section averaged flow velocity. Analogous to this function the grain related friction coefficient (c_f') and the form-drag-related friction coefficients (c_f'') are defined. The cross-section averaged velocity is considered determinative for both friction contributions. Therefore Eq. 4.22 can be rewritten as:

$$c_{f,b} = c_f' + c_f'' \qquad \text{(Eq. 4.24)}$$

The grain related friction coefficient is estimated using a White-Colebrook type formula:

$$\frac{u}{u_*'} = \frac{u}{\sqrt{gR_b'I}} = 6 + \frac{1}{\kappa}\ln\frac{R_b'}{k_s} \qquad \text{(Eq. 4.25)}$$

with:

$$c_f' = \left(\frac{u}{u_*'}\right)^{-2} \qquad \text{(Eq. 4.26)}$$

In these formulas R_b' is the grain related part hydraulic radius of the bed R_b. The latter can, in flume experiments with smooth sidewalls, be estimated using the method of Vanoni and Brooks (1957). The parameter κ is the Von Kármán constant, a turbulence related constant with value 0.4. The parameter I is the bed or water level slope; here I_e, the gradient of the energy level, is used. The models of Yalin and Engelund differ slightly in the way the White-Colebrook equation is applied. Yalin uses $k_s = D_{50}$; furthermore he assumes that grain friction only occurs at the stoss side of a dune. He corrects the grain friction coefficient using a factor Λ_{st}/Λ where Λ is the dune length and Λ_{st} is the length of the stoss side. Yalin uses the water depth instead of the hydraulic radius for the bed. Engelund uses $k_s = 2D_{65}$ and the hydraulic radius. Engelund (1966) and Yalin (1964) both use Carnot's formula for sudden expansions in pipe flow to estimate the expansion losses caused by the flow expansion behind dunes. Expressed as a friction coefficient the relation reads as:

$$c_f'' = \frac{\Delta^2}{2h\Lambda} \qquad \text{(Eq. 4.27)}$$

Adaptations for Supply-limited conditions

The bed form roughness predictor of Engelund and Yalin is analytically derived for a series of backward facing steps with a distance Λ between the steps. Under supply-limited conditions a distance appears between the dunes. However, this does not affect the application of Eq. 4.27 since the supply-limited dune length predictor (Eq. 4.3) predicts the length between the lee-faces (Λ) and not the dune length from toe to toe (L). Therefore the form drag is predicted using Eq. 4.27 under supply-limited conditions as well.

Apart from the variation of form drag and bedform dimensions due to supply limitation the grain friction is also variable. Variation in supply limitation introduces variation in the grain roughness because of two processes: 1) the coverage of the immobile layer that is composed of a usually coarser sediment with bedform of finer mobile sediment, and 2) the roughness of the coarse layer varies due to the infilling of the interstice space between the particles with finer grained sediment.

For the prediction of grain roughness a White-Colebrook type of formula is applied. In order to deal with the variation in infilling of the immobile layer and the partial coverage of the immobile layer the used k_s values will be varied and the roughness is calculated for the immobile layer and the bedload sediment separately. This approach is described below.

The grain roughness height is assumed to vary between the grain roughness height of the coarse immobile layer and the mobile sand bed. The grain roughness height is usually estimated as a factor (*X*) times a representative grain size.

$$k_s = X^* D_{xx} \qquad \text{(Eq. 4.28)}$$

Where D_{xx} is the grain size for which xx percent of the distribution is finer. If the volume of sand grains is small compared to the space between gravel particles, the sand will move through the interstice space of the gravel layer. The filling up of the pockets between the particles reduces the roughness of the gravel layer (Tuijnder et al., 2008). The model concept to predict this reduction of the coarse layer roughness is based on the model of Van der Zwaard (1974). In this concept the roughness height of the coarse layer is assumed to linearly decrease with an increasing thickness of the sand layer (*d*) until the coarse layer is saturated ($d = d_{sat}$) and transport starts to take place over the coarse layer rather than predominantly through the interstice space. Saturation of the gravel layer takes place over the interval:

$$0 < d < d_{sat} \qquad \text{(Eq. 4.29)}$$

It is assumed that d_{sat} is related to the grain size of the immobile layer. Using the schematization of the half spheres (Figure 4.8):

$$d_{sat} = {}^1\!/_2 D_{cl} \qquad \text{(Eq. 4.30)}$$

Over this interval the roughness height is assumed to decrease linearly with a factor *f*:

$$f = \left(1 - \frac{d}{d_{sat}}\right) \qquad \text{(Eq. 4.31)}$$

For $d \geq d_{sat}$ the layer is considered saturated and $f = 0$. The bedload sediment does not distribute itself evenly over the immobile layer because of local shear stress variations. Locally, the bed will be covered and at another location the bedload will fill up the immobile

layer to a lesser extent. Rhythmic bedforms are forming and migrating over and between the particles of the coarse layer. It has been observed that the flow cannot completely remove the sediment from the pockets between particles of the immobile layer without mobilizing the immobile layer. Therefore we take the value of $½D_{cl}$ as a minimum roughness height for the immobile layer for $d \geq d_{sat}$. The observed bed roughness in the experiments with a bare gravel bed showed that the equivalent roughness height (k_s value) of the bare gravel bed is approximately 3 * D_{cl} (See Figure 4.2, points on y-axis). Therefore the roughness of the coarse layer is modelled as:

$$k_{s,cl} = f * 3D_{cl} + (1 - f) * {}^{1}/_{2}D_{cl} \qquad \text{(Eq. 4.32)}$$

This model concept for the roughness of the coarse layer is illustrated in the upper panel of Figure 4.9. The upper panel shows how the equivalent roughness linearly decreases with increasing layer thickness until the saturation layer thickness is reached.

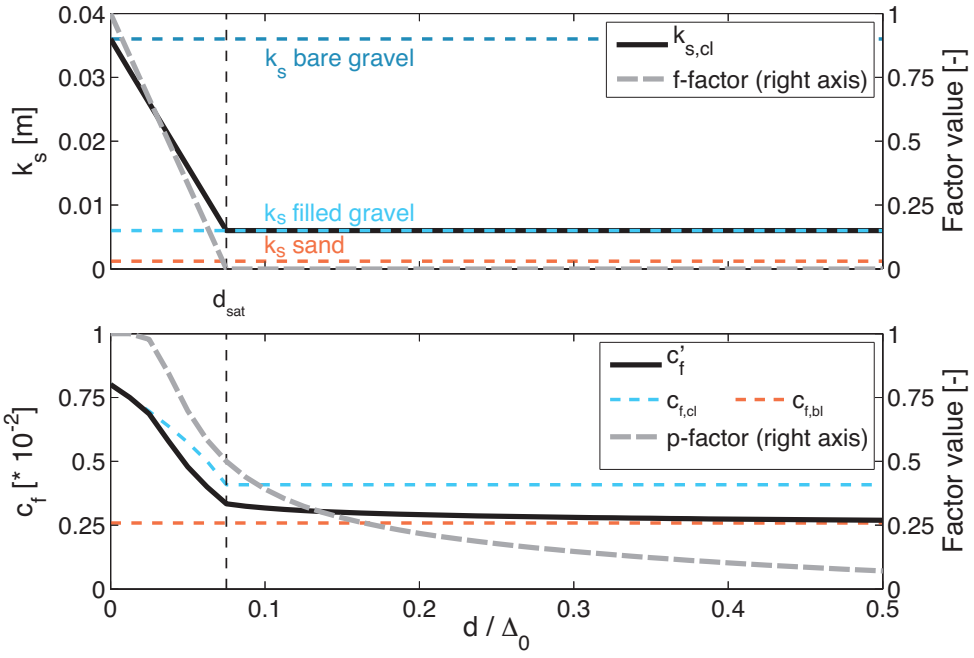

Figure 4.9: Illustration of the grain roughness estimation procedure. For this figure the data from DS-II Series 1 has been used.

For the bedload sediment the equivalent roughness is also estimated using Eq. 4.28. The representative grain sizes and multiplication factors found in literature vary significantly (Van Rijn, 1982). Yalin (1964) used $1D_{50}$, Engelund (1966) $2D_{65}$, and Van Rijn (1984) suggested using an average value of $3D_{90}$. We choose a value:

$$k_{s,bl} = 1D_{90} \qquad \text{(Eq. 4.33)}$$

Choosing a larger value ($3D_{90}$) resulted in an overprediction of the total roughness. The friction coefficient is estimated using a White-Colebrook type of equation:

$$c_{f,x} = \left(\frac{u}{u_*}\right)^{-2} = \left(6 + \frac{1}{\kappa}\ln\frac{R_b}{k_{s,x}}\right)^{-2} \qquad \text{(Eq. 4.34)}$$

The subscript *x* refers to the subscripts *cl* or *bl* for the coarse layer and bedload sediment respectively. We propose that the total grain friction factor is the weighted sum of the bedload part and the coarse layer part. These parts are weighted using factor *p*, the fraction of the bed where the immobile layer is uncovered:

$$c'_f = p * c_{f,cl} + (1-p) * c_{f,bl} \qquad \text{(Eq. 4.35)}$$

A method to estimate *p* was presented in Section 3.2. The combined influence of bedload and coarse layer related friction to the total grain friction is illustrated in the bottom panel of Figure 4.9. The exposure factor (*p*) of the bed determines how the friction factor for the coarse layer and the sand are averaged to a total grain friction factor. The total bed-related friction factor is again the sum of the grain and form drag related friction factors following Eq. 4.24. The method for roughness prediction that is presented above is summarised in the appendix in Section 4.7.

Results

The roughness model presented above has been applied to all experimental data (DS-I to DS-V) as described in Section 4.2 in order to compare the predicted roughness to the roughness calculated from the measurements. The measured dune dimensions and hydraulic parameters have been used as model input. In this way only the roughness model is tested. Figure 4.10 shows a comparison of the measured friction factor in DS-II ($c_{f,b\ exp}$) to the predicted friction factor ($c_{f,b\ pred}$). Panel 1 shows the friction factor calculated from the experimental data. Panel 2 shows the predicted roughness. The predicted value is composed of a grain and form roughness component (c_f' and c_f''). These are shown in the panels (2a and 2b) on the right. Panel 2a shows that the form roughness is zero if no sediment is present and grows with increasing sediment availability. Panel 2b shows the decreasing grain roughness with increasing infilling and coverage of the coarse layer. The combined effect is a decrease in roughness going from $d/\Delta_0 = 0$ to 0.2. If more sediment is added, the roughness starts to grow again to the alluvial roughness. Both the measured and the predicted roughness values show this trend. Figure 4.11 shows the predicted against the experimental friction coefficient for both the calibration data (DS-II) and the validation data (DS-I, III, IV and V). In general the average agreement between the predicted and measured friction coefficient is good. Only the lower values of the friction coefficient are slightly overpredicted on average.

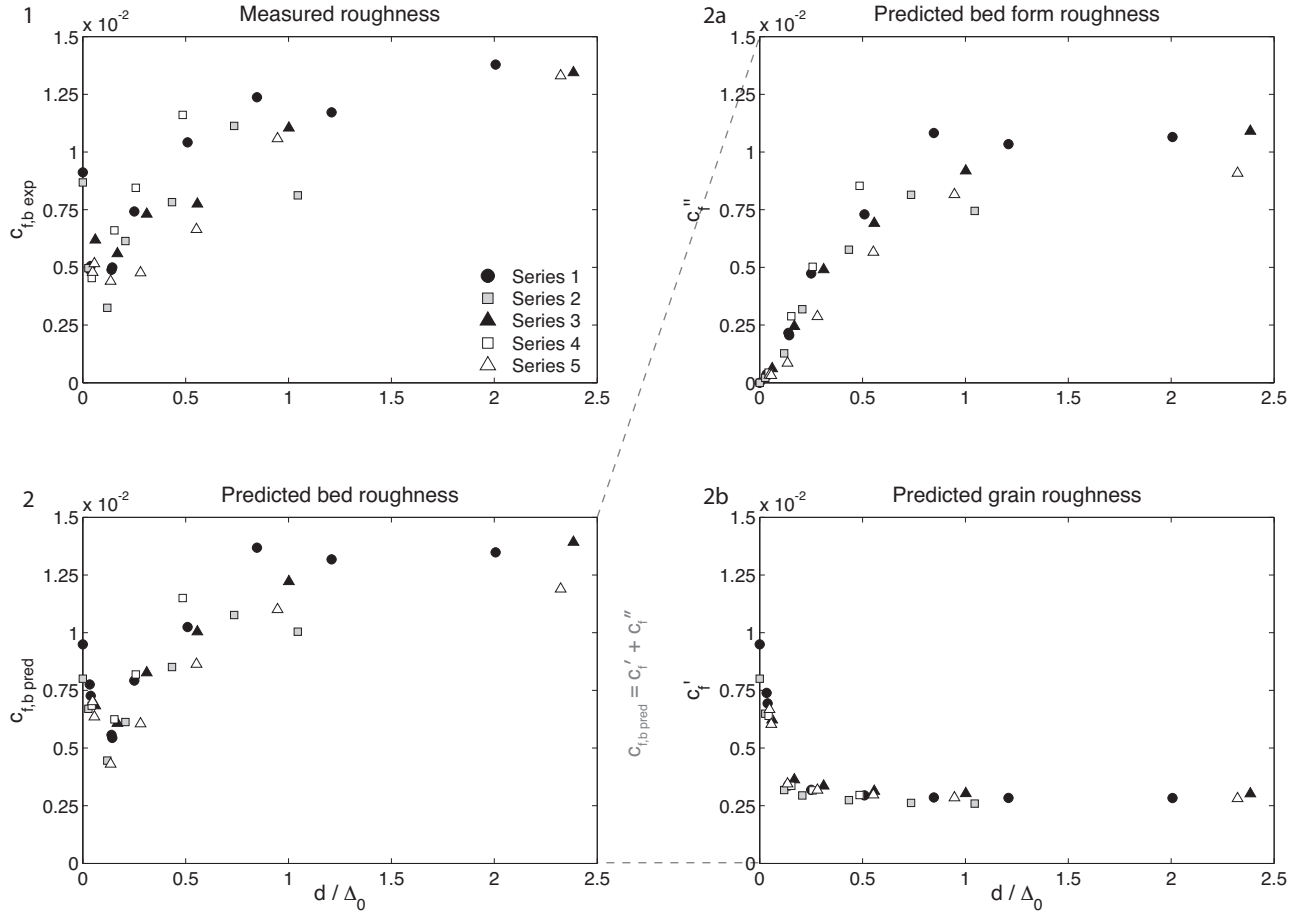

Figure 4.10: Comparison of the measured friction factor (panel 1) with the predicted friction factor (panel 2). Panel 2a and 2b show the contributions of the form (2a) and grain roughness (2b) to the predicted roughness.

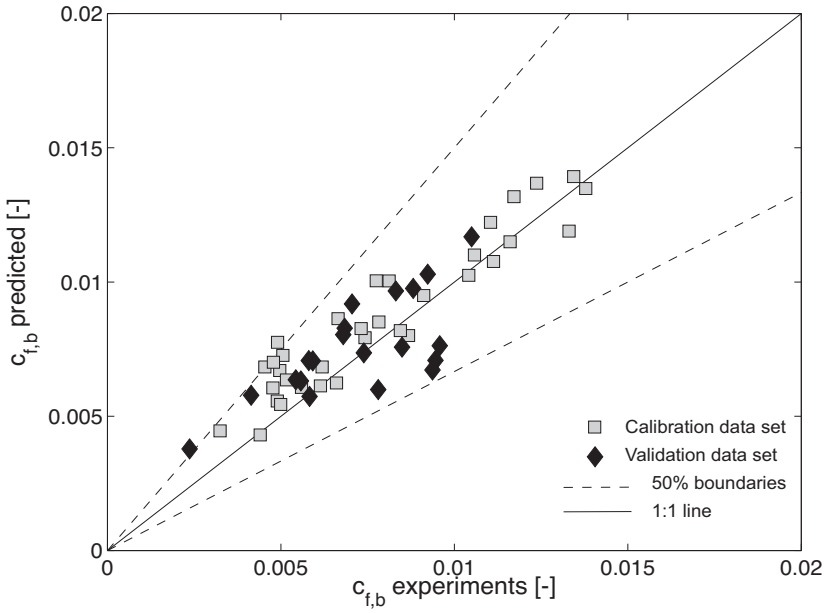

Figure 4.11: Plot of the roughness as predicted for the calibration data and validation data against the friction factor as calculated from the experimental results.

4.4 Integrated bed roughness prediction

Calculation procedure

In the previous sections the methods for the prediction of the bedform dimensions, the bed coverage and the resulting form and grain related flow resistance have been presented. These sub-models have to be used in combination if this method is to be used as a predictive tool for bed roughness estimation under supply-limited conditions. The combined performance of the sub-models will be explored in this section.

The bed roughness is needed to calculate the water depth in the case that the discharge and bed slope are known input variables. The water depth itself is needed in the roughness prediction procedure. This makes these parameters interdependent and an iterative approach has been used to solve the system. Figure 4.12 describes the method used to solve the system and predict the bed roughness. The equations solved here have all been presented in the previous sections, but for clarity, reference will be made to the summary of the formulations in the appendix in the following model description.

It is assumed that the discharge (Q), the bed slope (I), the grain size characteristics of the immobile layer (D_{cl}) and the bedload sediment (D_{50} and D_{90}), as well as the average layer thickness of the bedload sediment (d) are known as input variables. In Fig. 4.12 box 1 the water depth is calculated using the Chézy equation for equilibrium flow (Section 4.7.1), since the flume experiments were done with equilibrium flow. The first time an initial value is used for $c_{f,b}$. In order to calculate the water depth, the wall roughness also needs to be taken into account. The procedure to add the wall roughness is described in Appendix I. Subsequently, the alluvial dune dimensions are calculated in box 2 (Section 4.7.2) with this water depth. The effect of supply-limitation is taken into account in box 3. The bedform dimensions reduction functions are applied (Section 4.7.3) and the immobile layer coverage is estimated (Section 4.7.4). At that point all variables that are needed for the bed roughness prediction (box 4) are available (Section 4.7.5). This new bed roughness ($c_{f,b}$*) will probably deviate from the roughness that was initially used for the water depth calculation ($c_{f,b\ init}$). If this is the case the procedure should be repeated with new the estimated bed roughness as input instead. After some iterations the assumed roughness and the calculated roughness converge and a solution is found.

The integrated roughness model has been applied to all experimental data with and without the suggested sub-models for supply-limited conditions. The model without the adaptations for supply-limited conditions, the alluvial model, follows the short cut in Fig. 4.12 from box 2 to 4. For the roughness calculation a complete coverage of the immobile layer is used (p = 1) in the alluvial model. In this way the effect of the sub-models for SL-conditions can be demonstrated.

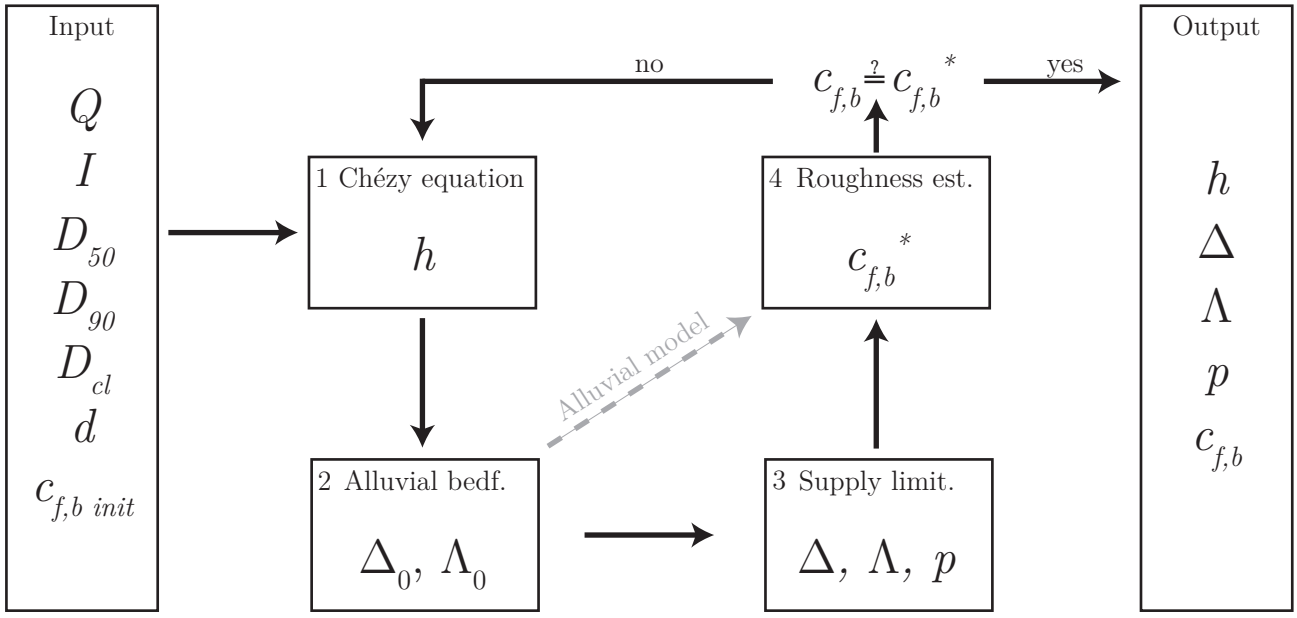

Figure 4.12: The iterative roughness prediction procedure.

Results

Figure 4.13 shows the results of the application of the integrated bed roughness prediction procedure that is described above (abbreviated as SL-model), and the results from the alluvial model on the experimental data. The SL-model (left column) predicts the dune height accurately. This is not trivial since now the predicted shear stress and water depth have been used instead of the measured values. The model predicts slightly larger dunes compared to the isolated test of the dune height prediction with measured roughness (see Fig. 4.5). The alluvial model (right column) clearly overpredicts the dune height, as could be expected from the results of the isolated test in Section 4.3. The results of the bedform length prediction show a bit more scatter, but are again much more accurate than the alluvial model. It is clear that the bedform dimensions are a very important factor in determining the bed roughness (friction factor); the alluvial model strongly over-estimates the bed roughness for the supply-limited experiments. The final roughness coefficient predictions from the SL-model show a much better agreement with the measured roughness than the alluvial model. On average the roughness model overpredicts the roughness a little, which coincides with the slightly overpredicted bedform dimensions. This feedback leads to a slightly overpredicted roughness compared to the isolated test of the roughness with measured dune dimensions in the previous section (Fig. 4.11).

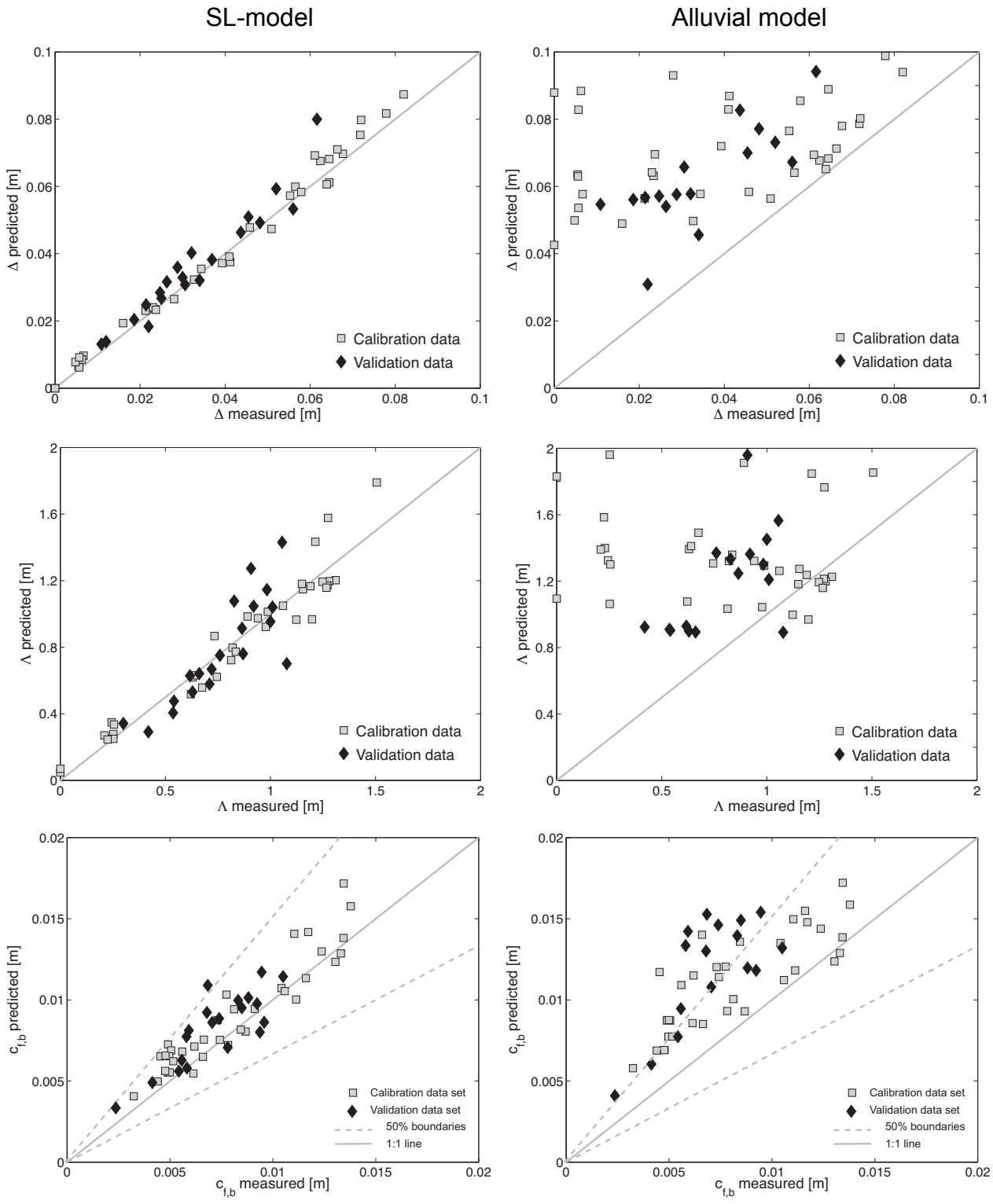

Figure 4.13: Plot of the results for the dune dimensions and roughness as predicted for the calibration data (gray) and validation data (black) against the experimental results. In the left column the supply-limited model has been applied; in the right column the alluvial model has been applied.

4.5 Discussion

The results of the integrated roughness prediction method, that includes the variation in bedform dimensions and immobile layer exposure, show obvious improvement over the alluvial method. Most of the used validation data comes from the supply-limited regime where the bedform dimensions are diminished but the form drag of these bedforms is still dominant over the grain friction. Therefore the most important factor that contributes to the improvement of the roughness prediction is the BDR-function.

For the extremely supply-limited regime the model concept by Van der Zwaard (1974) for the filling of the coarse layer with transport material has been used. This concept describes a sharp decline in bed roughness with increasing d that was also observed in the experiments of DS-II. It has been observed in the experiments that the sand that fills up the interstice space of the gravel stabilises there and cannot be eroded completely from the gravel layer anymore without mobilizing the gravel layer. The shear stress for initiation of motion of the sand that is hiding between the gravel increases up to the point where it equals the critical shear stress for the gravel. Therefore some sand remains immobile in the interstice space between the gravel particles as long as the gravel layer is stable. This sand still smoothens the bed and the bed does not reach the maximum roughness of the bare gravel layer anymore. The erodibility of the sand between the gravel particles probably depends on the grain size ratio between the immobile and mobile size fractions. For a more accurate prediction of the extremely supply-limited roughness therefore an advanced hiding-correction model concept may be used that can predict to what level the sediment can be eroded.

The model depends on the knowledge of the average layer thickness. In morphological models this knowledge is available if an immobile layer is defined in the model; the layer thickness results from a sediment balance. This approach is followed in the model concepts for transport over a coarse layer by Struiksma (1999) and Tuijnder et al. (2009b). However, supply-limited bedforms can also develop when a widely graded sediment is subjected to low shear stress and, due to partial transport, an immobile layer develops, like in DS-III and DS-IV. Prediction of the transport layer thickness in this situation needs an additional model concept for vertical sorting and critical shear stress in order to recognize an immobile layer.

Apart from the average layer thickness, also the alluvial dune height is needed to determine the level of supply limitation. The alluvial dune height can be defined in different ways. Here it has been defined as the dune height for an alluvial bed composed of the bedload sediment with the same water depth and flow velocity as occurring in the supply-limited situation. It is a practical definition if the model is to be applied in a morphological model where flow is generally non-uniform. The alluvial dune height can easily be predicted model using the supply-limited water depth and flow velocity as input. An alternative definition of the alluvial dune height would be to calculate the alluvial dune height that would develop for the same discharge and bed slope. However, this requires a new hydraulic solution for which the

alluvial roughness is estimated. This solution would only be used to calculate the alluvial dune dimensions. This makes that definition very impractical in its application.

The results of the integrated model using the supply limitation modifications still show some overprediction, even for the calibration data set. This is caused by limited amount of calibration that is done with the roughness model. A better result could be achieved if some calibration had been carried out for the form drag model. However, since more calibration for the specific conditions of the present experiments has only limited value, the choice was made to develop the roughness model with as little calibration as possible.

4.6 Conclusions

Under supply-limited conditions diminished bedform dimensions cause a decreased form drag and therefore a decreased bed roughness. The existing bedform dimension reduction model (Tuijnder et al., 2009) has been combined with a model for alluvial bedform dimensions. This combination proves to be able to accurately predict the bedform dimensions for a new independent set of laboratory experiments with supply-limited conditions. The bed form roughness prediction under supply-limited conditions is improved significantly by taking the reduced bedform dimensions into account.

In the strongly supply-limited regime, the bedform drag is very small and the grain roughness is dominant. The grain roughness appoaches the grain roughness of the immobile layer if the layer thickness of the mobile sand goes to zero. A new grain roughness model is proposed that is able to reproduce this observed behaviour. In this model, the coverage of the immobile layer with mobile sand is estimated using a simple Gaussian probability distribution of the vertical bed level fluctuations. With increasing coverage of the immobile layer the grain roughness approaches the grain roughness of the sand.

The integrated application of the new supply-limited roughness concepts side by side with alluvial roughness prediction methods shows that the new supply-limited roughness model clearly improves the accuracy of the roughness prediction.

Acknowledgements

This research project, which is part of the VICI project ROUGH WATER (project number TCB.6231), is supported by the Technology Foundation STW, the applied science division of the Netherlands Organization for Scientific Research (NWO) and the technology program of the Ministry of Economic Affairs. The laboratory experiments are funded by the Delft Cluster program ‘Natural Hazards’, work package A2 River Morphology (WP CT 043211).

Furthermore the authors would like to thank A. Dittrich and the rest of the staff of the Leichtweiss-Institute for Hydraulic Engineering at the Technical University Braunschweig in Germany for their cooperation in the experiments. Finally, the help of M. Spekkers and S. Janssen with the flume experiments was also greatly appreciated.

4.7 Appendix – Summarised formulation of roughness model

Below a summary of the bed roughness prediction model is given. Indented formulas give parameters to less indented formulas.

4.7.1 Equilibrium flow

In order to calculate the water depth, the wall roughness needs to be taken into account. The procedure to calculate the wall roughness is explained in Appendix I. This method results in a value for $c_{f,w}$. The wall and bed roughness are added as follows:

$$c_{f,t} = \frac{c_{f,b}}{1 + \frac{2h}{B}} + \frac{c_{f,w}}{1 + \frac{B}{2h}} \qquad \text{(Eq. 4A.1)}$$

From the Chézy equation the hydraulic radius is solved:

$$\tau_t = c_{f,t}\rho u^2 = \rho g R_t I_e \qquad \text{(Eq. 4A.2)}$$

$$R_t = \frac{c_{f,t}u^2}{gI_e} \qquad \text{(Eq. 4A.3)}$$

Since the flume width B is known the water depth can be calculated from the hydraulic radius:

$$h = \frac{BR_t}{B - 2R_t} \qquad \text{(Eq. 4A.4)}$$

Analogue to Eq. 4A.2 the wall-related hydraulic roughness is calculated as:

$$R_b = \frac{c_{f,b}u^2}{gI_e} \qquad \text{(Eq. 4A.5)}$$

4.7.2 Alluvial bedform dimension prediction

The alluvial bedform dimensions are predicted using the method of Van Rijn (1984). It has been calibrated with correction factors to correctly predict the alluvial experiments.

$$\Lambda_0 = 0.89 * 7.3h \qquad \text{(Eq. 4A.6)}$$

$$\frac{\Delta_0}{h} = 1.29 * 0.11 \left(\frac{D_{50}}{h}\right)^{0.3} \left(1 - e^{-0.5T}\right)(25 - T) \qquad \text{(Eq. 4A.7)}$$

$$T = \frac{\theta' - \theta_{cr}}{\theta_{cr}} \qquad \text{(Eq. 4A.8)}$$

$$\theta' = \frac{c_{f,90}u^2}{(\rho_s/\rho - 1)\, gD_{50}} \qquad \text{(Eq. 4A.9)}$$

$$c_{f,90} = g\left(18\log\frac{12R_b}{3 * D_{90}}\right)^{-2} \qquad \text{(Eq. 4A.10)}$$

4.7.3 Bedform dimension reduction function

The influence of supply-limitation on bedform dimensions can be taken into account by applying the BDR-functions (Tuijnder et al., 2009).

$$\frac{\Delta}{\Delta_0} = 1 - \exp\left(\frac{-d}{0.39\Delta_0}\right) \quad \text{(Eq. 4A.11)}$$

$$\frac{\Lambda}{\Lambda_0} = 1 - 0.96\exp\left(\frac{-d}{0.24\Delta_0}\right) \quad \text{(Eq. 4A.12)}$$

4.7.4 Estimation of immobile layer exposure

The exposed part of the immobile layer is calculated using a cumulative normal distribution evaluated at z_{til} = z_{cl} + ½D_{cl} = 0 + ½D_{cl}.

$$p = {}^1\!/_2\left(1 - \mathrm{erf}\left(-\frac{2.5({}^1\!/_2 D_{cl} - d)}{\Delta\sqrt{2}}\right)\right) \quad \text{(Eq. 4A.13)}$$

4.7.5 Bed roughness prediction

The bed roughness contains a form drag related component and a grain roughness component.

$$c_{f,b} = c'_f + c''_f \quad \text{(Eq. 4A.14)}$$

Form roughness

The form roughness is predicted using the roughness model by Yalin (1964) and Engelund (1977).

$$c''_f = \frac{\Delta^2}{2h\Lambda} \quad \text{(Eq. 4A.15)}$$

Grain roughness

The immobile layer and the bedload sediment have a separate roughness height. These are added using *p* as a weighting factor.

$$c'_f = p * c_{f,cl} + (1-p) * c_{f,bl} \quad \text{(Eq. 4A.16)}$$

The roughness height of the bedload sediment is estimated to be $1D_{90}$ for the experiments used here. The friction factor follows from a White-Colebrook type of formula.

$$c_{f,bl} = \left(6 + \frac{1}{\kappa}\ln\frac{R_b}{k_{s,bl}}\right)^{-2} \quad \text{(Eq. 4A.17)}$$

$$k_{s,bl} = 1D_{90} \quad \text{(Eq. 4A.18)}$$

The roughness height of the coarse layer varies with presence of sand on the coarse layer due to infilling of the space between the gravel particles. If the gravel is completely exposed the roughness height is estimated to be $3D_{cl}$ and decreases linearly to $½D_{cl}$ until the coarse layer is filled. This is assumed to be at $d = ½D_{cl}$.

$$c_{f,cl} = \left(6 + \frac{1}{\kappa} \ln \frac{R_b}{k_{s,cl}}\right)^{-2} \qquad \text{(Eq. 4A.19)}$$

$$k_{s,cl} = 3D_{cl} - 5d \text{ for } d \leq {}^1\!/_2 D_{cl} \qquad \text{(Eq. 4A.20)}$$

$$k_{s,cl} = {}^1\!/_2 D_{cl} \text{ for } d > {}^1\!/_2 D_{cl} \qquad \text{(Eq. 4A.21)}$$

Chapter 5

Modelling of Sediment Transport over Immobile Layers in Rivers using a Transport Reduction Approach*

Abstract

The dependency of the transport rate of sand on the availability of sand on top of an immobile gravel layer has been studied in flume experiments under equilibrium conditions. A decreasing sand transport rate was observed with a decreasing volume of sand per square meter (an increasing supply limitation) while the flow velocity and water depth were kept constant. It is shown that this decrease in the transport rate with decreasing sediment availability can be explained by I) a reducing bed shear stress due to decreasing bedform dimensions and II) a decreasing coverage of the bed with bedload sediment. We present a new sediment transport model concept for supply-limited conditions that takes these processes into account. This transport model is shown to be able to reproduce the results from the lab experiments well. Finally, the new transport model for supply-limited conditions is applied in the framework of a morphological modelling package (Delft3D) to simulate the morphological development that was observed in a new series of flume experiments under supply-limited non-equilibrium conditions. The results of these flume experiments are presented and compared to the results of the morphological simulations. It is shown that the new morphological model gives better predictions of the morphological development under supply-limited conditions than the current modelling approach.

* This chapter will be submitted for publication in parts.

5.1 Introduction

Morphodynamic models are a tool that can be used to simulate the future development of river systems. These models are applied to assess the effectiveness of possible measures taken in the river system. This way they can help in decision making in river management. Increasing complexity of the river management requires increasing detail in the morphodynamic river models (Havinga et al., 2009). This study focuses on one aspect of the morphodynamic modelling: the sediment transport over immobile layers.

Immobile layers develop naturally in river beds e.g. through amour layer development or more ephemeral immobile layer (pavement) formation below the transporting sediment. Moreover, immobile layers are made to prevent erosion. They have been created in outer bends to increase the erosion in the inner-bend and increase the navigable width of the river (Sloff et al., 2006).

The sediment transport on top of these immobile layers is usually supply-limited. This means that locally no additional sediment can be picked up and the transport rate is determined by upstream supply. The local sediment transport rate depends on the available amount of sediment on top of the immobile layer, characterized by the average layer thickness. The transport rate decreases with a decreasing amount of bedload sediment. Therefore, the amount of bedload sediment adapts to the upstream supply of sediment until the local transport rate matches the upstream supply under equilibrium conditions. This decreasing volume causes an incomplete coverage of the immobile layer and smaller bedform dimensions (Tuijnder et al., 2009).

The sediment transport rate needs to be predictable from the local conditions in order to make accurate simulations of morphodynamic behaviour. Generally, transport models do not take a limit on sediment availability into account. Such models, e.g. Meyer-Peter and Müller (1948) and Van Rijn (2007), are applicable under alluvial conditions. These models overpredict the transport rate if a limited volume of transportable sediment is present on the immobile layer. Fractional transport models for widely graded sediment mixtures, e.g. Parker (1990) and Wilcock (2003), may be applicable if the problem of transport over an immobile layer is considered to be a partial transport situation. In that case, the (surface) sediment composition needs to be known as input for the transport model. The combined grain size distribution of the immobile layer and the sediment on top of the layer is generally difficult to determine and varies strongly with the volume on top of the immobile layer.

An alternative method to take the reduction in transport rate due to supply-limitation into account has been proposed by Struiksma (1999). This model concept relates the reduction in the sediment transport rate, relative to the alluvial transport rate, to the availability of sediment on the immobile layer through a transport reduction function. The advantage of this model concept is that the grain size composition of the combined immobile layer and

transport sediment is not needed. Therefore, it can also be applied if the immobile layer is not a coarser sediment but e.g. a peat or clay layer. However, the shape of the reduction function was not accurately known. In this paper a set of new flume experiments with supply-limited transport over immobile layers is presented which provides the necessary data to obtain new insight in this transport reduction.

The general goal of this study is to improve the modelling of sediment transport over immobile layers in morphological river models. In order to achieve this we want to answer the following research questions:

I. How does the limited availability of bedload sediment on top of an immobile layer affect the sediment transport rate?

II. In what way can the observed transport rate variation due to supply-limitation be predicted with a transport model?

III. Does application of the new supply-limited transport model in a morphological model lead to better predictions of the morphological development?

In an earlier phase, the authors studied bedform dimensions and bed roughness under varying supply limitation in an extensive set of flume experiments (Tuijnder et al., 2009; Tuijnder et al., Subm/Ch. 4). These experiments were conducted under equilibrium conditions and were designed to study the effects of different levels of supply limitation. In the present study a part of these experiments, Data Set II, is used to gain insight into the relation between sediment availability and transport rate. In Section 5.2 the setup and procedure of these experiments are presented, special attention is given to the transport rate measurements since these have not been published before. Subsequently, in Section 5.3, the measured transport rates are analysed and used to test the Struiksma (1999) transport reduction concept.

From the new experimental data it becomes clear that the reduction in bed shear stress and bed coverage with transportable sediment are the most important parameters to explain the transport reduction. In Section 5.4 we present an adapted transport reduction model that explicitly takes the shear stress reduction and decreasing immobile layer coverage into account. In this model the sub-models for dune height prediction (Tuijnder et al., 2009) and roughness prediction (Tuijnder et al., Subm) under supply-limited conditions are applied. The new transport model is tested against the data from the equilibrium experiments.

Finally, in Section 5.5, we investigate the possibilities of a morphodynamic model to simulate the morphological development using the transport reduction approach. For this purpose, also a new set of morphological experiments was carried out. The setup of these experiments is described in Section 5.2. In Section 5.5 the results of these experiments are presented and compared to morphological simulations using the Delft3D morphological modelling software.

A comparison is made between the results of the original Struiksma transport reduction concept and the results of the adapted transport reduction concept.

5.2 Experimental setup and procedure

The main goal of the equilibrium experiments was to study the effect of a varying supply limitation on bedforms, roughness and sediment transport. In the equilibrium experiments the conditions were uniform along the flume. A limited amount of sand was distributed over an immobile gravel layer and was recirculated in the flume. In these experiments equilibrium flow was established and the experiment continued until a stationary condition developed and the equilibrium values of the system parameters like sediment transport, bedform dimensions and bed roughness could be determined. In the morphological experiments the goal was to observe the behaviour of a patch of sand on an immobile gravel layer. In these experiments the conditions were not uniform due to the presence of a migrating sand wave that varies in thickness.

In both types of experiments sand was transported over an immobile layer of gravel. The gravel layer was installed once before the experiments and stayed in place because the gravel was too coarse to be transported under the experimental conditions. The gravel had a relatively narrow grain size distribution with a D_{50} of 12 mm (see Figure 5.1). The sand also had a narrow grain size distribution; its D_{50} was 0.8 mm. The sand was quarz sand (>99.6%) and had a density of 2650 kg/m^3 according to its specification.

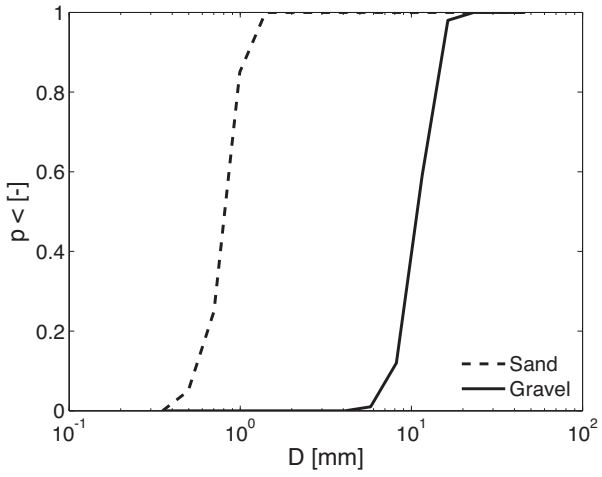

Figure 5.1: Grain size distribution of the sediments used in the experiments.

	D_{10}	D_{50}	D_{90}	σ_g
Sand	0.6	0.8	1.2	1.3
Gravel	7.8	10.9	15.4	1.3

Table 5.1: Characteristics of the used grain size distributions. The columns D_{10}, D_{50} and D_{90} indicate the grain size (mm) where respectively 10, 50 and 90% of the sediment is finer. The column σ_g shows the geometric standard deviation.

The large flume of the Leichtweiss Institute of the University of Braunschweig in Germany was used for the experiments. The flume, see Figure 5.2 for an schematic illustration, has a total length of approximately 30 m, of which 17.5 m were actually used for measurements. The width of the flume was reduced from 2 to 1 m, in order to reduce the required adaptation

length and prevent the formation of alternating bars (van Rijn and Klaassen, 1981). The sand was recirculated in the flume; the sand discharge at the downstream end of the flume was pumped back to the upstream end of the flume. In the sediment return pipe measurement devices to measure the discharge and turbidity (using a Negele Messtechnik ITM-4 turbidity sensor) of the sand water mixture were present. These were used to estimate the sediment transport in the equilibrium experiments. The flume is equipped with jacks that make it possible to adjust the bed slope to maintain a uniform flow. The bed level and water level were continuously measured with ultra sound sensors mounted on a carriage. Three sensors measured the bed level at three transects: one in the middle of the flume and two at 16.5 cm from both sidewalls. The water level was measured along a transect in the middle of the flume. The carriage drove up and down the flume in ca. 6 minutes.

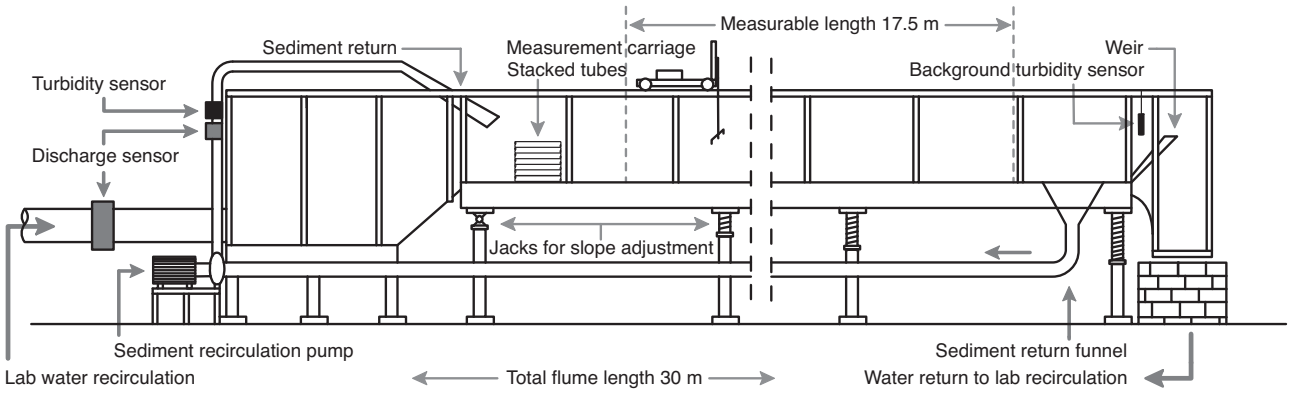

Figure 5.2: Side view of the used flume setup. The supply of water came from a constant-head tank ca 5 m above the level of the flume.

Method equilibrium experiments

Between the equilibrium experiments the average layer thickness (d) of the transport layer was increased stepwise in order to study the effects of the decreasing supply limitation on the average bedform dimensions, roughness and the sediment transport rate. Within each series the sediment volume was increased while the imposed flow conditions were kept constant. The flow velocity and water depth were varied between the series (Table 5.2). Series 1, 2 and 3 were conducted with a flow velocity of 0.52 m/s while the water depth was varied. Series 1, 4 and 5 had an equal flow depth but a varying flow velocity. Series 4 will not play an important role in this study; this series could not be completed because the mobilisation of the immobile layer due to increasing dune dimensions. Series 6 contains some additional alluvial experiments that were used for calibration of the alluvial sediment transport model.

The layer of sand was distributed evenly over the length of the flume before each experiment. At the beginning of an experiment the flume slope and the downstream weir were adjusted until a uniform flow with the desired water depth and flow velocity had been realized. The experiment was continued without further adjustment once the conditions were varying around a mean, and thus were in equilibrium. Under supply-limited conditions, less variation

in the conditions was observed over time than was the case under alluvial conditions. Therefore the experiments were continued for a few hours after an equilibrium was reached under supply-limited conditions, while the observations were continued for up to two days under alluvial conditions.

Exp Nr	d [m]	Q [m^3/s]	h [m]	I_e [-]	τ_b [N/m^2]	Δ [m]	Λ [m]	Δ_0 [m]	s [g/s]	c [m/h]	$p_{z<ztil}$ [-]
1-1	0.000	0.074	0.20	0.0007	1.25	0.000	0.00	0.080	0.0	0.0	0.92
1-2	0.003	0.105	0.20	0.0008	1.33	0.006	0.26	0.080	4.3	2.5	0.77
1-3	0.003	0.104	0.20	0.0008	1.38	0.006	0.29	0.080	3.8	2.5	0.71
1-4	0.011	0.104	0.20	0.0008	1.35	0.024	0.64	0.080	11.6	2.3	0.28
1-5	0.012	0.106	0.20	0.0008	1.41	0.023	0.65	0.080	7.9	2.3	0.27
1-6	0.020	0.105	0.20	0.0012	2.06	0.040	0.84	0.080	15.0	2.3	0.21
1-7	0.041	0.104	0.20	0.0016	2.87	0.057	1.13	0.080	21.2	1.9	0.06
1-8	0.068	0.104	0.20	0.0018	3.37	0.076	1.34	0.080	26.6	1.9	0.02
1-9	0.097	0.104	0.20	0.0019	3.32	0.077	1.46	0.080	25.5	1.9	0.00
1-10	0.161	0.105	0.20	0.0022	3.97	0.077	1.44	0.080	31.8	1.9	0
2-1	0.000	0.151	0.30	0.0008	2.17	0.000	0.00	0.091	0.0	0.0	0.96
2-2	0.003	0.156	0.30	0.0006	1.36	0.007	0.34	0.091	3.9	2.5	0.78
2-3	0.011	0.157	0.30	0.0004	0.90	0.024	0.74	0.091	6.0	1.3	0.31
2-4	0.019	0.156	0.30	0.0007	1.66	0.042	0.90	0.091	9.9	1.2	0.27
2-5	0.039	0.153	0.30	0.0008	2.06	0.065	1.23	0.091	13.6	0.9	0.12
2-6	0.067	0.157	0.29	0.0012	3.18	0.080	1.33	0.091	20.1	1.4	0.03
2-7	0.095	0.157	0.30	0.0009	2.24	0.086	1.64	0.091	16.5	1.0	0.01
3-1	0.004	0.079	0.15	0.0013	1.74	0.008	0.34	0.067	4.6	5.0	0.58
3-2	0.011	0.079	0.15	0.0012	1.56	0.022	0.64	0.067	10.8	3.0	0.24
3-3	0.021	0.077	0.15	0.0014	1.94	0.035	0.84	0.067	15.1	2.0	0.14
3-4	0.037	0.078	0.16	0.0014	1.95	0.048	1.06	0.067	18.1	2.0	0.04
3-5	0.067	0.079	0.15	0.0020	2.88	0.059	1.26	0.067	15.2	2.0	0.01
3-6	0.160	0.080	0.15	0.0026	3.70	0.068	1.37	0.067	32.1	2.7	0
4-1	0.004	0.135	0.20	0.0012	2.07	0.007	0.29	0.081	17.9	9.0	0.65
4-2	0.012	0.135	0.20	0.0017	3.01	0.028	0.69	0.081	35.0	8.0	0.31
4-3	0.021	0.116	0.20	0.0016	2.82	0.042	0.86	0.081	26.2	3.5	0.21
4-4	0.039	0.116	0.20	0.0021	3.91	0.059	1.03	0.081	38.2	3.5	0.08
5-1	0.003	0.093	0.20	0.0006	1.05	0.007	0.34	0.069	2.1	1.1	0.69
5-2	0.004	0.093	0.20	0.0007	1.12	0.006	0.32	0.069	1.5	1.0	0.62
5-3	0.009	0.092	0.20	0.0006	0.92	0.016	0.76	0.069	3.2	1.0	0.24
5-4	0.019	0.093	0.20	0.0006	1.05	0.033	0.95	0.069	6.0	0.9	0.15
5-5	0.038	0.093	0.20	0.0008	1.43	0.052	1.20	0.069	10.0	0.8	0.06
5-6	0.065	0.093	0.20	0.0012	2.24	0.067	1.37	0.069	11.1	0.7	0.01
5-7	0.160	0.094	0.20	0.0015	2.84	0.070	1.39	0.069	14.5	1.0	0
6-1	0.160	0.130	0.25	0.0017	3.87	0.083	1.47	0.083	25.2	1.6	0
6-2	0.157	0.135	0.25	0.0020	4.71	0.084	1.46	0.084		1.9	0
6-3	0.160	0.150	0.26	0.0022	5.21	0.095	1.49	0.095	45.2	2.5	0

Table 5.2: Experimental conditions and results for the equilibrium experiments (DS-II). Q is the discharge in the measurements section, h is the water depth, I_e is the slope of the energy level, τ_b is the bed shear stress, Δ and Λ are the average dune height and length, Δ_0 is the dune height under alluvial conditions, s is the transport rate over the width of the flume, c is the migration velocity of the dunes, $p_{z<ztil}$ is the fraction of the immobile layer that is exposed.

From the measurements in the equilibrium period the average bedform height and length, shear stress and sediment transport rate were determined. These are reported in Table 5.2. The average slope of the energy level was determined by making a least squares fit of a linear function to the energy level for every run of the measurement carriage; this was averaged over the equilibrium period. The total shear stress was calculated from the average slope of

the energy level. This was split into a bed shear stress and wall shear stress using the method of Vanoni and Brooks (1957). The bedform length and height were determined using a zero-crossing method described in Van der Mark (2007). The fraction of the bed where the immobile layer was exposed is reported in the column $p_{z<ztil}$. This is the fraction of measurements where a level lower than the level of the top of the immobile layer (z_{til}) was measured. The top of the coarse layer is assumed to be $½D_{cl}$ above the average immobile layer level, where D_{cl} is the average grain size of the immobile layer. If a lower level is measured, the immobile layer is exposed, see Tuijnder et al., (Subm/Ch. 4).

Transport measurements

The sediment transport rate (s [g/s]) was estimated using the turbidity measurement device in the return pipe of the sediment recirculation system. A relation was established between the measured turbidity and the sand concentration. The discharge through the return pipe was also measured. Therefore, the sediment discharge at the end of the flume can be estimated by multiplying the concentration and the discharge. Under the equilibrium conditions this transport rate is representative for the transport rate in the flume.

Another method to estimate the transport rate (q_s [m²/s]) uses the propagation velocity of the bedforms. This method is explored below because it provides a way to verify the results from the turbidity measurements. The sediment transport can be estimated by determining a bedform propagation velocity (celerity - c) and an average transport layer thickness (δ). This transport layer moves – by definition – with an average velocity equal to the bedform celerity. The transport layer thickness will generally be smaller than d – the average layer thickness of all available sand – because not all available sand on the gravel layer is mobilised with the passage of each dune. This means that an inactive sand deposit is present between the active dunes and the immobile gravel layer, see e.g. Fig. 3.4. In this figure, no inactive sand deposit is present in Exp 1-4 and 1-6 because the dune troughs lie on the immobile layer. In the other experiments the troughs are not always on the immobile layer and therefore $\delta < d$. The bedform shape parameter (α_{bf}) determines the relation between the average transport layer thickness and the dune height through the following relation:

$$q_s = \delta c = \alpha_{bf} \Delta c = \frac{V}{\Lambda \Delta} \Delta c \qquad \text{(Eq. 5.1)}$$

Where V is the volume of sediment (per unit width and including the pore volume) in a bedform with length Λ and height Δ of an average dune. This volume is generally not accurately known due to the irregularity of dunes. Therefore, no clear level can be given below which the sediment is not entrained during the passage of dunes, unless all dune troughs lie on the immobile gravel layer. Instead the probability of entrainment decreases gradually with increasing vertical distance to the average bed level (Ribberink, 1987). Wilbers (2004) analysed previously published datasets and concludes that the shape parameter

usually (± 70% of the observations) lies between 0.5 and 0.6. This would indicate convex dune profiles under alluvial conditions. However, this value has to be corrected for the difference in level between the dune trough and the level where the point of zero transport is located. This correction is approximately a factor 0.9. This results in a reported α_{bf} between 0.45 and 0.54.

Under supply-limited conditions ($d/\Delta_0 < 0.5$) the situation can develop where all dunes are separated by the immobile layer (Tuijnder et al., 2009). In that case, all sediment on the immobile layer is transported in the dunes and no exchange layer is present with sand that is only incidentally entrained. Due to the space between subsequent dunes, the value of α_{bf} is lower compared to alluvial conditions. It can be below 0.5 for triangular dunes as illustrated in Figure 5.3. If the immobile layer is exposed between each dune, the transport layer thickness (δ) equals the sediment layer thickness (d) and α_{bf} can be calculated from $\alpha_{bf} = d/\Delta$. The value of α_{bf} in the experiments without inactive sand layer was generally below 0.5. The dune profiles are convex ($\alpha_{bf} > 0.5$) yet the value of α_{bf} is reduced due to the increased space between the dunes as illustrated Figure 5.3.

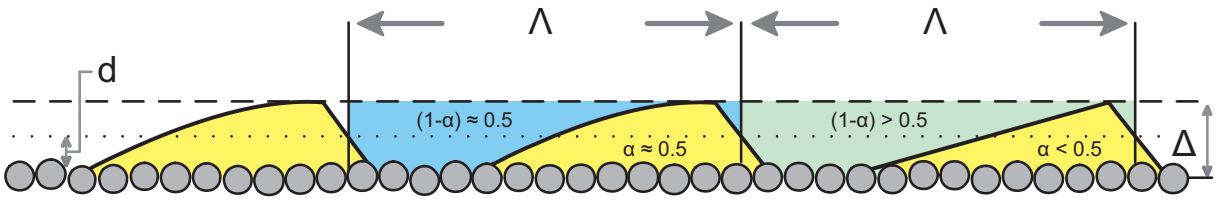

Figure 5.3: Illustration of the reducing effect of space between dunes on α_{bf}. The middle dune is convex and under alluvial conditions the shape parameter would be well above 0.5. Due to the additional space ($p\Lambda$) the blue shaded area and the yellow shaded area within the box formed with area $\Lambda^*\Delta$ are approximately equal in size. For triangular dunes α_{bf} is below 0.5.

In order to check the transport rates from the turbidity measurements (s) the value of α_{bf} can be calculated from Eq. 5.1. In order to do so, the bedform celerity (c) has been estimated by visually fitting 'celerity lines' as shown in the example in Figure 5.4. The transport rate s – which is given in g/s – has been converted to q_s –which is given in m^2/s including the pore volume – using $q_s = s/(1000\ \rho_s\ (1\text{-}p_s)\ B)$, where ρ_s is the density of the sediment, p_s the porosity and B the flume width. For the density a value of 2650 kg/m^3 is used and the porosity is assumed to be 0.4. Subsequently, α_{bf} has been solved from Eq. 5.1 using the values of s, Δ and c reported in Table 5.2.

Figure 5.5 shows the resulting values of α_{bf} against the dune height. The values of α_{bf} show a weak increasing trend with increasing dune height due to the decreasing supply-limitation. The trend agrees with the expected effect of the supply-limited conditions: with increasing sediment supply the bedforms become larger and the occurrence of space between dunes decreases, which causes an increase in α_{bf}. The values of α_{bf} are on average slightly lower than expected: they are 17% lower than the values that can be estimated from $\alpha_{bf} = d/\Delta$ if no

inactive layer is present. This difference may be caused by the estimation of Δ and c or the calibration of the transport measurement sensors: the turbidity sensor and the discharge sensor. Considering these results we consider the transport measurements to be reasonably accurate, though possibly slightly too low.

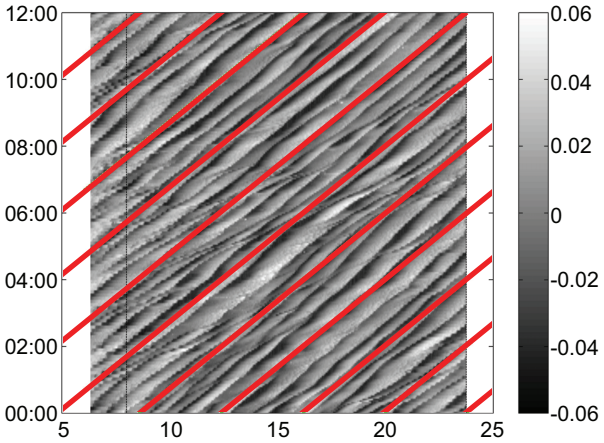

Figure 5.4: Bed level (gray level) against the x and time axes. The dune migration has been estimated by fitting the diagonal red lines to the migrating dune pattern.

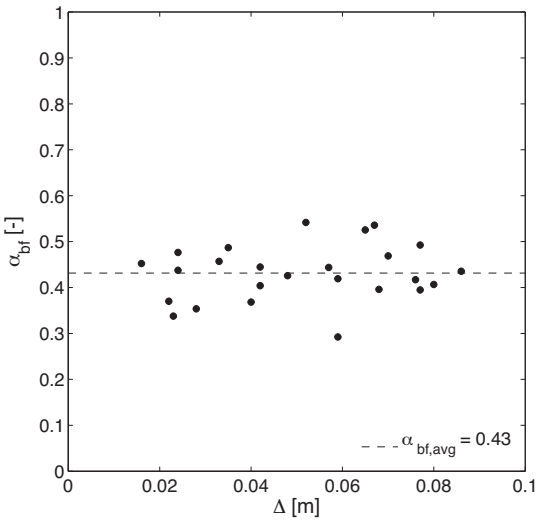

Figure 5.5: Values of α_{bf} that have been solved from Eq. 5.1 for the values of s, c and Δ from Table 5.2. Only data where d > 0.009 m are included since no dunes formed if d was smaller.

Morphological experiments

The morphological experiments were conducted to have an observation of the changing morphology of a migrating supply-limited sand body. In the (non-equilibrium) morphological experiments sand was initially distributed over the gravel layer between x = 6.5 and 13.5 m. The rest of the gravel layer was exposed. This sand body migrated downstream during the experiment. The sand was not recirculated; instead the sand discharge at the end of the flume was pumped away. Different experiments were carried out with a varying initial sand layer thickness. In experiment 1 the thickness was 4 cm, in experiment 2 it was 2 cm and in experiment 3 it was 1 cm. During all three experiments the same hydraulic conditions were imposed, the discharge was 104 l/s and the water depth was approximately 0.2 m. The bed slope was 0.0013. This setting resulted in approximate equilibrium flow without the sand body in place. The presence of the sand layer caused an acceleration of the flow and thus a deviation of the equilibrium flow. The results of these experiments are presented and discussed in Section 5.5. Moreover, they are compared to simulations with the morphological model Delft3D.

5.3 Transport reduction due to supply limitation

The local sediment transport rate varies with the availability of sediment – the average layer thickness – on top of the immobile layer. Without any additional data it is clear that: 1) The sediment transport is at transport capacity if more than a certain minimum layer thickness for alluvial transport (d_0) is present. 2) The sediment transport reduces to zero if the layer thickness is zero. This knowledge has been used by Struiksma to develop a transport reduction function. In this section the transport reduction as observed in the equilibrium experiments is presented. Subsequently, the transport reduction concept as proposed by Struiksma (1999) is tested using the measured transport rates.

Observed transport reduction

Figure 5.6 shows the measured sediment transport rate together with the bedform length and height, the immobile layer exposure and the bed shear stress, which are parameters that influence the transport rate. The columns are the different experimental series that were conducted under different hydraulic conditions; for each column the water depth and flow velocity were constant and the amount of sand on the immobile layer increased. The strength of a supply limitation can be expressed as the ratio of the average layer thickness of the transported sediment (d) and the dune height that develop under alluvial conditions (Δ_0), under the same flow velocity and water depth. This ratio is used for the x-axis in order to see the effect of variation in supply limitation.

The first two rows show the bedform height and length. It can be seen that a decreasing sediment availability (d/Δ_0 <) leads to decreasing bedform dimensions. The third row shows the exposure of the immobile layer, the relative bed area where a level lower than the top of the immobile layer (z_{til}) was observed. This area increases with decreasing sediment availability.

The fourth row shows the variation in bed shear stress with varying supply limitation. The bed shear stress decreases with decreasing sediment availability due to the decreasing bedform dimensions. Once the coarser sub-layer becomes fully exposed the bed shear stress can increase again (Tuijnder et al., Subm/Ch. 4), however, this effect is small for these experiments.

The last row shows the reduction in the sediment transport rate with a decreasing sediment availability. The combination of decreasing shear stress and decreasing bed coverage leads to a decreasing transport rate with decreasing sediment availability. The increasing shear stress with increasing immobile layer exposure under strongly supply-limited conditions (d/Δ_0 < 0.25) does not cause an increasing sediment transport rate because the grain shear stress is mostly caused by grain friction from the immobile gravel and the sand coverage (1-p) decreases quickly in this regime.

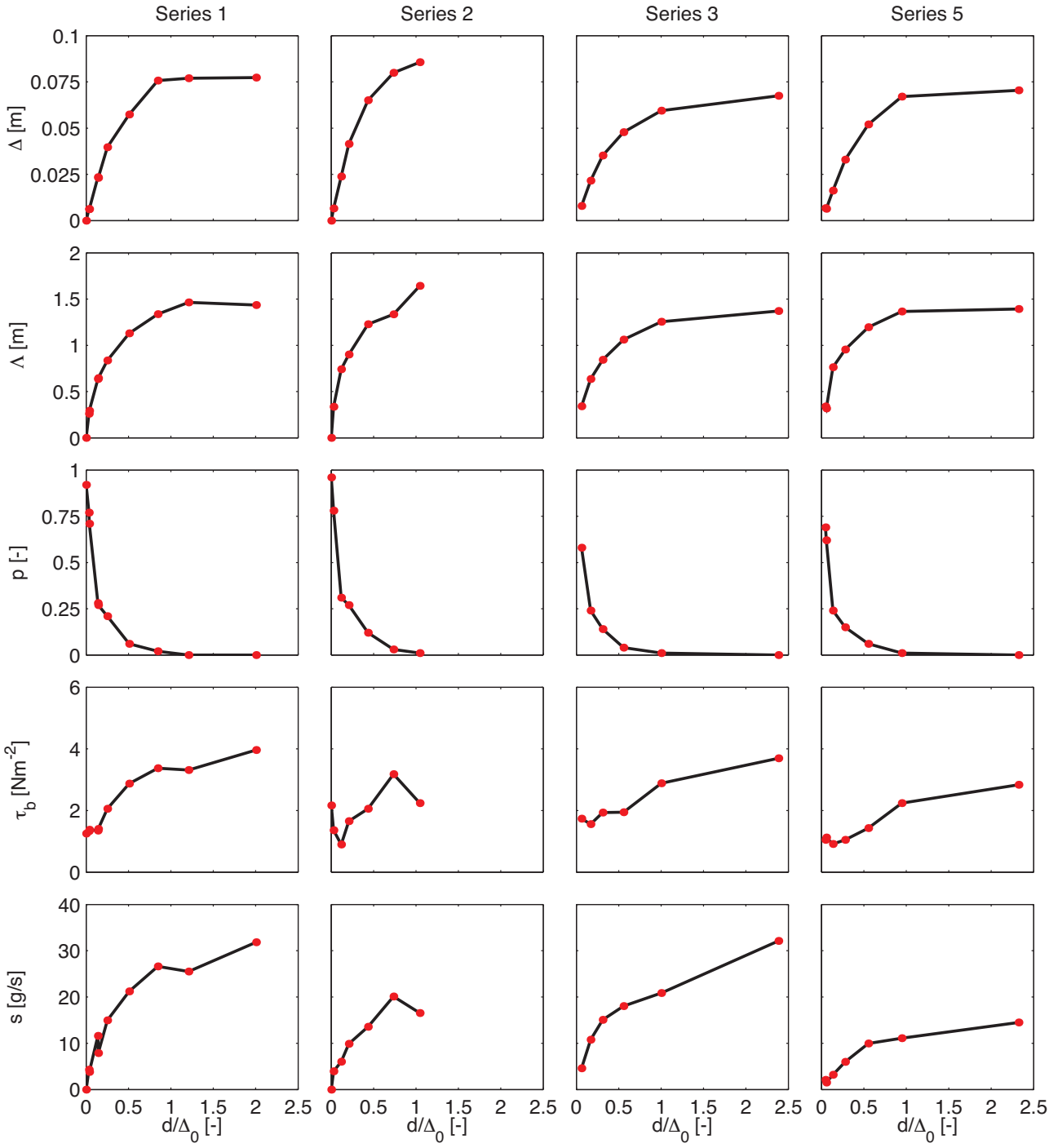

Figure 5.6: Variation of sediment transport and transport related factors in the equilibrium experiments. The squares in the lower row indicate the sediment transport estimated from dune migration.

Existing model concept – Struiksma Model

Struiksma (1985, 1999) proposed to relate the supply-limited transport rate (s) to the alluvial transport rate ($s_{0,a}$) using a reduction function. This function describes how the transport reduces with decreasing sediment availability, between the alluvial transport rate and the completely sediment starved bed with zero transport (d=0). It was proposed to relate the reduction in sediment transport between the alluvial rate and zero to the ratio of d over d_0, this is the minimum layer thickness required for alluvial conditions.

$$s = \psi s_{0,a} \text{ with } \psi = f\left(\frac{d}{d_0}\right) \qquad \text{(Eq. 5.2)}$$

Where $s_{0,a}$ is the alluvial sediment transport rate and ψ is the reduction function. A linear and a sinusoidal reduction function have been defined (Struiksma, 1985):

$$\psi = \frac{d}{d_0} \text{ for } \delta < \delta_0 \qquad \text{(Eq. 5.3)}$$

$$\psi = \sin\left(\frac{\pi}{2}\frac{d}{d_0}\right) \text{ for } d < d_0 \qquad \text{(Eq. 5.4)}$$

The sinusoidal function is believed to be more correct by Struiksma (1985) because of an assumed smooth transition from supply-limited to alluvial at $d = d_0$. The minimum alluvial layer thickness d_0 is an important parameter in this function. In the Struiksma concept it is assumed that the supply limitation becomes noticeable if $d < d_0 = ½\ \Delta_0$. The alluvial sediment transport rate ($s_{0,a}$) in this concept is the transport that occurs under an alluvial roughness and shear stress. Struiksma assumes a constant alluvial roughness and shear stress in the supply-limited regime. The effect of the reduction in roughness due to the smaller bedforms that develop under supply-limited conditions on the sediment transport rate is included in the reduction function.

Figure 5.7 shows a comparison of the Struiksma transport reduction model with the observed transport reduction. The measured transport rate (s_{meas}) in Series 1, 3 and 5 has been divided by the alluvial transport rate ($s_{0,a}$) that was observed in an equilibrium experiment with the same flow velocity and water depth as indicated in Table 5.2. The experimental data shows a gradual transition from supply-limited to alluvial conditions. Therefore, indeed the sinusoidal reduction function is to be preferred over the linear function. The black line is the reduction model with a value of $d_0 = 0.5\ \Delta_0$ as proposed in Struiksma (1985). The figure shows that the real measured transport reduction takes place over a larger range than predicted using this model. Based on the experimental data a value of $d_0 = 1.5\ \Delta_0$ should be used to improve the reduction model. It should be noted however, that the observed transport reduction is somewhat steeper for a smaller sediment availability ($d/\Delta_0 < 0.5$) than predicted using the sinusoidal function and $d_0 = 1.5\ \Delta_0$.

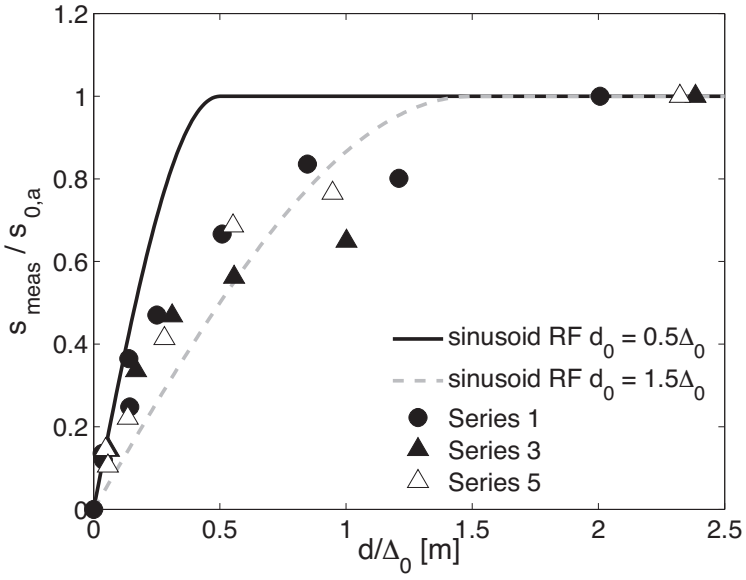

Figure 5.7: Comparison of the transport reduction as derived from the experimental data and the Struiksma reduction model for different values of d_0.

5.4 Model for bedload transport over immobile layers

The model for bedload transport over immobile layers that is presented below essentially follows the same procedure as the Struiksma transport reduction concept. We extended this model in two ways. Firstly, the transport reduction model of Struiksma assumes a constant roughness for a varying supply limitation. However, the roughness decrease with decreasing sediment availability causes a shear stress decrease that can partly explain the transport decrease. Therefore we propose to take the roughness decrease into account. A second extension is the used transport reduction function. The remaining reduction in transport rate that cannot be explained with a shear stress decrease is now related to the variation of the area of the immobile layer at the surface of the river bed.

In this section first the effect of a shear stress decrease due to supply-limitation on the transport rate is studied using the measured shear stress. Subsequently a model to predict the supply-limited transport rate is presented. Finally, the proposed method to predict the sediment transport rate under supply-limited conditions is tested against the equilibrium experiments.

Transport reduction due to shear stress reduction

Since we are dealing with bedload transport of a uniform sediment, a Meyer-Peter and Müller type of formula should be able to predict the transport rate. This model is expressed in dimensionless parameters as:

$$\phi = a\,(\mu\theta - \theta_{cr})^{b} \qquad \text{(Eq. 5.5)}$$

The values for the Meyer-Peter and Müller model are: a = 8 (without pore volume), θ_{cr} = 0.047 and b = 3/2. The dimensionless shear stress parameter (Shields parameter) is defined as:

$$\theta = \frac{\tau_b}{(\rho_s - \rho_w) g D_{50}} \qquad \text{(Eq. 5.6)}$$

The ripple factor μ is defined as:

$$\mu = \left(\frac{C}{C_{90}} \right)^{\frac{3}{2}} \qquad \text{(Eq. 5.7)}$$

In this equation *C* is the Chézy parameter related to the bed. This roughness parameter relates the bed shear stress to the flow velocity as is shown in the following equation:

$$\tau_b = \rho g \frac{u^2}{C^2} = \rho g R_b I_e \qquad \text{(Eq. 5.8)}$$

The second equal sign is only valid under equilibrium flow and is in another form also known as the Chézy equation. In the roughness model the friction factor (c_f) is used. These are related through:

$$C = \sqrt{\frac{g}{c_{f,b}}} \qquad \text{(Eq. 5.9)}$$

C_{90} is the estimated Chézy value for the grain roughness. This is estimated using a White-Colebrook type of formula expressed in the Chézy parameter. The (Nikuradse) roughness height is estimated using $1D_{90}$:

$$C_{90} = 18 \log \left(\frac{12 R_b}{D_{90}} \right) \qquad \text{(Eq. 5.10)}$$

The relation with the actual volumetric transport rate is given by:

$$\phi = \frac{q_s}{\sqrt{(\rho_s / \rho_w - 1) g D_{50}^3}} \qquad \text{(Eq. 5.11)}$$

The subscript 0 refers to alluvial conditions. The transport rate in the flume experiments is expressed in g/s therefore the volumetric rate has to be converted using the sediment density. This model has been calibrated to give -on average- correct predictions for the alluvial experiments. See Figure 5.8 for the calibration result. For this purpose the experiments which are marked with an ‘a’ in Table 5.2 have been used. The values b = 1.46 and θ_{cr} = 0.034 were found with a least squares analysis of the model. Fitting these parameters gave a slightly better fit than using a combination of the coefficients a and either b or θ_{cr}.

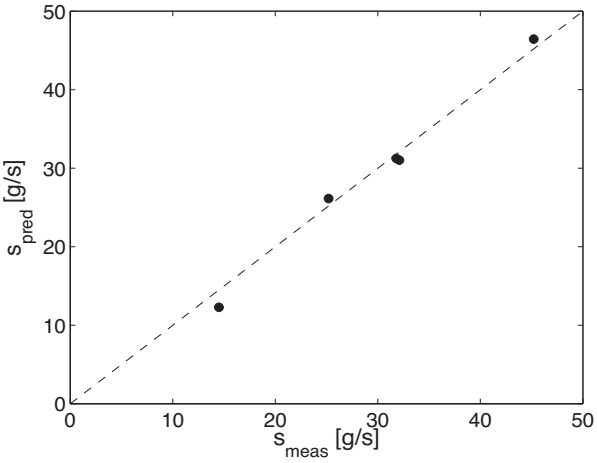

Figure 5.8: Calibration result of the transport model using the alluvial experiments. The model used for the predictions had the following parameters: a = 8, b = 1.46 θ_{cr} = 0.034

This model is applied to the 4 series of supply-limited experiments in order to see how much the measured transport decrease can be explained by the shear stress decrease and how much is caused by other factors. In Figure 5.9 both the measured and calculated sediment transport rates are shown. The sediment transport rate has been calculated with the measured bed shear stresses and the calibrated model. The crosses in Figure 5.9 indicate the calculated sediment transport rate. Above d/Δ_0 = 0.5 the calculated and measured transport rates are in agreement. This means that the shear stress reduction explains most of the transport reduction in this mildly supply-limited regime. Below approximately d/Δ_0 = 0.5 the shear stress decrease does not account for all of the decrease in sediment transport rate, the predicted transport rate is higher than the measured transport rate. In this range of strong supply-limitation the measured reduction should be explained by other factors, such as the reduced sand coverage of the bed.

In the following text, this transport rate calculated with the supply-limited shear stress and the alluvial transport model will be called the supply-limited reference transport rate ($s_{0,s}$). A model to predict the supply-limited shear stress as well as the transport reduction factor is presented in the following sections.

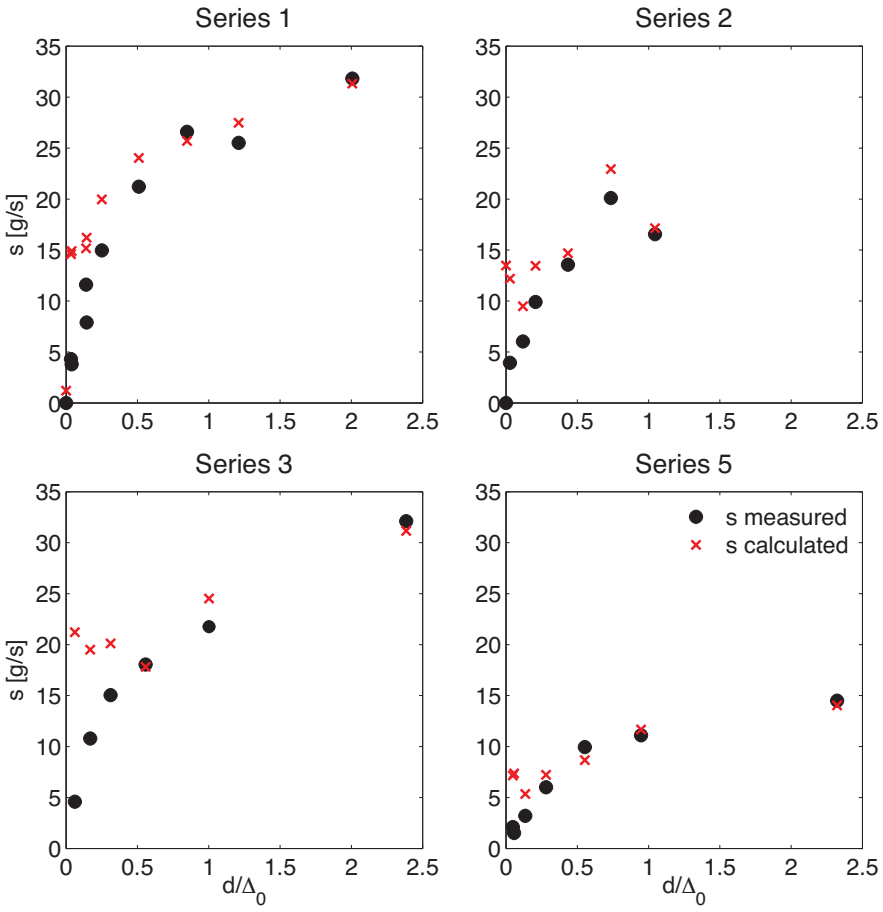

Figure 5.9: Transport reduction due to a decrease in sediment availability compared with the transport rate that follows from the alluvial sediment transport prediction. The decreasing shear stress explains a part of the observed decrease.

Transport reduction due to immobile layer exposure

The supply-limited sediment transport rate is calculated by reducing the reference transport rate with a reduction factor. The local transport rate becomes very small where the average layer thickness decreases to the extent that the immobile layer becomes exposed. With an increasing exposure of the immobile layer an increasing part of the bed shear stress is not effectively transporting sediment. Instead the energy is dissipated by friction with the immobile layer. Therefore it is assumed that the reference transport rate should be decreased with the fraction of the bed where the immobile layer is exposed in order to calculate the actual supply-limited transport rate. This assumption is only reasonable if the main transport mode is bedload transport over the immobile layer and not if a significant proportion of the transport takes place through the interstice space of the immobile layer.

In this way the adapted supply-limited transport model can now be written as:

$$s = s_{0,s} * (1 - p) \qquad \text{(Eq. 5.12)}$$

In this relation, p is the fraction of the bed where the immobile layer is exposed. Figure 5.10 shows the ratio $s_{meas}/s_{0,s}$ as a function of d/Δ_0. The measured shear stress in each experiment

has been used to calculate $s_{0,s}$. Compared to Figure 5.7 the transport ratio remains 1 with decreasing d/Δ_0 over a larger range. The transport ratio starts to decrease approximately at $d/\Delta_0 = 0.5$ instead of $d/\Delta_0 = 1.5$ because the effect of the shear stress decrease is now included in the calculation of $s_{0,s}$.

The coverage of the immobile layer (1-p), where p is the exposure of the layer, is also indicated in Figure 5.10. The crosses show the measured values of (1-p), where $p = p_{z<ztil}$ as reported in Table 5.2. The coverage has also been predicted with the model for immobile layer exposure that was proposed by Tuijnder et al. (Subm/Ch. 4) and is presented below (Eq. 5.21 - 5.22). This reduction in the measured and predicted coverage (1-p) agrees well with the observed transport rate reduction ($s_{meas}/s_{0,s}$) for the equilibrium experiments. This supports the use of Eq. 5.12 and suggests that the transport rate indeed scales with the bed coverage and that the bed coverage can be used as a reduction factor for the reference transport rate.

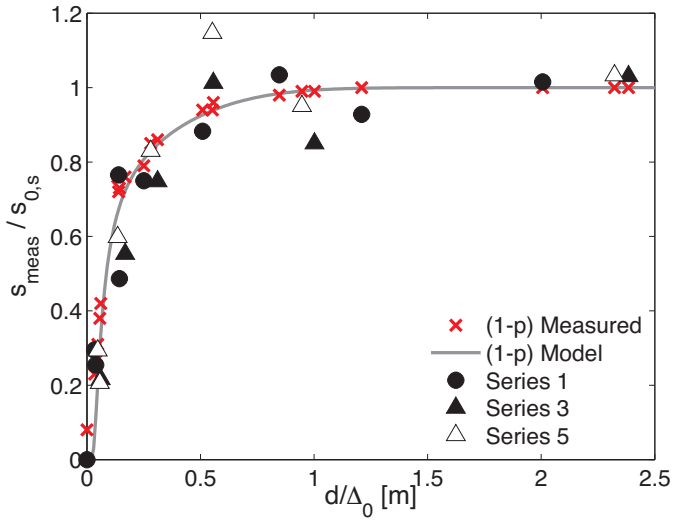

Figure 5.10: Comparison of the transport reduction as derived from the experimental data and the reduction model that used the fraction of the bed covered with bedload sediment.

The reference transport rate $s_{0,s}$ and the immobile layer exposure need to be predicted in order be able to predict the supply-limited transport rate. In order to predict $s_{0,s}$ a model for the bed shear stress and therefore for the supply-limited bed roughness is needed as well as a model for the coverage of the immobile layer with sand. Here we use the bed roughness and immobile layer exposure models presented by Tuijnder et al. (Subm/Ch. 4). These model concepts are summarised below.

Bedform dimensions

Dunes are a large source of roughness in the mildly supply-limited regime where still enough sediment is present for dune formation. The dune dimensions in this regime are not only dependent on shear stress and grain size as under alluvial conditions, but also on the sediment availability. This dependency was studied using the equilibrium experiments and resulted in a bedform dimensions reduction (BDR-) function. This function takes the effect of

a limited average layer thickness (d) relative to the alluvial dune height (Δ_0) into account. This BDR-function needs to be combined with a model for alluvial dune dimensions to actually predict dune dimensions. For the alluvial bedform dimensions the dune height predictor by Van Rijn (1984) is used. This model reads as:

$$\frac{\Delta_0}{h} = 0.11 \left(\frac{D_{50}}{h}\right)^{0.3} \left(1 - e^{-0.5T}\right)(25 - T) \quad \text{(Eq. 5.13)}$$

$$\Lambda_0 = 7.3h \quad \text{(Eq. 5.14)}$$

T is the mobility parameter. It is defined as:

$$T = \frac{\theta' - \theta_{cr}}{\theta_{cr}} \quad \text{(Eq. 5.15)}$$

For θ_{cr}, the critical Shields parameter for initiation of motion, the fit of the Shields curve (Shields, 1936) by Brownlie (1981) and modified by Parker has been used. The grain related Shields parameter (θ') is estimated using:

$$\theta' = \frac{\tau'}{(\rho_s - \rho) g D_{50}} \quad \text{(Eq. 5.16)}$$

$$\tau' = c_{f,90} \rho u^2 \quad \text{(Eq. 5.17)}$$

$$c_{f,90} = g \left(18 \log \frac{12 R_b}{3 * D_{90}}\right)^{-2} \quad \text{(Eq. 5.18)}$$

The sediment characteristics (D_{50} and D_{90}) of the bedload sediment are used. Furthermore, for the grain related roughness ($c_{f,90}$) a roughness height of 3*D_{90} is used as proposed by Van Rijn. These values are related to the bedload sediment only, not the total surface sediment, because the model is applied to get an estimation of the dune dimensions under alluvial conditions. The prediction of the alluvial dune dimensions has been calibrated using the alluvial experiments (indicated with an 'a' in Table 5.1) from the calibration data set as well as 5 additional alluvial experiments. The correction factor for the dune height is 1.29 and for the dune length it is 0.89.

The BDR-functions are applied to take the influence limited sediment availability into account. These functions read as:

$$\frac{\Delta}{\Delta_0} = 1 - \exp\left(\frac{-d}{\alpha_h \Delta_0}\right) \quad \text{(Eq. 5.19)}$$

$$\frac{\Lambda}{\Lambda_0} = 1 - \beta \exp\left(\frac{-d}{\alpha_l \Delta_0}\right) \quad \text{(Eq. 5.20)}$$

These functions describe a growth of the dune dimensions with increasing sediment availability (d/Δ_0). The parameter values are α_h = 0.39, α_l = 0.24 and β = 0.96.

Immobile layer exposure

It is shown by Tuijnder et al. (Subm/Ch. 4) that the fraction of the bed where the immobile layer is exposed can be written as an error function:

$$p = 0.5 * (1 - \mathrm{erf}(-z)) \quad \text{(Eq. 5.21)}$$

Where z is defined as:

$$z = 2.5 \frac{1/2 D_{cl} - d}{\Delta\sqrt{2}} \quad \text{(Eq. 5.22)}$$

Bed roughness

In order to predict the bed roughness the bedform roughness and the grain roughness are estimated. The roughness model by Engelund (1977) is applied using the supply-limited dune dimensions and a modified grain roughness model. The total bed roughness, expressed as a friction factor, is the sum of the form drag related component (c_f') and a grain roughness component (c_f''):

$$c_{f,b} = c_f' + c_f'' \quad \text{(Eq. 5.23)}$$

The form drag related roughness is predicted using the form drag model that was derived by Yalin (1964) and Engelund (1977):

$$c_f'' = \frac{\Delta^2}{2h\Lambda} \quad \text{(Eq. 5.24)}$$

For the grain roughness prediction a White-Colebrook type of model is applied. The immobile layer and the bedload sediment have a separate roughness height. These are added using p as a weighting factor.

$$c_f' = p * c_{f,cl} + (1 - p) * c_{f,bl} \quad \text{(Eq. 5.25)}$$

The roughness height of the bedload sediment is estimated to be $1D_{90}$ for the experiments used here.

$$c_{f,bl} = \left(6 + \frac{1}{\kappa} \ln \frac{R_b}{k_{s,bl}}\right)^{-2} \quad \text{(Eq. 5.26)}$$

$$k_{s,bl} = 1D_{90} \quad \text{(Eq. 5.27)}$$

The roughness height of the coarse layer varies with presence of sand on the coarse layer due to infilling of the space between the gravel particles. If the gravel is completely exposed the

roughness height is estimated to be 3 D_{cl} and decreases linearly to ½D_{cl} until the coarse layer is filled. This is assumed to be at d = ½D_{cl}.

$$c_{f,cl} = \left(6 + \frac{1}{\kappa} \ln \frac{R_b}{k_{s,cl}}\right)^{-2} \quad \text{(Eq. 5.28)}$$

$$k_{s,cl} = 3D_{cl} - 5d \text{ for } d \leq {}^1/_2 D_{cl} \quad \text{(Eq. 5.29)}$$

$$k_{s,cl} = {}^1/_2 D_{cl} \text{ for } d > {}^1/_2 D_{cl} \quad \text{(Eq. 5.30)}$$

The total roughness, as measured in the flume experiments in this study, is the sum of the wall roughness and bed roughness. The roughness of the wall and bed is estimated using the method of Vanoni and Brooks (1957). For more details about the supply-limited roughness model reference is made to Tuijnder et al. (Subm/Ch. 4).

Application of integral model to equilibrium experiments

In a morphological model the prediction of the sediment transport depends on the roughness prediction. Therefore the combined roughness model and transport reduction function are tested below. The previously described model for supply-limited transport rate predictions is applied to hindcast the equilibrium experiments in order to test the model concepts.

The discharge, bed slope, flow width and the grain sizes of the immobile layer and the bedload sediment of the experiments are the starting point for the transport predictions. Based on these variables first the dune dimensions (Eq. 5.13-5.20), immobile layer exposure (Eq. 5.21-5.22), the bed roughness (Eq. 5.23-5.30) and the flow velocity and water depth are predicted. Chézy's law for equilibrium flow is used to calculate flow depth and velocity. This is done iteratively since the roughness depends on the flow depth and velocity and vice versa. After the roughness, depth and velocity are solved, the sediment transport is predicted. The reference transport rate $s_{0,s}$ is predicted using Eq. 5.5-5.11 and subsequently the transport is reduced using Eq. 5.12.

Inaccuracies in one of the sub-models propagate through the model and appear to some extent in all parameters due to the iterative nature of the system. For this reason, even sub-models that were previously calibrated using measured input data can give inaccurate results because of inaccurately predicted input. The form drag prediction, which was previously uncalibrated, has been calibrated to improve the results of the integral model. The model has been calibrated by introducing a calibration factor (α_{cf}) in Eq. 5.24 this reads as:

$$c_f'' = \alpha_{cf} \frac{\Delta^2}{2h\Lambda} \quad \text{(Eq. 5.31)}$$

A calibration factor α_{cf} = 0.8 in the form drag predictor results on average in a better roughness and shear stress prediction and therefore in a better sediment transport prediction.

In Figure 5.11 the measured and predicted results are shown for Series 1, 2, 3 and 5 of the equilibrium experiments. The first two rows show the prediction of the bedform dimensions. The red line shows the measured values, the predictions using the calibrated model are shown with the black line and the uncalibrated model is shown with the dashed gray line. The third row shows the estimated bed coverage. These variables are input for the prediction of the bed roughness ($c_{f,b}$) in the fourth row and the bed shear stress in the fifth row. The variables in rows 1-5 are solved iteratively, once a solution has been found the ripple factor (sixth row) and the sediment transport (seventh row) are calculated.

The agreement between the measured and predicted parameters in Figure 5.11 is generally good for the dune height (Δ), length (Λ) and immobile layer coverage (p). The bed roughness ($c_{f,b}$) is slightly overpredicted on average with the uncalibrated model, which leads to an underprediction of the sediment transport rate. This is caused by a reduction in μ if the roughness is overpredicted (C < in Eq. 5.7). The calibration factor α_{cf} improves the average prediction of the roughness and the sediment transport rate. However, it can be seen that the uncalibrated results is actually better for Series 2 and 5. The deviation between the measured and predicted transport rates is smaller than 30% for 75% of the predictions and smaller than 50% for 85% of the predictions. The largest deviations occur for the smallest measured transport rates, even though the absolute differences are small. It can be concluded that the integrated model predicts the measured transport rates in a satisfactory way.

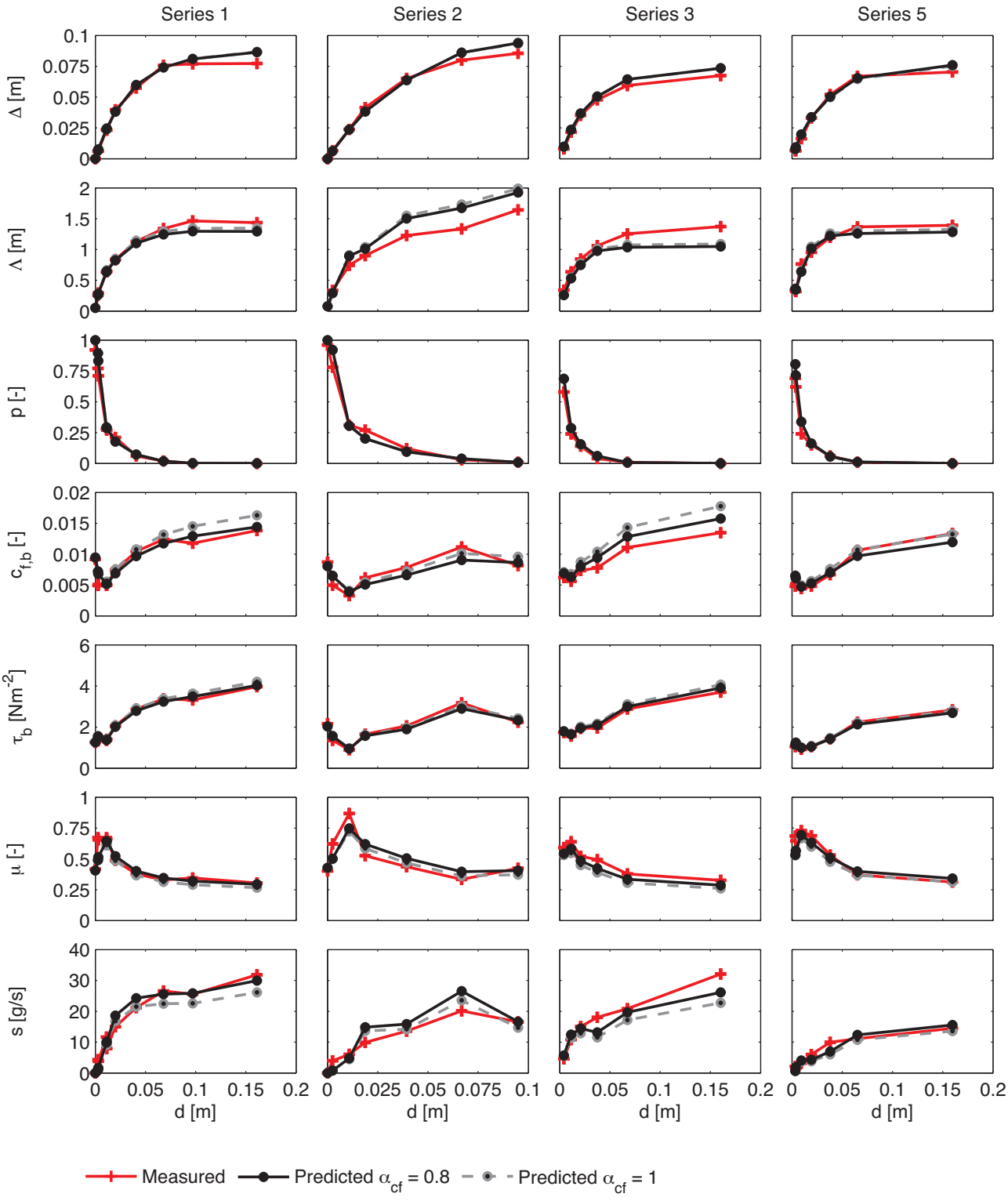

Figure 5.11: Comparison of measured variables to predicted variables with the integrated roughness and transport prediction.

5.5 Application in morphodynamic modelling

In this section the two modelling approaches are compared in the framework of a morphological model, Delft3D (Lesser et al., 2004). The model is applied to simulate the three morphological flume experiments as described in Section 5.2. On the one hand we apply the new 'Bedform Behaviour Based' (BBB-) model, where the supply-limited transport rate is calculated on the basis of the varying immobile layer coverage and the bedform dependent bed roughness. On the other hand we apply the 'Struiksma model', with a constant bed roughness and the sinusoidal reduction that starts at $d = ½\ \Delta_0$. For the Struiksma model a Chézy value of 32 $m^{½}/s$ has been used; this gives equilibrium flow under the average water depth and bed slope. The assumption of equilibrium flow (the Chézy equation) as used in the previous section is not valid and no longer needed, since Delft3D solves the shallow water equations.

The initial conditions are defined to match the initial conditions of the morphological experiments as described in Section 2.2: a sand layer of constant layer thickness is defined over the range $x = 6.5$ to $x = 13.5$. The measured downstream water level is used as boundary condition in the model to make the water level agree with the measured water level. For the side-walls free slip boundary conditions are imposed. This ensures that the solution is a two dimensional solution, with no lateral bed level variation. The bed shear stress reducing effect of the side walls is taken into account by applying the method of Vanoni and Brooks (1957).

The used grid has a cell length of 50 cm longitudinally. This means that the grid is too coarse to simulate dune development, as is generally also the case for applied morphological river models. The simulation was run with a time step (*dt*) of 30 s. Increasing *dt* with a factor 2 or decreasing it with a factor 5 gave very similar results. The results with the 5x smaller time steps are slightly more diffusive, which is probably caused by increased numerical diffusion.

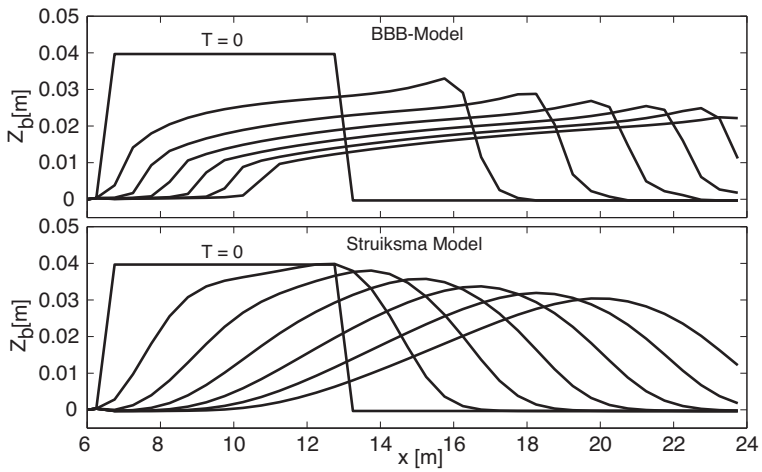

Figure 5.12: Morphological development for the Struiksma model and the BBB-model. There is one hour between two consecutive profiles.

The computed morphological development is different for the Struiksma reduction concept and the new BBB-model. This is illustrated in Figure 5.12 with the morphological development as simulated for Experiment 1. This figure shows the average bed level for the initial situation and the morphological development at one hour intervals. The solution for the new BBB-model shows a steep wave front and a well-defined tail; non-linear advective behaviour is dominant. Whereas the character of the Struiksma model is more that of a linear advection-diffusion equation. Contrary to the BBB-model, the Struiksma model does not maintain a well defined tail of the wave.

Simulation of morphological experiment 1

The simulations are compared to the experiments in order to know which behaviour is more realistic. Figure 5.13 shows the results of the experiments and both model concepts against an x and t (time) axis. This shows the migration pattern of the bed wave and, in case of the experimental data, also the individual bedforms. The result of Experiment 1, which was started with a 4 cm thick sediment layer, shows divergent behaviour with a front that moves clearly faster than the tail of the wave. The velocity of the front decreases gradually. The highest dunes occur towards the front of the migrating sand wave. Figure 5.13 shows that the divergent behaviour of the experiments is well represented by the BBB-model. The Struiksma model predicts a gradual decrease of the bed level at the back side, where in reality an abrupt transition is observed.

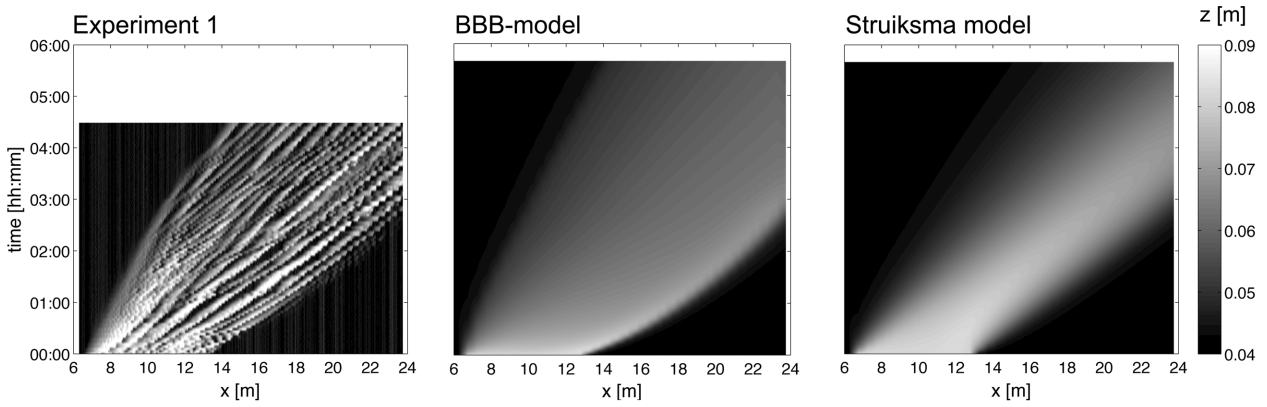

Figure 5.13: Measured and predicted bed level of experiment 1 against x and time axes. This representation is suitable for seeing the morphological development of the sand wave. The experimental results show the individual bedforms and their migration. This is invisible in the simulations as the average bed level behaviour is simulated and the effect of the bedforms is parameterised.

The models simulate the behaviour of the average bed level. Therefore, the models should be compared to the average bed level. In order to do so, the bed level measurements have been filtered with a moving average filter; this smoothes out the appearance of individual bedforms. A moving average filter with a hann-window with a width of 2 m has been applied on the average of the three bed level sensors. The result is shown in Figure 5.14.

Figure 5.14 compares the predictions of the two models with the bed level measurements in Exp. 1 after 2 hours in a longitudinal profile in the centre of the flume. The irregular gray line shows the bed level measurements and shows that the migrating sand wave consists of a train of migrating bedforms. It also shows that the front and back of the sand wave are quite abrupt. The black line is the filtered bed level. This line is still wavy due to the bedforms. The filter would have to be stronger to completely smooth out the bedforms. However, the abrupt front and tail of the sand wave would be lost with a stronger filter. The blue line shows the predicted average bed level by the new BBB-model, while the red line shows the predictions of the Struiksma model. The filtered bed level shows that the sand wave has an abrupt leading edge, followed by a relatively constant average level in the middle and an abrupt trailing edge. This behaviour is better represented by the new BBB-model. This model predicts abrupt edges and a slightly sloping middle section at approximately the same level as the filtered bed level. The Struiksma-model also predicts a steep leading edge, but it overpredicts the average bed level in the middle and underpredicts towards the trailing edge. Furthermore, the model does not reproduce the abrupt trailing edge; instead a smooth transition is predicted. The BBB-model also provides predictions of the average dune height, as shown by the dashed gray line. While the model concepts for the dune height prediction assume equilibrium conditions, here they are applied to non-stationary conditions. Despite the non-stationarity, the bedform heights are accurately predicted.

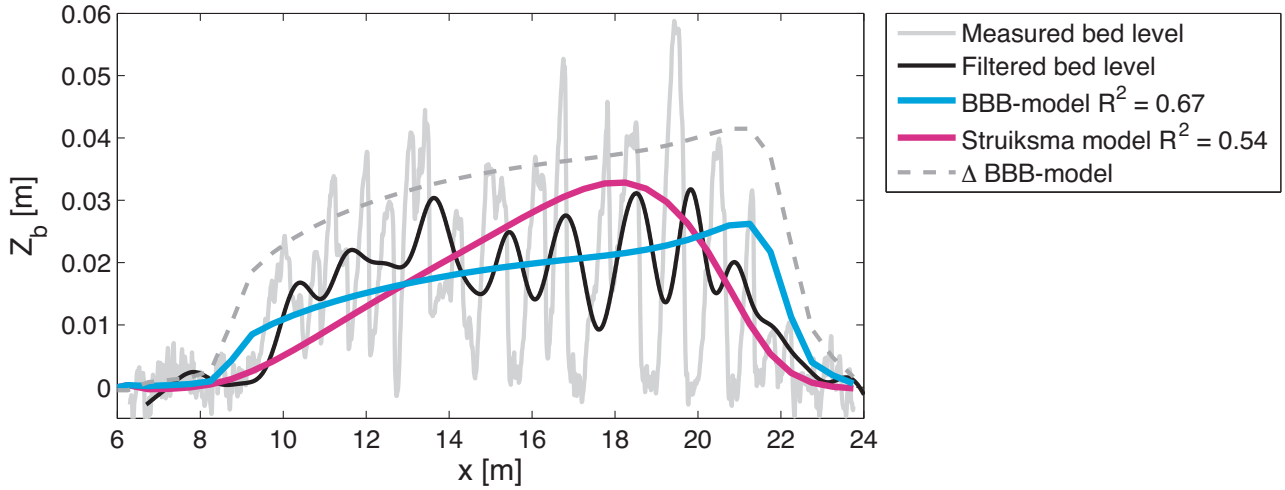

Figure 5.14: Comparison of the measured bed level in Exp. 1 with predicted bed levels and dune height using the BBB-model and Struiksma model after 2 hours.

We calculated R^2, the coefficient of determination, in order to quantitatively estimate which model predicts the average bed level better. This coefficient is usually applied to statistical models, it can however also be applied to provide a relative measure for the quality of a deterministic model prediction (Nash et al., 1970). This parameter is calculated as:

$$R^2 = 1 - \frac{\sum_i^n (p_i - o_i)^2}{\sum_i^n (o_i - \bar{o})^2} \qquad \text{(Eq. 5.32)}$$

Where p_i and o_i are the predicted and measured bed level for index i, $\bar{o}$ is the average measured bed level and n is the total number of observations. The fit of both models to the filtered measured bed level has been calculated for the range x = 6.75 – 23.75 m. For the situation after 2 hours, as shown in Fig. 5.14, the R^2 is 0.67 for the BBB-model and R^2 is 0.54 for the Struiksma model, which indicates that the new BBB-model gives a better prediction.

Simulation of morphological experiment 2

Figure 5.15 shows that the sand wave is less divergent in Experiment 2. The leading edge and trailing edge are more parallel than in Experiment 1. This is well represented by both simulations. This figure also shows that the edges of the sand wave are well-defined. This is shown even more clearly in the measured bed level line in Figure 5.16. Again the behaviour of the simulation using the Struiksma concept is more diffusive than the BBB-model. Therefore the Struiksma model predicts gradual transitions from sand wave to immobile layer where abrupt edges are observed. The dune height is again predicted well by the BBB-model, however at the tail of the wave the dune height is slightly underpredicted while the small dunes at the leading edge are slightly overpredicted.

The R^2 values for both models are roughly equal: 0.83 for the BBB-model and 0.81 for the Struiksma model. However, it should be noted that the small wave lengths, like this abrupt change in bed level at both edges, are lost to a certain degree due to the bed level filtering. The makes the edges more diffusive, which is an advantage for the Struiksma model. It can be concluded that qualitatively the BBB-model is preferable, and also quantitatively the new BBB-model is slightly better.

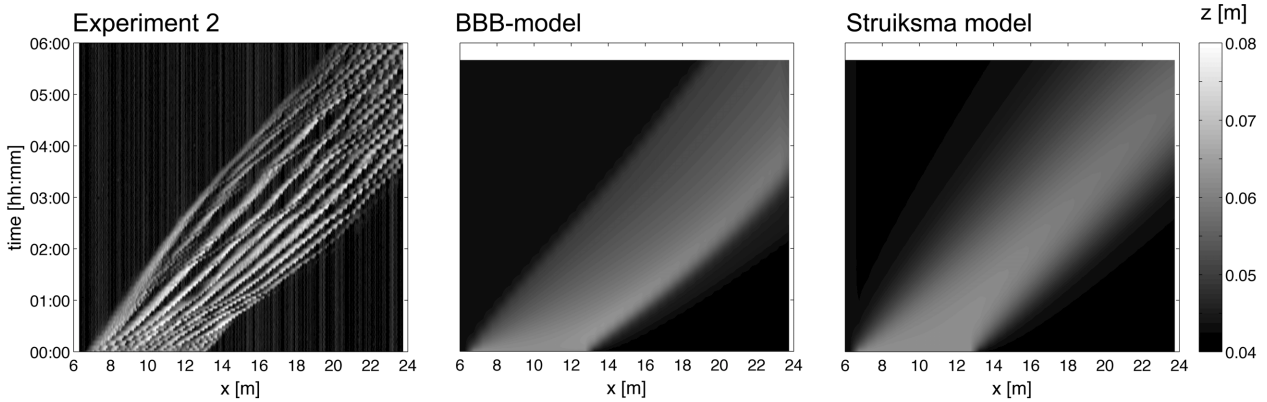

Figure 5.15: Measured and predicted bed level of Exp. 2 against *x* and time axes.

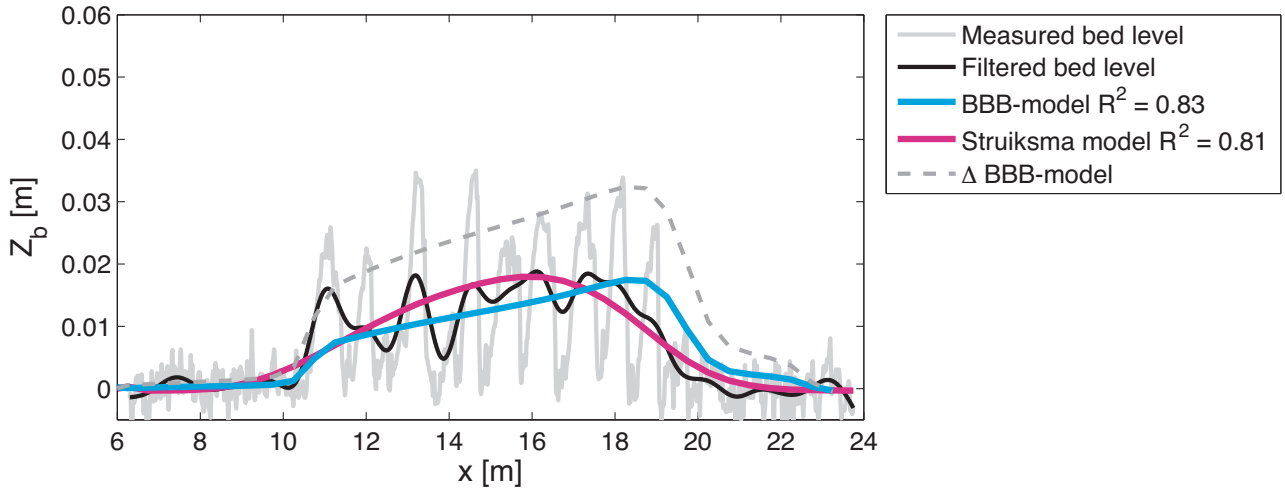

Figure 5.16: Comparison of the measured bed level in Exp. 2 with predicted bed levels and dune height using the BBB-model and Struiksma model after 2 hours.

Simulation of morphological experiment 3

Figure 5.17 shows the bed level development during Experiment 3. This figure shows that the sediment converges in a large dune at the trailing end of the bed wave. After 2 hours a region of small bedforms can be seen that precedes larger dunes at the back of the sand wave (see also Fig. 5.18). The BBB-model also predicts this pattern where the sediment converges at the tail of the sand wave. The pattern predicted by the Struiksma model is very similar to that in the previous experiments: the same smooth migrating bed wave. The R^2 is calculated from x = 10 – 23.75 m for this model, since the rest of the bed was without sand. Again the BBB-model (R^2 = 0.49) is slightly better than the Struiksma model (R^2 = 0.44).

Overall it can be concluded that the new BBB-model only gives a slightly better overall bed level preduction than the Struiksma model. However, the bed level patterns like the abrupt edges and the divergence or convergence of sediment are better reproduced by the BBB-model.

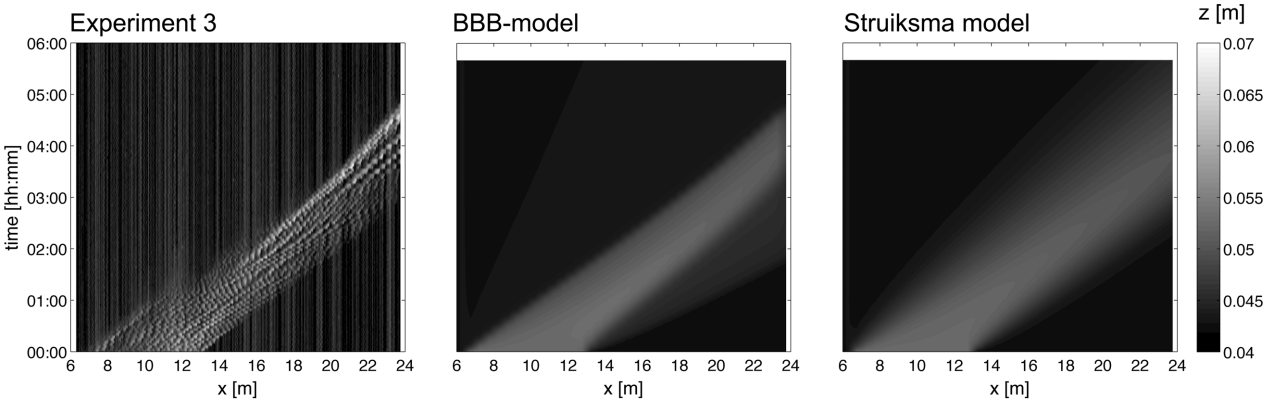

Figure 5.17: Measured and predicted bed level of Exp. 3 against *x* and time axes.

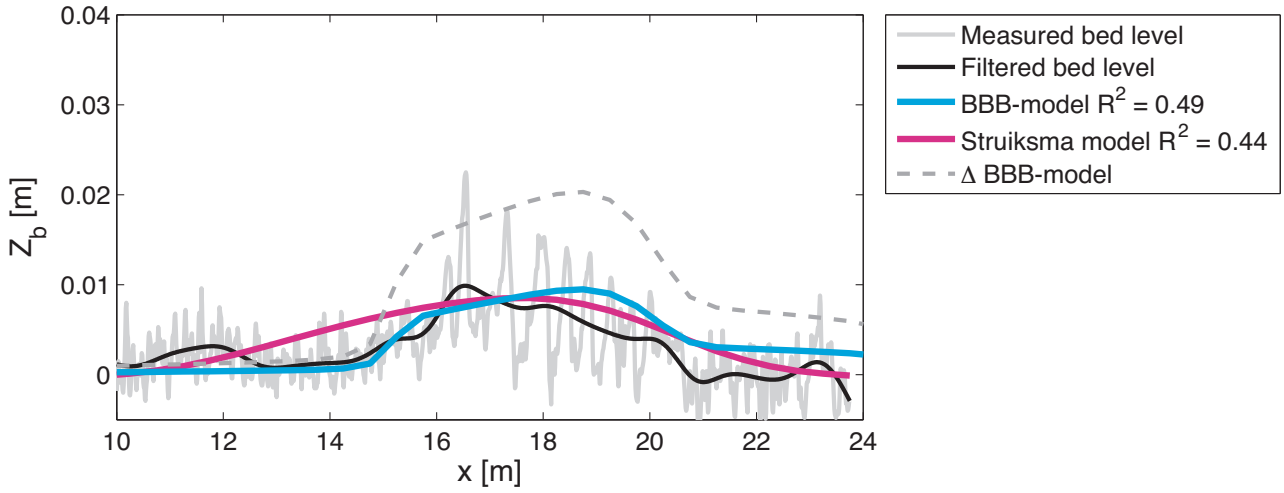

Figure 5.18: Comparison of the measured bed level in Exp. 3 with predicted bed levels and dune height using the BBB-model and Struiksma model after 2 hours.

5.6 Discussion

The transport reduction concepts presented here provide a method to predict the transport rate of mobile sediment partially covering an immobile layer. An alternative model concept would be the application of a fractional transport model that is able to predict transport rates in partial transport conditions and uses the complete surface sediment composition (gravel and sand). Which model is more appropriate depends on the situation.

For situations where the bedload sediment is distinctly different from the immobile layer the reduction concepts are appropriate models. Partial transport models are generally not validated for the combined grain size distribution of the bedload sediment and immobile layer sediment, especially if the size difference is large. Furthermore, it is not obvious how to determine the combined grain size distribution of the combined immobile layer sediment and bedload sediment, that can be used as input for a surface based transport model for sand gravel mixtures. The advantage of the transport reduction concept is that the transport calculation is always based on the constant bedload transport composition. Moreover, the transport reduction concept also provides a more useful approach for situations where the immobile layer does not consist of immobile loose sediment, e.g. peat, clay or concrete layers.

The transport model used here to calculate s_0 is a classical transport model, based on the Meyer-Peter and Müller model, that has been calibrated to give optimal performance for the conditions encountered in the experiments. This choice has been made to avoid an extensive analysis of the applicability of many available transport models under supply-limited conditions and to focus on the different approaches in dealing with bed roughness calculation: a fixed Chézy value vs. a roughness predicted based on local conditions. In this way it can be shown that the morphodynamic behaviour indeed can be improved by adding more physical processes to roughness predictions.

However, a drawback of the choice for the MPM-like transport model is the behaviour of the ripple factor μ, which proves to be sensitive for the decreasing bed roughness. This causes an increase in the transport rate with increasing supply limitation in the morphological experiments, where the experiments do not show any sign of an increase in the transport rate. The present solution, to use a fixed value for the μ-parameter in de morphological simulations, is effective though not very elegant. Therefore a further study on the transport rate prediction in supply-limited systems is valuable to reduce the need for extensive calibration.

One of the main differences between the Struiksma reduction model and the new model is the choice of the reference situation. In order to apply the Struiksma model the alluvial sediment transport rate is needed and, in order to predict this, the alluvial roughness is needed. When considering a certain supply-limited situation, e.g. one of the equilibrium experiments, this alluvial roughness is not known a priori and needs to be predicted. In the new approach the transport reduction is related to the alluvial sediment transport rate that would occur under the actually present supply-limited roughness and shear stress (the reference transport rate), instead of the alluvial roughness and shear stress. Therefore no prediction of an alluvial shear stress and roughness is needed.

This method of using the actual shear stress for calculation of the reference transport rate rather than the alluvial shear stress, reduces the range over which a transport reduction function is needed. A value of $d_0 = 0.5\ \Delta_0$ was chosen for the start of the reduction in transport rate by Struiksma (1999). Considering the experimental results in Section 3 this layer thickness is too small for the Struiksma reduction model. A value of $d_0 = 1.5\ \Delta_0$ results in a better agreement between the measurements and the Struiksma-model (Figure 5.7). The start of the supply limitation is gradual in the new BBB-model concept and therefore no value needs to be specified for the onset of supply limitation. If we do want to specify a value for the onset of supply limitation a value of $d_0 = 1\ \Delta_0$ is a good estimation (Figure 5.10).

The model concepts for the bedform dimensions are in principle only valid for equilibrium conditions. The predictive model does not account for the time and length needed by the bedforms to develop to equilibrium conditions; instead the final equilibrium value is predicted directly. Because of the integrated nature of the model, the other model predictions, like roughness and sediment transport, are strictly speaking only reliable under equilibrium conditions. If this constraint of equilibrium conditions is strictly obeyed the model concepts cannot be applied for morphodynamic simulations at all, since morphological changes only occur under non-equilibrium conditions. Therefore, we assume that it is appropriate to apply equilibrium models under quasi-equilibrium conditions. This means that the adaptation time and length of the bedforms have to be small compared to the time and length scale of morphodynamic changes. In the morphological experiments 1-3 the length of the sand wave that is propagating over the immobile layer is not much longer than the wave length of the

dunes. For example, effects of the lack of the modelling of the adaptation mechanism can be seen in Figure 5.14. The measured bed level in this Figure between 9 and 13 m shows that the bedform height increases in the positive x-direction, the troughs become deeper and the crests become higher. The bedforms are developing to their supply-limited equilibrium dimensions over this range. The predicted bedform height is indeed a bit too high over this range. On the other hand, the dune height predictions are not far off and good results are obtained even without taking the adaptation length and time into account. Nevertheless, it is recommended to study the application of adaptation models for bedforms in non-stationary alluvial conditions under non-stationary supply-limited conditions (e.g. Rauen et al., 2009).

5.7 Conclusions

Below the conclusions are presented for each of the research questions.

I. How does the limited availability of bedload sediment on top of an immobile layer affect the sediment transport rate?

From the results of the equilibrium experiments it is concluded that the sediment transport rate is affected by the supply limitation through two processes: I) a decreasing bed shear stress due to decreasing bedform dimensions and II) a decreasing coverage of the bed with bedload sediment. The onset of the influence of supply limitation on transport reduction occurs at approximately $d/\Delta_0 = 1.5$. This initial reduction is gradual and is caused by a shear stress reduction. If the sediment availability is below $d/\Delta_0 = 1$ the reduction cannot be explained by the shear stress reduction alone. The increasing exposure of the immobile layer needs to be taken into account.

II. In what way can the observed transport rate variation due to supply-limitation be predicted with a transport model?

The transport reduction concept of Struiksma (1985) has been adapted to take the variation in bed roughness and immobile layer coverage into account. This new transport reduction model makes use of sub-models for bed roughness variation and immobile layer coverage variation due to supply limitation from Tuijnder et al. (Subm/Ch. 4). It is shown that this model leads to an improved prediction of the reduction in transport rate caused by supply-limitation. Furthermore, it is shown that the transport rate observations from the equilibrium experiments can be reproduced with a good accuracy with the proposed model.

III. Does the application of the new supply-limited transport model in a morphological model lead to better predictions of the morphological development?

A comparison of a series of morphological experiments with morphological simulations using the Struiksma transport model and the improved BBB-transport model shows that a more

realistic behaviour is obtained with the BBB-model. Especially the abrupt front and tail of the sand wave are better represented if this transport model is applied. Also the overall quantitative prediction of the bed-level changes is slightly improved by the new model.

Acknowledgements

This research project, which is part of the VICI project ROUGH WATER (project number TCB.6231), is supported by the Technology Foundation STW, applied science division of the Netherlands Organization for Scientific Research (NWO) and the technology program of the Ministry of Economic Affairs. The laboratory experiments are funded by the Delft Cluster program 'Natural Hazards', work package A2 River Morphology (WP CT 043211). The morphological simulations have been carried out in the context of the Deltares TO-project: "Rivierkundige onderzoeksthema's", subproject "Los zand, grind, en harde klei" number 1200186-002.

Furthermore the authors would like to thank A. Dittrich and the rest of the staff of the Leichtweiss-Institute for Hydraulic Engineering at the Technical University Braunschweig in Germany for their cooperation in the experiments; the help of M. Spekkers and S. Janssen with the flume experiments was also greatly appreciated. Finally, the authors would also like to thank K. Sloff, A. Spruyt de Boer and W. Ottevanger from Deltares for their help with the morphological simulations.

Chapter 6

Discussion and Conclusions

6.1 Discussion

Applicability of model concepts

The model concepts presented in this thesis are derived for the supply-limited dune regime, with bedload dominated sediment transport. This can occur where permanently immobile layers are present, but also if a sand-gravel mixture is partially mobile and forms a temporary immobile layer. Additional model concepts are still required that can predict the formation and break up of immobile sediment layers in variable flow conditions

Furthermore, the model concepts that are presented here have been developed with experiments from distinctly bimodal sediment mixtures composed of two well-sorted fractions. For these mixtures it is clear which fractions are mobile and which are immobile. However, supply-limited conditions can also develop in poorly sorted sediments where it is much less clear which size fractions remain immobile and which are (partially) mobile (see e.g. Blom et al., 2003). Possibly, the predictions of bedform dimensions, bed roughness and transport rates under these conditions can also be improved by applying a fractional transport model (e.g. Wilcock and Crowe, 2003) in combination with the model concepts proposed here.

In principle, the validity of the bedform dimensions reduction function is also limited to the regime where dunes develop under alluvial conditions. However, the bedform dimension reduction approach, in which the relative bedform dimensions are related to the relative layer thickness, may also be applicable in other regimes, e.g. the flow ripple regime. Rauen et al. (2009) conducted experiments with ripple development in a diverging channel. In these experiments a supply-limitation developed locally. Rauen et al. concluded that 'the bedforms did not reach the equilibrium stage', because of a supply-limitation. Compared to the findings in this thesis it could be concluded that the ripples reached a supply-limited equilibrium rather than an alluvial equilibrium. Because of the supply-limitation it was impossible to predict the steady state dimensions. Possibly, the ratio of the supply-limited ripple dimensions and the alluvial ripple dimensions can also be related to the sediment availability in a similar way as has been demonstrated for dunes in this thesis.

The model concepts described here may even be applicable outside of the fluvial setting for which the present study was conducted. Longsdale and Malfait (1974) described the occurrence of a field of dunes and barchans in the deep sea that developed on a valley floor at

a depth of ±2650 m. These bedforms formed in forminiferal sands. These are sands that have been formed by the deposition of the outer shells of foraminifera that sink to the ocean floor once they die. Foraminifera are a plankton-like life form that build a shell of calcium carbonate (Whittow, 1984). Presumably, density currents periodically transport the forminiferal sand and formed a field of supply-limited dunes on the immobile valley floor.

Sediment starved vs. isolated dunes

The model concepts for immobile layer exposure and bedform dimension prediction presented in this thesis assume the presence of sediment-starved dunes. Sediment starved dunes are dunes that become lower in reaction to a supply-limitation. At the same time the dune length, measured between two successive lee sides, decreases as well. This reaction to a supply limitation was observed in the experiments with a coarse immobile layer presented in this thesis. Similar sediment starved dunes were observed in flume experiments on a much smaller scale by Dreano (2008) and in flume experiments with a bimodal sand-gravel mixture (Kuhnle et al., 2006). Similar to our experiments, these flume experiments were conducted with uniform stationary flow conditions that are suitable for dune development under alluvial conditions. However, a different reaction to supply limitation is the formation of isolated dunes instead of sediment-starved dunes. These dunes gather enough sediment to reach normal alluvial dimensions. In this situation, the supply limitation causes increasing lengths between the dunes with increasing supply limitation. This type of reaction, the formation of isolated bedforms, was observed in the Rhine by Carling (2000). The controls for the formation of isolated bedforms instead of sediment starved dunes are not completely clear yet. The occurrence of repeated flood waves could be a cause, but also external topographic controls are likely to play a role.

Prediction of alluvial bedform dimensions

The alluvial bedform dimensions play an important role in the prediction of the supply-limited bedform dimensions and therefore the bed roughness. The water depth and bed shear stress of the supply-limited conditions are used as input for Van Rijn's alluvial bedform model (Van Rijn, 1984) in the proposed prediction method. The predicted alluvial dune height with supply-limited parameters ($\Delta_{0,SL}$) will deviate somewhat from the alluvial dune height predicted with alluvial parameters ($\Delta_{0,A}$). The reason to choose for this approach is that in this way the bedform dimensions predictions are not dependent on the flow velocity and water depth that would exist in the different situation; a situation that is potentially in a different bedform regime like e.g. the upper plane bed regime.

It could be argued however, that the water depth and shear stress that exist in the presence of the alluvial dunes should be used. In principle, it is possible to determine the alluvial water depth and shear stress using the same iterative method that is used to determine the supply-

limited values (see Chapter 4). Although, that means a considerable increase in the computational effort.

The predictions of the alluvial dune height using both methods are compared in the figures below in order to see whether these methods give fundamentally different results. In the experiments of DS-II we have measurements of both the alluvial and supply-limited conditions. $\Delta_{0,SL}$ has been calculated by using the measured supply-limited water depth and shear stress as input to Van Rijn's alluvial bedform dimensions model. $\Delta_{0,A}$ is the dune height that has been predicted with Van Rijn's model using the measured alluvial water depth and shear stress. The ratio of these values is shown in Figure 6.1. It can be seen that the difference of the two methods is approximately 10% under supply-limited conditions and it decreases towards the alluvial conditions. For the alluvial experiments the ratio $\Delta_{0,A}$ /$\Delta_{0,SL}$ is one by definition.

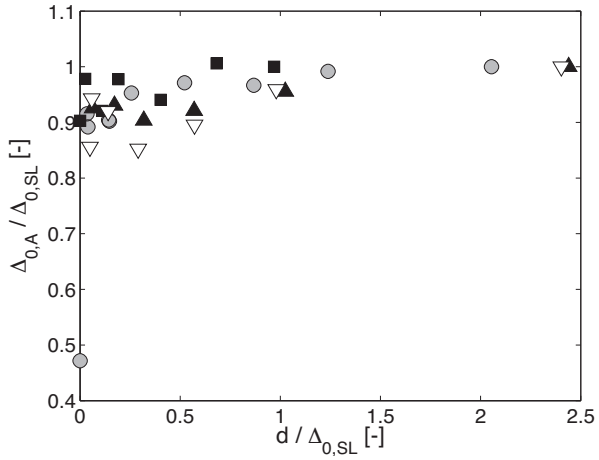

Figure 6.1: The difference in predicted bedform height due to the use of the alluvial conditions or the supply-limited conditions as input for the bedform dimensions model.

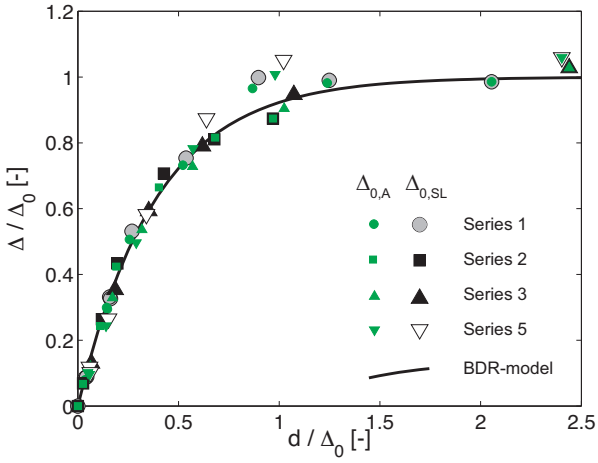

Figure 6.2: Effect of the different approaches on the prediction of supply-limited dune heights. The small green symbols show the result using the alluvial conditions to predict the alluvial dune height. The difference is very small.

Figure 6.2 shows the effect of this difference in the scaling of the supply-limited dune height with the transport layer thickness. The figure shows the bedform dimensions reduction (BDR) model that was fitted to the measured data in Chapter 3. The points shown in the figure are the measured bedform dimensions and layer thickness divided by the predicted alluvial dune height using the alluvial method (in green) and the supply-limited method (in gray). The points keep following the BDR-model no matter which method is used. The relatively small difference between both methods is further reduced by the fact that both the supply-limited dune height and the transport layer thickness are scaled by the alluvial dune height. It is concluded from this exercise that both methods lead to the same predicted supply-limited dune height. However, the use of $\Delta_{0,SL}$ is computationally much more convenient, since only the actual supply-limited shear stress needs to be solved.

6.2 Conclusions

Below the conclusions of the present study are given by answering the research questions that were posed in the introduction.

I. What is the influence of the volume of bedload sediment as present on top of an immobile layer on the bedform characteristics in general, and particularly on the average bedform dimensions?

To answer this question, laboratory experiments were carried out in conditions (water depth, flow velocity and grain size) which were in principle suitable for dune development. In supply-limited conditions dunes can also develop as long as the volume of bedload sediment is sufficient. It can be concluded from these experiments that both the dune height and length decrease with decreasing availability of bedload sediment.

The research question above has been formulated with the general term 'bedforms' because the dunes that develop under supply-limited may lack some of the characteristics of alluvial dunes. Alluvial dune dimensions scale with the water depth (Van Rijn, 1984; Carling, 1999 and references therein). However, in the supply-limited regime the sediment supply is a stronger control on the bedform dimensions than the water depth, and the scaling of the dune length with water depth ($\Lambda \approx 7\ h$) is lost. Dunes are still observed until the sediment availability, expressed as d/Δ_0 decreases to approximately 0.2. For a stronger supply limitation ($d/\Delta_0 < 0.2$), flow parallel sand ribbons with superimposed ripples are formed.

Apart from the response of average dune dimensions on the supply limitation also the regularity of the dunes changes. We found that the presence of the immobile layer leads to more regular bedforms. A dominant wave length was clearly present in the spectra whereas under alluvial conditions the spectral energy is more distributed over a range of wave lengths.

II. How can the bedform dimensions be predicted under supply-limited conditions?

Alluvial dune dimensions (Δ_0, Λ_0, the dune height and length) are predictable by using one of the available prediction methods with input of grain size, shear stress and water depth. In Chapter 3 it has been shown that the ratio of the average transport layer thickness (d) to the alluvial bedform height (Δ_0) determines the maximum supply-limited bedform dimensions relative to the alluvial bedform dimensions (Λ/Λ_0 and Δ/Δ_0). Two new bedform dimension reduction functions were proposed which extend the alluvial dune dimension predictors to the supply-limited regime.

III. What is the effect of variation in supply-limitation on the bedform roughness and the grain roughness?

The laboratory experiments provided the following insights in the qualitative influence of supply limitation on bed roughness: Variation in supply-limitation causes variation in

bedform dimensions and in the coverage of the (usually coarser) immobile layer with sand. The decrease in bedform dimensions with an increasing supply limitation leads to a decreasing bedform roughness. An increasing supply limitation also leads to an increased exposure of the immobile layer. The bedload sediment and the immobile layer generally have a different grain roughness height. Therefore, the coverage of the immobile layer with bedload sediment becomes an additional relevant parameter for the roughness prediction under supply-limited conditions. With increasing coverage of the immobile layer the grain roughness height approaches the value of the bedload sediment. The roughness height of the immobile layer itself appeared to decrease with increased infilling of the space between the particles of the immobile layer.

IV. In what way can the roughness prediction for supply-limited conditions be improved?

The roughness model of Engelund (1966) has been modified for application in the supply-limited regime. In order to better predict the bed roughness under supply-limited conditions the effects of the 'reduced' bedform dimensions and the variability in the coverage and roughness heights are included.

The bedform dimension reduction function presented in Chapter 3 has been combined with a model for alluvial bedform dimensions (Van Rijn, 1984) for prediction of the supply-limited bedform dimensions. It could be shown that the form roughness predictor can be applied unaltered, using these supply-limited bedform dimensions. The grain roughness prediction is split into two parts: where the bedforms cover the immobile layer a representative grain size for the bedload sediment is used; where the immobile layer is exposed a variable roughness height is applied.

A new model concept to predict the exposure of the immobile layer has been presented. In this model a Gaussian bed level probability distribution function is assumed for the supply-limited dune field. This function predicts a percentage of the bed below the top of the immobile layer (z_{til}). It could be shown that the relative area of the bed where the immobile gravel layer is exposed (p) agrees well with the predicted area below the top of the immobile layer.

The grain roughness height of the bedload sediment can be estimated using the usual roughness height predictors (e.g. Van Rijn, 1984). Using $k_s = D_{90}$ of the sand worked well in the cases presented in this thesis. The roughness height of the immobile layer varies due to variable infilling of the interstice space between the coarser particles of the immobile layer. If the immobile layer is clean, the roughness height for the gravel can be used. The value $3D_{cl}$ worked well in our case. In the new model this 'clean' immobile layer roughness decreases linearly to the lower roughness of the immobile layer that is saturated with sand. The total grain roughness, expressed as a friction factor, of the bedload sediment and the immobile

layer are added according to their presence at the bed surface, using p and 1-p as weighting factors.

The roughness predicted with the new model generally showed a good agreement with the measured roughness of the lab experiments. It is concluded that the inclusion of the described supply-limited processes in a physics-based empirical roughness model strongly improves the accuracy of the roughness predictions. Application of 'alluvial' roughness model concepts to a supply-limited situation will generally result in an overprediction of the bed roughness.

V. How can the sediment transport be calculated in supply-limited situations from the local flow and sediment conditions on top of an immobile layer?

Based on flume experiments it has been shown in Chapter 5 that the roughness and immobile layer exposure variations, caused by supply-limitation, have a clear effect on the sediment transport rates. The bed shear stress is not effective for sand transport over that part of the bed where the immobile layer is exposed. The experimental results indicate that the supply-limited transport rate scales with the bed coverage by mobile sediment. A new transport model concept is proposed that relates the supply-limited transport to I) the relative bed coverage with sand and II) a reference transport rate. The latter can be predicted using a classical transport model with input of the bed shear stress adjusted for supply limitation.

VI. How can morphological simulations be improved in case of supply-limited sediment transport?

This question has been answered by I) carrying out a new set of flume experiments in supply-limited non-equilibrium conditions, and II) simulating these experiments with Delft3D after implementation of the new sub-models for supply-limited conditions.

The current state of art in the modelling of supply-limited transport over an immobile layer is the application of a transport reduction approach as proposed by Struiksma (1985). In this modelling approach roughness variation due to supply-limitation is ignored and the reaction of the sediment transport rate to the supply-limitation is approximated with simple geometric reduction functions because the actual transport reduction was not known.

In Chapter 5 this model concept has been extended to include the roughness variation due to supply-limitation. Furthermore, a new transport reduction function has been developed based on the observed transport reductions in the equilibrium flume experiments. After implementation of the new model concepts for bed roughness and the sediment transport rate in Delft3D, this model has been used to simulate the new morphological experiments. The results of the simulations show improved morphological predictions compared to the model concept of Struiksma (1985). This shows that improved morphodynamic predictions can be realized by improving the roughness prediction and the relation between sediment supply and the sediment transport rate.

6.3 Recommendations

The author recommends studying the following issues to further improve the understanding and modelling of bedform behaviour, bed roughness and sediment transport under supply-limited conditions.

Very few data sets are still available with a systematic approach towards the study of supply-limited transport. The data that can be collected from literature is diverse and multiple variables are usually different between experiments. This makes it difficult to derive relations from these data. For further model improvement, a general recommendation is that new series of experiments should be carried out in which parameters are systematically varied one by one.

The model concepts presented here become unreliable if the grain size ratio of mobile and immobile layer is large, especially if the sediment is transported in suspension. The author would consider it useful to extend the available experimental data sets with data sets in which the supply limitation is varied for different size ratios of the immobile sediment to the mobile sediment. The focus in this thesis is on conditions where transport is predominantly taking place *over* the immobile layer, due to the relatively small grain size ratio (≈15). For larger values of this ratio the transport *through*, rather than *over*, the immobile layer becomes more important. Larger shear stresses are possible without mobilizing the immobile layer for these larger grain size ratios. Therefore, also suspension becomes an important transport mechanism. This regime has received little attention in lab experiments (see Grams, 2006 and Wren, 2009). Combination of the new model concepts proposed here with model concepts for suspended transport over immobile layers can extend the applicability of the models to a wide range of conditions.

The grain size distribution in the presented experiments was always bimodal with two completely separated uniform grain size distributions. Validation and/or model extension towards widely graded continuous grain size distributions is desirable. In widely graded sediment mixtures the critical shear stress for initiation of motion is size dependent. Therefore, development of immobile layers that cause supply-limited conditions is possible. It is recommended to further investigate the application of the models as presented in this thesis to these partial transport conditions. It should be realized that additional model concepts are required that can predict the formation and break up of immobile sediment layers.

References

Allen, J.R.L. (1976) Computational models for dune time-lag: general ideas, difficulties and early results. Sedimentary Geology, 15, pp. 1–53.

Allen, J.R.L. (1984) Sedimentary structures: Their character and physical basis. Elsevier, Amsterdam.

Bakker, B. (1982) Determination of bed form dimensions in the sand flume; description and some results of program DULOC (in Dutch). Technical report R 657-XLV. Delft Hydraulics Laboratory, Delft, The Netherlands.

Bendat, J.S. and Piersol, A.G. (2000) Random Data Analysis and Measurement Procedures. John Wiley & Sons, New York.

Bennett, S.J. and Bridge, J.S. (1995) The geometry and dynamics of low-relief bed forms in heterogeneous sediment in a laboratory channel, and their relationship to water flow and sediment transport. J. Sed. Res., A64(1), pp. 29-39.

Blom, A., Ribberink, J.S., and de Vriend, H.J. (2003) Vertical sorting in bedforms: Flume experiments with natural and trimodal sediment mixture. Water Resour. Res., 39(2) 1025, doi:10.1029/2001WR001088.

Brownlie, W.R (1981) Prediction of flow depth and sediment discharge in open channels. Rep. No. KH-R43B Lab. of Hydr. Res. California Institute of Technology, Pasadena, California

Carling, P.A (1999) Subaqueous gravel dunes. Journal of Sedimentary Research 69 (3), pp. 534-545.

Carling, P.A., Williams, J.J., Gölz, E. and Kelsey, A.D. (2000) The morphodynamics of fluvial sand dunes in the River Rhine, near Mainz Germany. I. Hydrodynamics and sediment transport. Sedimentology, 47, pp. 253–278.

Cartwright, D.E. and Longuet-Higgins, M. S. (1956) The Statistical Distribution of the Maxima of a Random Function. Proc. Roy. Soc. London. Series A, Math. and Phys. Sc., Vol. 237, Num. 1209, pp. 212-232.

Chiew, Y.M. (1991) Bed features in Nonuniform sediments. J. Hydraul. Eng. 117(1), pp. 116-120.

Chow, V.T. (1959) Open-channel hydraulics, McGraw-Hill, New York, USA.

Dalrymple, R. W. and Rhodes, R. N. (1995) Estuarine dunes and bars. Geomorphology and sedimentology of estuaries. Developments in Sedimentology, Vol. 53, pp. 359-422.

Coleman, S.E., Zhang, M.H., and Clunie, T.M. (2005) Sediment-Wave development in subcritical water flow. J. Hydraul. Eng. 131(2), pp. 106-111.

Curran, J.C., and Wilcock, P.R. (2005) Effect of sand supply on transport rates in a gravel-bed channel. J. Hydraul. Eng. 131(11), pp. 961-967.

Dietrich, W., Kirchner, J., Ikeda, H. and Iseya, F. (1989) Sediment supply and the development of the coarse surface layer in gravel-bedded rivers. Nature 340, pp. 215–217.

Dreano, J., Valance, A., Cassar, C., and Lague, D. (2008) Experimental study of deposit morphology and sediment transport in a flume. Proceedings Marine and River Dune Dynamics (MARID) 1-3 April 2008 Leeds U.K., pp. 97-102.

Endo, N., Sunamura, T., and Akimoto, H. (2005) Barchan ripples under unidirectional water flows in the laboratory: Formation and planar morphology. Earth Surf. Proc. Land. 30 (13): pp. 1675-1682.

Engelund, F. (1966) Hydraulic resistance of alluvial streams, J. Hydr. Eng. Div.,92 (HY2).

Engelund, F. and Hansen, E. (1967) A Monograph on Sediment Transport. Copenhagen, Denmark: Technisk Forlag.

Engelund, F. (1977) Hydraulic resistance for flow over dunes, Progress report 44, Institute for Hydrodynamic and Hydraulic Engineering, Tech. Univ. Denmark.

Fredsøe, J. (1982) Shape and dimensions of stationary dunes in rivers. J. Hydraul. Eng., 108, pp. 932-947.

Frings, R.M (2007) From gravel to sand: Downsream fining of bed sediments in the lower Rhine. PhD-Thesis. Faculteit Geowetenschappen Universiteit Utrecht, Utrecht, Netherlands.

Gill, M.A. (1971) Height of sand dunes in open channel flows. J. Hydraul. Eng., HY12.

Giri, S. and Shimizu, Y. (2006) Numerical computation of sand dune migration with free surface flow. Water Resour. Res. 42(10) doi: 10.1029/2005WR004588.

Grams, P.E (2006) Sand transport over a coarse and immobile bed. PhD-Thesis, Johns Hopkins University, Baltimore, Maryland, USA.

Havinga, H. Schielen, R.M.J., and van Vuren S. (2009) Tension between navigation, maintenance and safety calls for an integrated planning of flood protection measures. In Vionnet, C., García, M. H., Latrubesse, E.M., Perillo, G.M.E. (Eds.) Proc. River, Coastal and Estuarine Morphodynamics: RCEM 2009, Publ. Taylor & Francis, London, ISBN 978-0-415-55426-8, Vol I, pp. 137-143.

Hino, M. (1968) Equilibrium-range spectra of sand waves formed by flowing water. J. Fluid mech., 34, pp. 565-573.

Kleijwegt, R.A. (1992) On sediment transport in circular sewers with non-cohesive deposits. Thesis Technical Universitty of Delft, Delft, Netherlands.

Kleinhans, M.G., and Van Rijn, L.C. (2002) Stochastic prediction of sediment transport in sand-gravel bed rivers. J. Hydraul. Eng. 128(4), pp. 412-425.

Kleinhans, M.G., Wilbers, A.W.E. Swaaf, A. and Van den Berg, J.H. (2002) Sediment supply limited bedforms in sand-gravel bed rivers. J. Sed. Res., 72(5) pp. 629-640.

Koll, K. and Dittrich, A. (2001): Influence of sediment transport on armoured surfaces. Int. J. Sed. Res., 16(2) pp. 201-206

Kuhnle, R.A., Horton, J.K., Bennett, S.J., and Best, J.L. (2006) Bed forms in bimodal sand-gravel sediments: laboratory and field analysis. Sedimentology, 53, pp. 631-654.

Leclair, S. (2002) Preservation of cross-strata due to the migration of subaqueous dunes: an experimental investigation. Sedimentology, 49, pp. 1157-1180.

Lesser, G.R., Roelvink, J.A., van Kester, J.A.T.M., Stelling, G. (2004) Development and validation of a three-dimensional morphological model. J. Coast. Eng., 51, pp. 883-915.

Livesey, J.R., Bennett, S.J., Ashworth, P.J., and Best, J.L., (1998) Flow structure, sediment transport and bedform dynamics for a bimodal sediment mixture, in Gravel-Bed Rivers in the Environment, edited by P.C. Klingeman, R.L. Beschta, P.D. Komar, and J.B. Bradley, pp. 149-176. Water Resourc. Publ., LLC, CO.

Lonsdale, P. and Malfait, B. (1974) Abyssal dunes of foraminiferal sand on the carnegie ridge. Geol. Soc. Am. Bull. 85, pp. 1697-1712.

McCulloch, D.S. and Janda, R.J. (1964) Subaqueous river channel barchan dunes. J. Sed. Petrol, 34, pp. 694.

McLelland, S.J., Ashworth, P.J., Best, J.L., and Livesey, J.R. (1999) Turbulence and Secondary flow over sediment stripes in weakly bimodal bed material. J. Hydraul. Eng., 125(5), pp. 463-473.

Meyer-Peter, E. and Müller, R. (1948) Formulas for bed-load transport. In: Report from the 2nd Meeting of the International Association for Hydraulic Structures Research (IAHR), Stockholm, Sweden, pp. 39–64.

Nabi, M.A (2008) A 3D model of detailed hydrodynamics with sediment transport for simulation of subaqueous dunes. In Proc. Int. Conf. Fluvial Hydraulics, Çesme, Izmir, Turkey, Sept. 3-5, 2008., Turkey, pp. 1423-1431.

Nash, J.E. and Sutcliffe, J.V. (1970) River flow forecasting through conceptual models part I — A discussion of principles, Journal of Hydrology, 10 (3), pp. 282–290.

Nikora, V.I., Sukhodolov, A.N. and Rowinski, P.M. (1997) Statistical sand wave dynamics in one-directional water flows. J. Fluid mech., 351, pp. 17-39.

Nordin, C.F. (1971) Statistical properties of dune profiles. US Geol. Surv. Prof. Pap., 562-F.

Nordin, C.F. and Algert, J.H. (1966) Spectral analysis of sand waves. J. Hydraul. Eng., 92(HY5), pp. 95-114.

Paola, C., Parker, G., Seal, R., Sinha, S.K., Southard, J.B., and Wilcock, P.R. (1992) Downstream fining by selective deposition in a laboratory flume. Science 258 (Dec) pp. 1757-1760.

Parker, G (1990) Surface-Based bedload transport relation for gravel rivers. J. Hydraul. Res. 28(4) pp. 417-436.

Parker, G. and Andrews, E.D. (1985) Sorting of Bed Load Sediment by Flow in Meander Bends. Water Resour. Res., 21(9) pp. 1361–1373.

Rauen, W.B., Lin, B. and Falconer, R.A. (2009) Modelling ripple development under non-uniform flow and sediment supply-limited conditions in a laboratory flume. Estuar. Coast. Shelf Sci. 82 pp. 452-460.

Ribberink, J.S. (1987) Mathematical modelling of one-dimensional morphological changes in rivers with non-uniform sediment. PhD-Thesis, Technical University of Delft, Delft, The Netherlands

Shields, A. (1936) Anwendung der Aehnlichkeitsmechanik und der Turbulenzforschung auf die Geschiebebewegung. Mitteilungen der Preussischen Versuchsanstalt für Wasserbau und Schiffbau. Rep. No. 26, Berlin

Sieben, J. (2008) Taal van de rivierbodem: parameters voor morfodynamiek in rivieren. Rijkswaterstaat Waterdienst Rapport WD 2008-49

Simons, D.B. and Richardson, E.V. (1966) Resistance to flow in alluvial channels. US Geol. Surv. Prof. Pap., 422-I.

Sloff, C.J., Mosselman, E. and Sieben, J. (2006) Effective use of non-erodible layers for improving navigability. In R.M.L. Ferreira, E.C.T.L. Alves, J.G.A.B. Leal & A.H. Cardoso (Eds.) Proc. River Flow 2006, Lisbon, 6-8 Sept., 2006, Publ. Taylor & Francis, London, ISBN 978-0-415-40815-8, Vol.2, pp.1211-1220

Southard, J. and Boguchwal, L. (1990) Bed configuration in steady unidirectional water flows. part 2. Synthesis of flume data. Journal of Sedimentary Petrology 60, pp. 658–679.

Struiksma, N. (1985) Celerity and deformation of bed perturbations travelling over a non-erodible layer. Report W308, Delft Hydraulics, Delft, The Netherlands

Struiksma, N. (1999) Mathematical modelling of one-dimensional morphological changes in rivers with non-uniform sediment. Proceedings IAHR symposium on River, Coastal and Estuarine Morphodynamics (RCEM), Genova, pp. 89-98

Tuijnder, A. P., Ribberink, J. S., and Hulscher, S. J. M. H. (2007) Predicting the occurrence of dunes under supply limited conditions. In Dohmen-Janssen, C. M. and Hulscher, S. J. M. H. (Eds.) Proc. River, Coastal and Estuarine Morphodynamics: RCEM 2007, Publ. Taylor & Francis Group, Vol I, pp. 633-639.

Tuijnder, A.P., Ribberink, J.S. and Hulscher, S.J.M.H. (2009) An experimental study into the geometry of supply-limited dunes. Sedimentology, 56, pp. 1713-1727, doi: 10.1111/j.1365-3091.2009.01054.x

Tuijnder A.P., Ribberink, J.S. and Hulscher, S.J.M.H. (2009b) Morphodynamic modelling of rivers under supply-limited conditions. In Vionnet, C., García, M. H., Latrubesse, E.M., Perillo, G.M.E. (Eds.) Proceedings River, Coastal and Estuarine Morphodynamics, RCEM 2009, Publ. Taylor & Francis, London, ISBN 978-0-415-55426-8, Vol I, pp. 877 - 882

Tuijnder, A.P., Ribberink, J.S. and Hulscher, S.J.M.H. (Subm/Ch. 4) Riverbed roughness prediction under supply-limited conditions.

Tuijnder, A.P., Ribberink, J.S. and Hulscher, S.J.M.H. (Subm/Ch. 5) Modelling of Sediment Transport over Immobile Layers in Rivers using a Transport Reduction Approach.

Tuijnder, A.P., Spekkers, M.H., Ribberink, J. S. and Hulscher, S.J.M.H. (2008) Bed roughness under supply-limited conditions. In Altinakar M., Kokpinar M.A. et al., (Eds.) Proc. of the Int. Conf. on Fluvial Hydraulics, River Flow 2008, Cesme, Izmir, Turkey, Sept 3-5, 2008, pp. 395-405.

Vanoni, V.A. and Brooks, N.H. (1957) Laboratory Studies of the Roughness and suspended load of alluvial streams. Report E-68. Sedimentation Laboratory, California Institute of Technology, Pasadena.

Van den Berg, J. H. and Van Gelder, A. (1993) A new bedform stability diagram, with emphasis on the transition of ripples to plane bed in flows over fine sand and silt. Special Publication 17, Int. Assoc. of Sedimentol. Santa Barbara, Calif.

Van der Mark, C.F. (2009) A semi-analytical model for form drag of river bedforms, Ph.D. thesis, University of Twente, Enschede, the Netherlands

Van der Mark, C.F. and Blom, A. (2007) A new and widely applicable tool for determining the geometric properties of bedforms. CE&M Research Report 2007R-003/WEM-002 ISSN 1568-4652, University of Twente, Enschede, The Netherlands

Van der Mark, C.F., Blom, A. and Hulscher, S.J.M.H. (2008) Quantification of Variability in Bedform Geometry. J. Geophys. Res., 113(F03020), doi:10.1029/2007JF000940

Van der Scheer, P., Blom, A. and Ribberink, J.S. (2001) Transport Formulas for Graded Sediment. Rep. No. 2001R-003/MICS-022 Civil Engineering and Management University of Twente, The Netherlands

Van der Zwaard, J.J. (1974) Roughness aspects of sand transport over a fixed bed. In: Proceedings XVth IAHR-Congress 1973

Van der Zwaard, J.J. (1974a). Ruwheidsonderzoek waal - invloed van bodemtransport op de ruwheid van een vaste laag - tekst, tekeningen en bijlagen. verslag modelonderzoek M 988 deel I, WL–Delft Hydraulics.

Van der Zwaard, J.J. (1974b). Ruwheidsonderzoek waal - invloed van bodemtransport op de ruwheid van een vaste laag - tabellen en foto's. verslag modelonderzoek M 988 deel II, WL–Delft Hydraulics.

Van Rijn, L.C. (1982) Equivalent roughness of alluvial bed Journal J. Hydraul. Eng. 108 HY10

Van Rijn, L.C. (1984) Sediment Transport, Part III: Bed Forms and Alluvial Roughness. J. Hydraul. Eng., 110(12), pp. 1733-1754.

Van Rijn, L.C. (1990) Principles of Principles of Fluid Flow and Surface Waves in Rivers, Estuaries, Seas and Oceans. Aqua publications, Blokzijl, Netherlands 400 p. ISBN: 90-800356-1-0

Van Rijn, L.C. (2007) Unified View of Sediment Transport by Currents and Waves. I: Initiation of Motion, Bed Roughness, and Bed-Load Transport. J. Hydraul. Eng. 133-6, pp. 649-667

Van Rijn, L.C., and Klaassen, G.J. (1981) Experience with straight flumes for movable bed experiments. WL–Delft Hydraulics. Report No. 255 May 1981

Vanoni, V.A. and Brooks, N.H. (1957) Laboratory Studies of the Roughness and suspended load of alluvial streams. Report E-68. Sedimentation Laboratory, California Institute of Technology, Pasadena.

Venditti, J.G., Nelson, P.A., and Dietrich, W.E. (2008) The domain of bedload sheets. In Proc. Int. Workshop Marine Sandwave and River Dune Dynamics III University of Leeds UK 2008.

White, W.R., Paris, A., and Bettes, W.R. (1980) The frictional characteristics of alluvial streams. In: Proc. Instn. Civ. Engrs, pp. 737-750.

Whiting, P.J., Dietrich, W.E., Leopold, L.B., Drake, T.G., and Shreve, R.L. (1988) Bedload sheets in heterogeneous sediment. Geology, 16, pp. 105-108.

Wilbers, A (2004) The development and hydraulic roughness of subaqueous dunes. Ph.D. thesis, University of Utrecht, Utrecht, the Netherlands.

Wilcock, P.R (1993) Critical shear stress of natural sediments. J. Hydraul. Eng. 119 (4), pp. 491-505.

Wilcock, P.R., and Crowe, J.C. (2003) Surface-Based transport model for mixed-size sediment sediment. J. Hydraul. Eng. 129 (2), pp. 120-128.

Wilcock, P.R., and McArdell, B.W. (1997) Partial transport of a sand/gravel sediment. Water Resour. Res. 33 (1), pp. 235-245.

Wren, D.G., Langendoen, E.J., and Kuhnle, R.A. (2009) Flow and sand transport over an immobile gravel bed. In Proc. 33rd IAHR Congress Water Engineering for a Sustainable Environment, August 9-14, 2009

Yalin, M.S. (1964), On the average velocity of flow over a mobile bed, La Houille Blanche, 1, pp. 45–53.

Yalin, M.S (1977) Mechanics of Sediment Transport. Second edition, 298 pp, Pergamon Press, Oxford, United Kingdom.

Yalin, M.S. (1985) On the determination of ripple geometry. J. Hydraul. Eng. 111 (8), pp. 1148-1155.

Zhang, Y. (1999) Bed form geometry and friction factor of flow over a bed covered by dunes. MSc Thesis, University of Windsor, Windsor, Canada.

Used Symbols

Greek

α_h	growth parameter BDR-model
α_l	growth parameter BDR-model
β	intercept parameter BDR-model
Δ	dune height
θ	dimensionless shear stress
κ	Von Karman's constant
Λ	dune length
μ	mean / ripple factor
ρ	density
σ	standard deviation
τ	shear stress
ψ	transport reduction factor

Latin

b	power parameter in transport model
B	flume width
c_f	friction coefficient
C	Chézy friction coefficient
d	layer thickness
D	grain diameter
D_{xx}	grain size for which XX percent is finer
f	fill-factor of the coarse layer
f_g	Gaussian probability density function for bed level
f_Δ	Rayleigh probability density function for (Δ/2)
g	gravitational acceleration
G_{zz}	spectral density
h	water depth
I	slope
I_e	slope energy level
k_s	Nikuradse equivalent sand roughness height
L	dune length toe-toe
L	characteristic length (Chapter 3)
p	fractional bed coverage
$p_{z<ztil}$	fraction of bed observed below level z_{til}
Q	discharge
q_s	sediment discharge [m^2/s]
R	hydraulic radius
s	sediment transport rate [g/s]
$s_{0,a}$	Alluvial sediment transport rate for alluvial shear stress
$s_{0,s}$	Alluvial sediment transport rate for supply-limited shear stress
t	elapsed simulation time
u	Flow velocity
u_*	friction velocity
x	horizontal axis, streamwise direction
y	horizontal axis, flow normal direction
z	vertical axis, flow normal direction
z_{cl}	average level of coarse layer
z_{til}	level of the top of the immobile layer

Sub and superscripts

$'$	grain related
$''$	form related
0	Alluvial reference situation
10	10-th percentile of distribution
50	50-th percentile of distribution
90	90-th percentile of distribution
a	alluvial shear stress used for reference transport
b	bed
bl	bedload
c	critical
cl	coarse layer
cr	critical
e	energy
meas	measured
pred	predicted
s	supply-limited
sl	supply-limited
st	stoss
sat	saturation
t	total
til	top immobile layer
w	wall

Appendix I

Wall Roughness Correction

Total shear stress

The energy losses in the experiments are derived from the bed level, water level and discharge measurements. The energy losses in an equilibrium flow can be calculated from the slope of the water and bed level since these are the same on average. However, a true equilibrium flow is difficult to realise and in the experiments the conditions were varying around an equilibrium. In the experiments of DS-III the equilibrium flow was only approximated. Therefore the energy losses need to be calculated from the slope of the energy level in order to take the slight acceleration or deceleration of the flow into account (Chow, 1959). The energy level is expressed as:

$$z_e = z_w + \frac{u^2}{2g} \qquad \text{(Eq. A1.1)}$$

The slope of the energy level (I_e) in stream wise direction is determined by making a linear least squares fit to the energy level, over the observation length. The total bed shear stress follows from:

$$\tau_t = \rho g R_t I_e \qquad \text{(Eq. A1.2)}$$

R_t is the total hydraulic radius:

$$R_t = \frac{hB}{B + 2h} \qquad \text{(Eq. A1.3)}$$

The average of the water depth and the energy slope are used in order to calculate the average total shear stress over the equilibrium period.

Division of shear stress and roughness

The total shear stress consists of contributions from the wall and from the bed and generally the roughness of these surfaces will be different. For the simple rectangular flume the wall shear stress acts on two sidewalls over the depth ($2h$) and the bed shear stress acts over the width of the flume (B). Therefore the total shear stress is divided into wall and bed shear stress following:

$$(2h + B)\tau_t = 2h * \tau_w + B * \tau_b \qquad \text{(Eq. A1.4)}$$

The roughness parameter that is used in this thesis is the friction coefficient, (c_f) which is defined as:

$$\tau_x = c_{f,x}\rho u^2 \qquad \text{(Eq. A1.5)}$$

The friction coefficient is therefore the Darcy-Weisbach friction factor (f_{dw}) divided by 8. The method to divide the shear stress and roughness over the wall and bed that is applied is the method presented by Vanoni and Brooks (1957). The same average flow velocity is assumed to determine the bed and wall shear stress. Therefore the flow velocity disappears if Eq. A1.4 and A1.5 are combined. The friction coefficients are added using this equation:

$$c_{f,t} = \frac{c_{f,b}}{1+\frac{2h}{B}} + \frac{c_{f,w}}{1+\frac{B}{2h}} \qquad \text{(Eq. A1.6)}$$

Thus, the wall roughness needs to be known in order to calculate the bed roughness.

Smooth wall

Vanoni and Brooks presented a method to determine the wall resistance of a smooth wall in a turbulent flow. They present a curve where f_{dw} is related to Re/f_{dw} to determine the $f_{dw,w}$, where $f_{dw,w}$ is the wall-related friction factor and Re the Reynolds number:

$$Re = \frac{4uR_t}{\nu} \qquad \text{(Eq. A1.7)}$$

ν is the kinematic viscosity. Instead of the graph of Vanoni and Brooks a fit of this graph, as found in Van Rijn (1990) has been used to determine the wall roughness. Expressed in c_f this relation reads as:

$$c_{f,w} = \frac{1}{8}\left(0.0026\left(\log\left(\frac{Re}{8c_{ft}}\right)\right)^2 - 0.0428\log\left(\frac{Re}{8c_{ft}}\right) + 0.1884\right) \qquad \text{(Eq. A1.8)}$$

Rough wall

If the assumption of a smooth wall is not reasonable and the wall roughness height ($k_{s,w}$) is known, the following formulation can be used:

$$c_{f,w} = \frac{g}{\left(18\log\left(\frac{12R_w}{k_{s,w}}\right)\right)^2} \qquad \text{(Eq. A1.9)}$$

This is a White-Colebrook type of formula expressed as a friction factor instead of a Chézy roughness parameter. R_w can be expressed in known variables using the following relations:

$$\tau_t = \rho g R_t I_e = c_{f,t}\rho u^2 \qquad \text{(Eq. A1.10)}$$

$$\tau_w = \rho g R_w I_e = c_{f,w}\rho u^2 \qquad \text{(Eq. A1.11)}$$

u and I_e are assumed to be equal, therefore:

$$R_w = R_t \frac{c_{f,w}}{c_{f,t}} \qquad \text{(Eq. A1.12)}$$

Equations A1.9 and A1.12 can be solved iteratively.

Solution for bed and wall roughness

The bed roughness can be determined once a solution for the wall roughness has been found. For the experimental data the variables *h*, *B* and *u* are known. Therefore a solution for the bed roughness can be directly found using Eq. A1.6 and subsequently the bed shear stress can be found using Eq. A1.5.

However, the wall roughness prediction methods are also used the hindcast the total roughness and shear stress in Chapters 4 and 5. The bed roughness model presented in Chapter 4 predicts a value for $c_{f,b}$, but the wall roughness needs to be taken into account as well in order to calculate the water depth. In that case the equilibrium water depth and total bed roughness are not known in advance and an iterative procedure is used solve the system. In Figure A1.1 the solution scheme is described.

The bed slope and discharge are the boundary conditions for the predictions. The bed roughness ($c_{f,b}$) is predicted using the method described in Chapter 4 and is therefore also considered a known variable. The wall roughness ($k_{s,w}$) is either known or the sidewalls are smooth. Initially the water depth and the total roughness are unknown. Therefore an initial value for the water depth is estimated from the Chézy equation for equilibrium flow. Initially the wall roughness is assumed to be equal to the bed roughness. With these assumptions the wall roughness can be predicted using one of the methods described above. Once the wall roughness is known the total roughness can be calculated and the water depth can be recalculated. Figure A1.1 describes how these two nested iteration loops are executed.

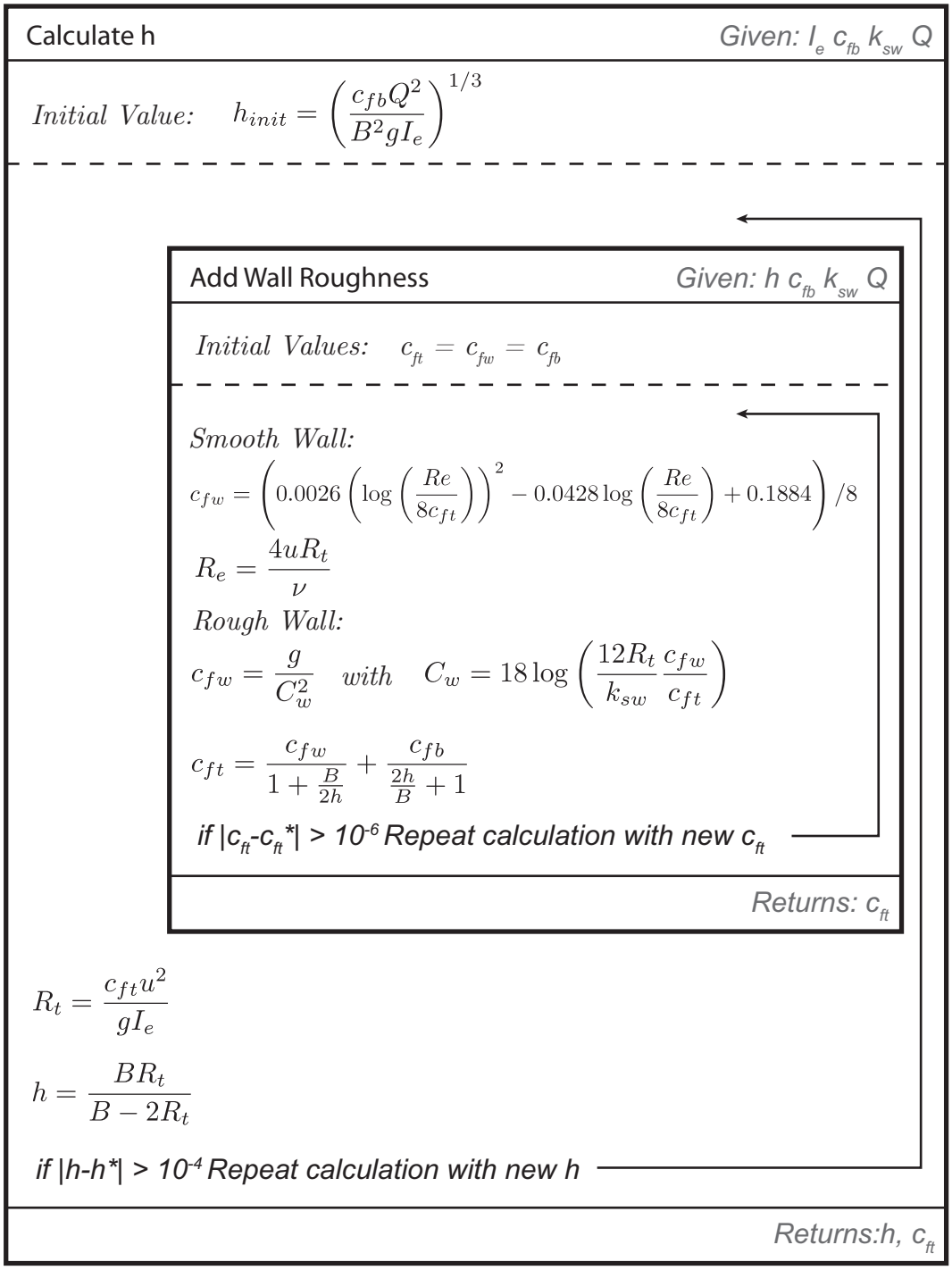

Figure A1.1: Solution scheme for adding the wall roughness to the bed roughness in a predictive application of the wall roughness correction formulation.

Appendix II

Choice of Filter Width for Bedform Recognition

The bedform dimensions have been determined using the procedure described in Van der Mark and Blom (2007). Below the method is briefly explained and the choice of a filter length is discussed.

The method consists of the following steps: First outliers are removed. Then the data are detrended. Subsequently the dune troughs and crests are selected. To find these, the bed level is low-pass filtered, with a hanning-window, to remove high frequency features. The crossings of the filtered bed level and the average bed level are selected. The unfiltered signal is used to determine the bedform amplitude in order to prevent a decrease in amplitude because of the low-pass filtering. The dune height reported here is the difference in level between the highest point between an up and down crossing of the average bed level and the lowest point between a down and an up-crossing. An up-crossing is located on the stoss-side of a dune, a down-crossing on the lee side. The dune length is defined as the difference in *x*-direction between two successive down crossings.

For the data sets II, IV and V no real detrending was needed for selection of bedforms with up and down crossings. The bed level sensor moved parallel to the (tilted) flume bottom and the immobile layer, and the sand layer thickness in the measurement sections is constant on average. Fitting a trend line results in the horizontal line at the average bed level (Figure 2.5). For the data sets I and III in the small flumes detrending was needed.

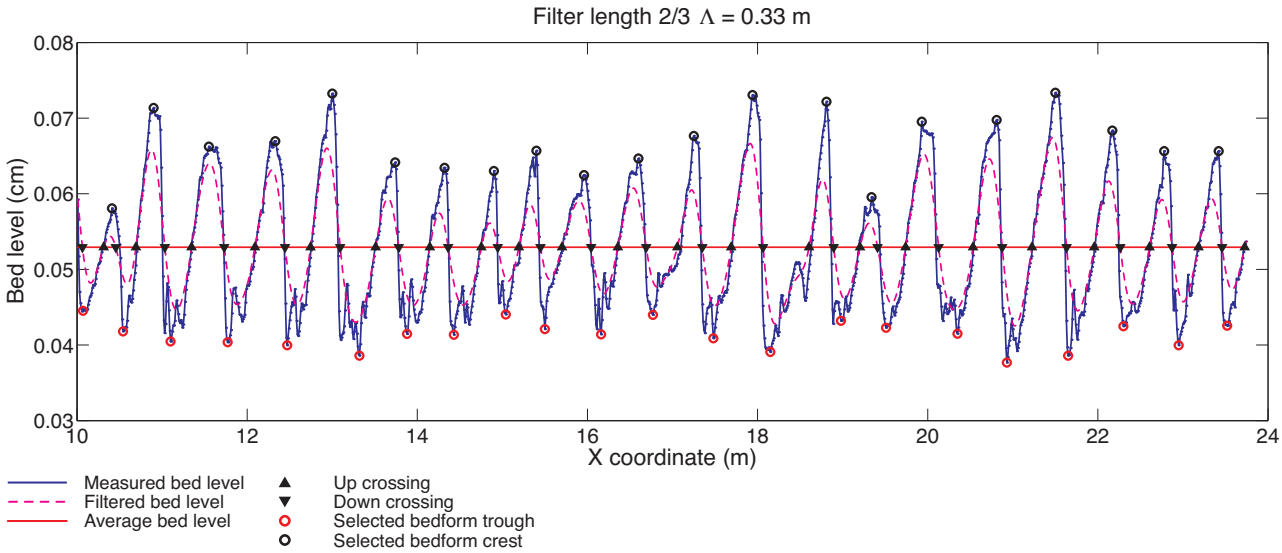

Figure 2.5: Result of the bedform recognition algorithm for one of the supply-limited experiments (DS-II Exp 1-4). A strong filter has been applied to the bed level, ff=2/3, but still all bedforms are recognized without problems. Therefore these supply-limited experiments are rather indifferent to the choice of the filter width.

The choice of the filter width determines which bedforms are recognized by the average bed level crossing method that is applied to find bedforms. Van der Mark and Blom (2007) propose to relate the length of the filter to the dune length as estimated by a spectral moments method using:

$$P = \mathrm{ff}(\Lambda/dx + 1) \qquad \text{(Eq. A2.1)}$$

P is the filter width in points, ff is the filter length factor, Λ is the estimated bedform length, *dx* the distance between measurements. A filter factor of 1/6 worked well for the data of Van der Mark and Blom (2007). Inspection of the results of the bedform recognition algorithm revealed that small bumps near the average bed level were sometime recognized using a filter factor of 1/6. This is shown in the left panel of Figure 2.6. The dashed line, which is used to find bedforms, is the bed level that is filtered with filter factor of 1/6. Two small bumps are still visible at the average bed level. If these bumps are present in the filtered line and cause an up and down crossing of the average bed level (the black triangles in Fig. 2.6) these bumps are recognized as bedforms. If the window length is increased, using ff=1/3, these bumps are no longer recognized as bedforms (Fig. 2.6 right). This increases the average dune height and length. Figure 2.7 shows the effect of the choice of the filter on the average dune dimensions of DSII Series 1. The average bedform dimensions increase with increasing filter length because an increasing number of small bedforms is not included. The most supply-limited experiments, 1-4 and 1-6, are indifferent to the filter width because the bedforms in these experiments were very regular, as shown in Figure 2.5. The more alluvial experiments are more irregular and react therefore stronger to a change in filter width.

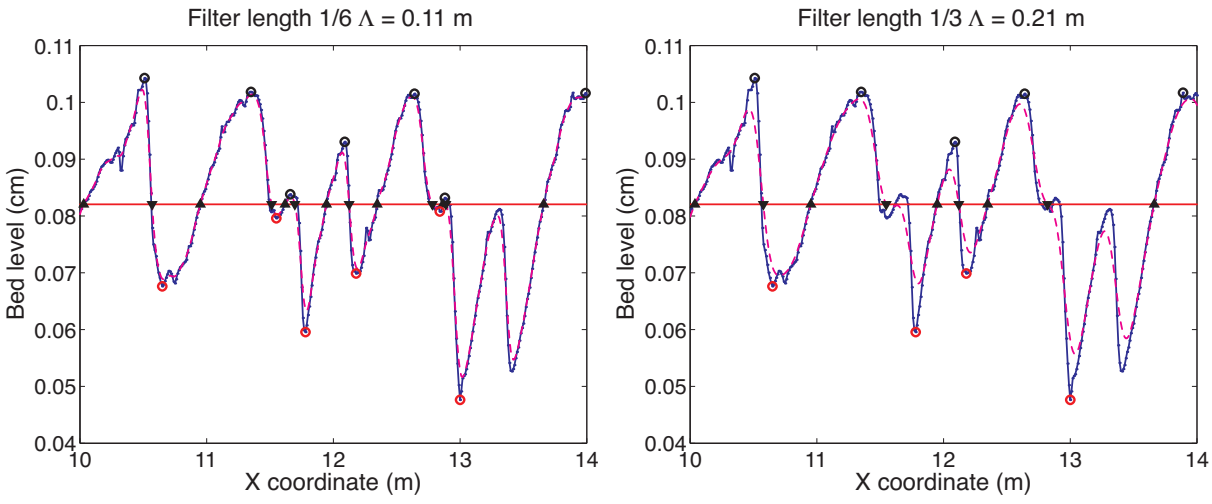

Figure 2.6, Effect of variation in the filter width on the recognition of small-scale features as bedforms. These bed levels were measured in DS-II Exp 1-7.

Van der Mark and Blom (2007) used a figure like Figure 2.7 to determine an optimum filter factor. Below ff = 1/6 the bedform height quickly increased and above ff 1/6 the line flattened. This feature is not as apparent for the data in this thesis. The bedform height increases nearly linearly with increasing filter width. Therefore it is not clear from Fig. 2.7 what value would

be best. Based on the Figure 2.6 and similar figures for other experiments, it has been decided that small features like shown in Figure 2.6 should not be recognized by the algorithm. Therefore the value for the filter factor of 1/3 has been chosen.

The difference in average bedform height between using a value of 1/6 and 1/3 is for these experiments in the worst case approximately 6%. This is for alluvial experiments. For supply-limited experiments the uncertainty reduces to 0%.

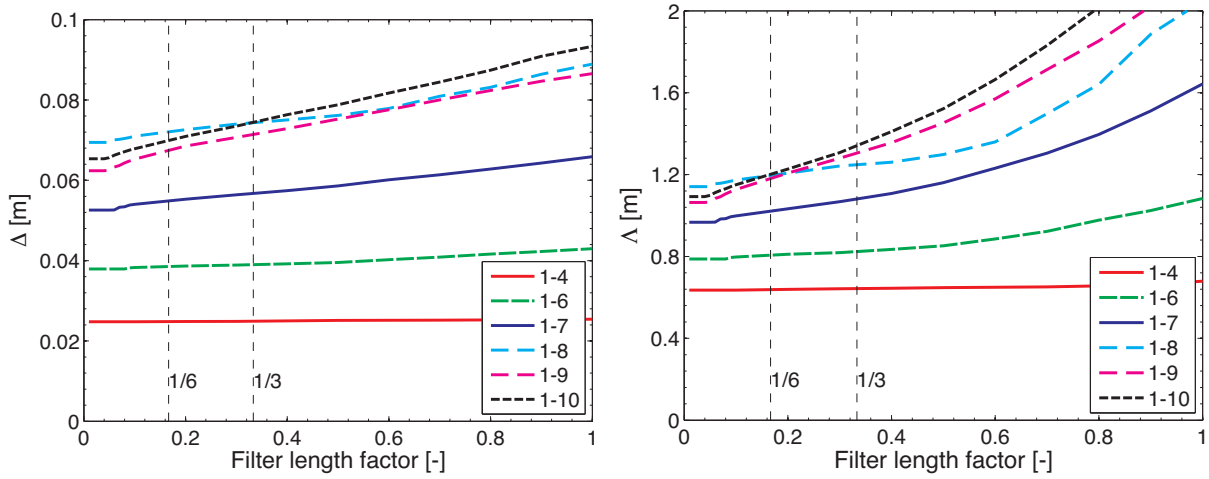

Figure 2.7, Effect of the variation of the filter factor on the bedform dimensions. The experiment numbers refer to the experiments from DS-II Series I.

Appendix III

Calculation of the Geometric Standard Deviation

The standard deviation is a measure for the width of the grain size distribution. Often, the log-transform of the grain size distribution can be approximated by a normal distribution. Therefore the sedimentological ϕ and ψ scales have been introduced, where $\psi = -\phi$ (Parker and Andrews, 1985). The ψ parameter is defined as:

$$\psi = \frac{\ln(D)}{\ln(2)} \qquad \text{(Eq. A3.1)}$$

The geometric standard deviation is the standard deviation calculated from the log-transformed grain size distribution and subsequently transformed back to the original units of D (Parker, Man 54). The standard deviation for a discretized distribution is calculated from:

$$\sigma_\psi = \sqrt{\sum_{i=1}^{n} ((\psi_i - \psi_m)^2 p_i)} \qquad \text{(Eq. A3.2)}$$

Where σ_ψ is the standard deviation of the log-transformed distribution, n is the number of classes in the grain size distribution, ψ_m is the mean value of ψ and p_i is the fraction of the sediment in class i.

$$\psi_m = \sum_{i=1}^{n} (\psi_i p_i) \qquad \text{(Eq. A3.3)}$$

The geometric standard deviation is the reverse transform of σ_ψ:

$$\sigma_g = 2^{\sigma_\psi} \qquad \text{(Eq. A3.4)}$$

The following definition is often used to calculate σ_g:

$$\sigma_g = {}^1/_2 \left(\frac{D_{84}}{D_{50}} + \frac{D_{50}}{D_{16}} \right) \qquad \text{(Eq. A3.5)}$$

However, this equation only gives the same result as the more general definition of Eq. A3.1 – A3.5 if the grain size distribution is log-normal. This approach is not used since the bi-modal sediment mixtures in many of the experiments can not be approached by a log-normal distribution and therefore the Eq. A3.1 – A3.5 have been used to calculate σ_g.

List of Publications

Kroon, A., Tuijnder, A.P., Spanhoff, R., & Aarninkhof, S.G.J. (2005). Seasonal effects and the impact of the beach morphology on the variability of water line positions. In Agustin Sanchez-Arcilla (Ed.) Proceedings of the 5th International Conference, April 4-8, 2005, Barcelona, Spain, doi: 10.1061/40855(214)63

Tuijnder, A.P., Ribberink, J.S., and Hulscher, S.J.M.H. (2007) Predicting the occurrence of dunes under supply limited conditions. In Dohmen-Janssen, C.M. and Hulscher, S.J.M.H. (Eds.), Proceedings river, coastal and estuarine morphodynamics: RCEM 2007, Publ.: Taylor & Francis Group, Vol I, pp. 633-639.

Tuijnder, A.P., Spekkers, M.H., Ribberink, J. S. and Hulscher, S.J.M.H. (2008) Bed roughness under supply-limited conditions. In: In Altinakar M., Kokpinar M.A. et al. (Eds.) Proc. of the Int. Conf. on Fluvial Hydraulics, River Flow 2008, Cesme, Izmir, Turkey, Sept 3-5, 2008, Vol I, pp. 395-405.

Tuijnder, A.P., Ribberink, J.S. and Hulscher, S.J.M.H. (2009) An experimental study into the geometry of supply-limited dunes. Sedimentology, 56, pp. 1713-1727, doi: 10.1111/j.1365-3091.2009.01054.x

Tuijnder A.P., Ribberink, J.S. and Hulscher, S.J.M.H. (2009) Morphodynamic modelling of rivers under supply-limited conditions. In Vionnet, C., García, M. H., Latrubesse, E.M., Perillo, G.M.E. (Eds.) Proc. River, Coastal and Estuarine Morphodynamics, RCEM 2009, Publ. Taylor & Francis, London, ISBN 978-0-415-55426-8, Vol I, pp. 877 - 882

Tuijnder, A.P. & Havinga, H. (2009). Onderzoek verfijnt modellen voor sedimenttransport. Land + water : magazine voor civiele- en milieutechniek 49(9), pp. 28 – 30.

Tuijnder, A.P., Ribberink, J.S. and Hulscher, S.J.M.H. (Subm) Riverbed Roughness Prediction under supply-limited conditions.

Tuijnder, A.P., Ribberink, J.S. and Hulscher, S.J.M.H. (Subm) Modelling of sediment transport over immobile layers in rivers using a transport reduction approach.

Tuijnder, A.P., Spekkers, M.H. and Ribberink, J.S. (Subm) Development of supply-limited transport due to vertical sorting of a sand-gravel mixture. Proc. River Flow 2010 Braunscheig, Germany.

Tuijnder, A.P. and Ribberink, J.S. (Subm) Prediction of bedform dimensions, bed roughness and sediment transport under supply-limited conditions in rivers. In Proc. 1st IAHR European Division Congress, Edinburgh, United Kingdom.

About the Author

I was born the 29th of January 1980 in Dordrecht, the Netherlands. During my youth I lived in Zwijndrecht where I went to high school at the Develstein College. I took the VWO-exams in 1998. After school I preferred to play with LEGO and later on with Märklin model trains. As for sports: I first swam a lot but later switched to running; my favorite distance was 20 km.

Between 1998 and 2004 I studied geography at the University of Utrecht. I followed courses on a.o. sedimentology, geomorphology, (quaternary) geology, fluvial and coastal morphology, fluid dynamics and sediment transport. The several field works during my study took me from the Dutch polder via the Teutoburger Wald, Harz, French Alps and Denmark to Java and Kalimantan in Indonesia. In the weekends I worked at a telephone shop until I could get student-assistantships for soil science and the computer service department. In my leisure time I kept running, but since I bought a racing bike I decided to join the triathlon club and picked up the swimming again.

In 2004 I worked at the Netherlands Environmental Assessment Agency (RIVM/MNP) where I was mainly assisting in the development of a statistical method to predict the distribution of plant and bird species.

In 2005 I started my PhD-research at the Water Engineering and Management group at the University of Twente in Enschede and I moved to Deventer with my girlfriend Ilse. In Deventer a great triathlon club was started in 2006 of which I am a member. Besides that I like travelling and nature photography, preferably a combination of these. My most beautiful journeys thus far were to New Zealand and Iceland.

Since the end of 2009 I have a postdoc position and I am working on the development of model concepts for vertical sorting of grain size fractions and the formation of immobile layers in river beds. This work is commissioned by Deltares and Rijkswaterstaat.

Morphodynamic models are an important tool for river mangement, as they provide insight into the effects of interventions and the natural development of rivers. These models depend on accurate predictions of the bed roughness and the transport of sediment. In this thesis, the effect of a limited volume of mobile sediment on the river bed –a supply limitation– on bedform dimensions, bed roughness and sediment transport rates is studied in an extensive set of new flume experiments. The new insights into these effects are used to formulate new models and adapt existing model concepts to predict these variables in morphodynamic models under supply-limited conditions.

ISBN 978-90-9025123-3
University of Twente, the Netherlands